

Fluid Bed Particle Processing

Peter Dybdahl Hede



Download free books at

bookboon.com

Peter Dybdahl Hede

Fluid Bed Particle Processing



Fluid Bed Particle Processing

1st edition

© 2013 Peter Dybdahl Hede & bookboon.com

ISBN 87-7681-153-0

Contents

Fluid Bed Particle Processing	7
1 Introduction to fluid bed processing	8
1.1 Types of fluid beds	9
1.2 Important fluid bed parameters	10
1.3 The Geldart classification of particles	12
1.4 Advantages and disadvantages of fluid bed operations	13
2 The process and principles of Wet agglomeration	15
2.1 Introduction to the stages of the granulation processes	15
2.2 Wetting and nucleation	16
2.3 Granule growth behavior	26
2.4 Breakage and attrition	31
2.5 Simulation of the agglomeration process – a brief review on population balance theory	32
2.6 Summing up on wet agglomeration – Qualitative guidelines for parameters influencing agglomeration	33

**YOU THINK.
YOU CAN WORK
AT RMB**

**RAND
MERCHANT
BANK**
A division of FirstRand Bank Limited
Traditional values. Innovative ideas.

Rand Merchant Bank uses good business to create a better world, which is one of the reasons that the country's top talent chooses to work at RMB. For more information visit us at www.rmb.co.za

Thinking that can change your world

Rand Merchant Bank is an Authorised Financial Services Provider



Click on the ad to read more

3	Granule coating principles and properties in fluid beds	36
3.1	Parameters describing the coating process and result	37
3.2	Product, system and operating parameters affecting the coating process and efficiency	38
3.3	Influence of product and formulation variables on coated granule morphology	41
3.4	Agglomeration or Coating?? – Qualitative trends and attempts of finding a boundary parameter	43
3.5	Qualitative description of key parameters governing the coating process – a first attempt to encircle an operating window	45
4	Mechanical properties of granules and coating layer – strength and breakage mechanisms	47
4.1	Properties characterising the granule strength	47
4.2	Types of breakage mechanisms	50
4.3	Towards a quantitative prediction of breakage mechanisms	53
4.4	Qualitative trends of parameters affecting breakage	56
4.5	Modern approach – a brief review on computer simulation of granule breakage	57
4.6	Strength test methods – a brief review	58
4.7	Summing up on granule strength	61
5	Summary	62



Discover the truth at www.deloitte.ca/careers

Deloitte.

© Deloitte & Touche LLP and affiliated entities.



Click on the ad to read more

Table of symbols	63
Literature	68
Appendix A1: Derivation of the equation 2.5	80
Appendix A2: From equation 2.5 to equation 2.7	84
Appendix A3: Derivation of the dimensionless spray flux	85
Appendix A4: Derivation of the Stokes viscous number and the Stokes critical viscous number	86
Appendix A5: Derivation of equation 3.1 describing the coating thickness	89
Appendix A6: Derivation of equation 3.4	91
Notes	94



**I WANT TO CHANGE DIRECTION,
AND THE WORLD.**

GOT-THE-ENERGY-TO-LEAD.COM

We believe that energy suppliers should be renewable, too. We are therefore looking for enthusiastic new colleagues with plenty of ideas who want to join RWE in changing the world. Visit us online to find out what we are offering and how we are working together to ensure the energy of the future.

RWE
The energy to lead



Fluid Bed Particle Processing

The present text introduces the use of fluidised bed processing in the context of wet granulation and coating. The text also covers introductory information about the mechanical properties of dry granules. This is a scientific field rarely taught at universities or engineering schools around the world although it has enormous and ever increasing relevance to the chemical and biochemical industries. Often students are left with nothing but qualitative tendencies and hands-on experience as no textbook yet covers all relevant subjects treated in this text.

Being part of the powder technology field it is the aim of this text to narrow the gap between applied engineering and quantitative models and theory. The text is aimed at undergraduate university or engineering school students working in the field of chemical or biochemical engineering. Newly graduated as well as experienced engineers may also find relevant new information as emphasis is put on the newest scientific discoveries and proposals presented in recent years of scientific publications. In order to provide a firm theoretical background several of the relevant formulas have been derived in the appendix which is often impossible to find elsewhere even in scientific literature. It is the hope that such theoretical considerations may help the reader to understand how particle technology is closely related to other branches of chemical science and chemical engineering. The literature list may also hopefully be an inspiration for further reading in the small but highly important field of fluid bed processing.

I alone am responsible for any misprints or errors but I will be grateful to receive any critics and suggestions for improvements.

Copenhagen, September 2006

Peter Dybdahl Hede

1 Introduction to fluid bed processing

The principle of a fluid bed is to maintain particles in suspension in a close area by blowing air through the particle bed. The state of the bed depends thereby on the air velocity and on the particle properties. A fluidised bed behaves like a boiling liquid. For instance will an object placed in the fluid bed float depending on its density, and the upper limited surface of the fluid bed remains horizontal if the bed is inclined (Teunou & Poncelet, 2002). Agglomeration in fluid beds is achieved by spraying the binder liquid onto the bed. The agitation forces combined with the drying air will ensure permanent collisions between the wetted particles thereby causing agglomeration. Drying in fluid beds can likewise be achieved by agitating the bed with hot air but without liquid addition. The drying end-point is detected by a sudden rise in the outlet air temperature and an equalization of the outlet air dew point to that of the inlet air. Coating in fluid beds is analogous to the agglomeration process and the coating liquid is sprayed onto the bed as well, although process conditions are changed in order to hinder agglomeration (Faure et al., 2001). The principle of a typical fluid bed set-up can be seen in figure 1.

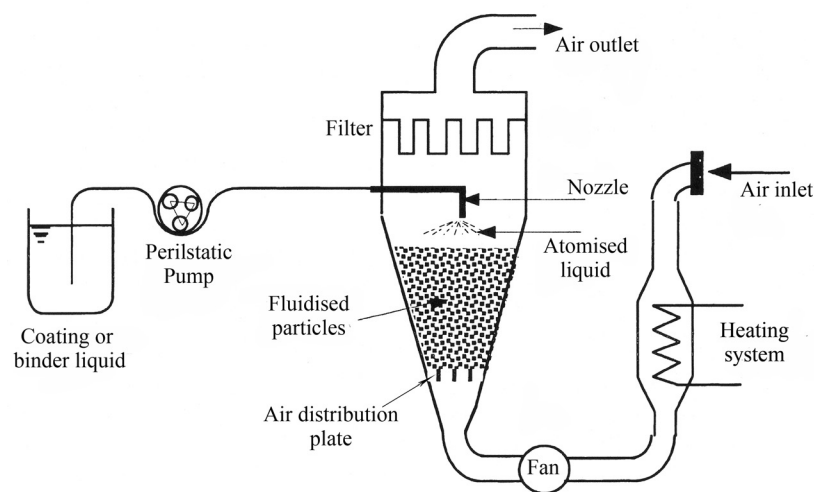


Figure 1: The principle of a typical (top spray) fluid bed set-up

Sketch of a typical top-spray fluid bed with a conical fluidisation chamber that makes sure that the fluidisation velocity in m/s is greatest in the bottom of the chamber and lowest nearest the nozzle
(Based on Teunou & Poncelet, 2002).

Fluid bed granulation is in some ways different from other types of mixer granulation because the gas supplied to produce particle agitation also is responsible for binder/coating solvent evaporation and heating of the particles. In addition the increase in particle size and the liquid addition to the bed is associated with many changes in fluidisation characteristics, especially the mixing properties of the fluid bed. Other phenomena of the like and the fact that trajectories of particles are not predictable, makes fluid bed processing difficult to model and optimise without extensive use of experiments. Nevertheless, fluid beds have found many applications and a range of types have been developed for different purposes, not only in the biotech industry (Tardos et al., 1997).

1.1 Types of fluid beds

Fluid beds used for granulation or coating are classified according to the nozzle position (top, bottom or side) and to the operating conditions (continuous or batch) (Guignon et al., 2002). Continuous fluid beds are widely used in the food industry but rarely in production of enzymes. Batch fluid bed reactors have a cylindrical or conical shape. Air is distributed through a bottom grid with an adequate partition and size of holes. Reactors are equipped with one or several nozzles and sometimes with a mechanical stirrer as well (Guignon et al., 2002). In general there exist four basic types of batch granulation systems useable for enzyme granules. The four types can be seen in figure 2.

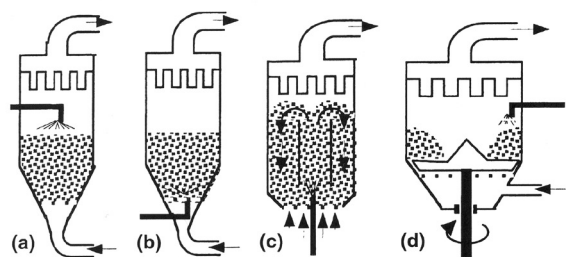


Figure 2: Different types of batch fluid beds.

a) Top-spray, b) Bottom-spray, c) Wurster type, d) Rotor with side-spray (Teunou & Poncelet, 2002).

Top-spraying is the oldest and simplest technique with the spray nozzle placed at the top of the chamber and air blowing from the bottom. It is still widely used for wet granulation but the efficiency and quality regarding coating is generally poor and it is now often replaced by bottom-spray or the Wurster type (Teunou & Poncelet, 2002). Generally, granules prepared by top-spray have a looser structure and are more porous than granules prepared from the other fluid bed types (Rubino, 1999).

The collisions between particles and liquid droplets are considerably increased with the use of the bottom spray type. Introducing liquid from the bottom gives a shorter distance between nozzle and bed thereby reducing the premature drying of binder/coating liquid before impact and leads to a larger coating efficiency. This type of fluid bed is very efficient for coating but the risk of unwanted agglomeration during coating is higher than in a top spray due to the higher concentration of wet particles (Teunou & Poncelet, 2002).

Work by Wurster in the fifties led to an improvement of the bottom spray bed called the Wurster system. By inserting a fixed cylinder into the chamber the circulation of the particles is changed and the drying rate increased, reducing the risk of agglomeration. This fluid bed type is particularly suited for coating (Teunou & Poncelet, 2002).

A fourth type of reactor is called the rotor system. The reactor consists of a disc rotating in the fluidising chamber and the liquid solutions are added tangentially from the top of the reactor. The combination of rotation and bottom-up air flow provides specific properties such as higher spherical shape and density to the resulting particles. This type of fluid bed system is mainly used for coating, although the coating quality is similar to that obtainable with the Wurster type (Teunou & Poncelet, 2002).

1.2 Important fluid bed parameters

The most important parameters regarding air velocities in a fluid bed are the minimum fluidisation velocity U_{mf} and the settling or terminal velocity U_t both in m/s. U_{mf} is the velocity at which fluidisation is incipient. It is one of the most important design parameters and is used for processes as drying, coating and agglomeration. In general U_{mf} can be described by the Ergun equation (Linoya et al., 1990):

$$U_{mf} = \frac{\eta_{gas}}{\rho_{gas} d_p} \left\{ \left(\beta_{E1}^2 + \beta_{E2} \cdot Ar \right)^{1/2} - \beta_{E1} \right\} \quad (1.1)$$

where η_{gas} is the gas viscosity, ρ_{gas} the gas density, d_p the diameter of particles and β_{E1} and β_{E2} are the Ergun parameters depending on the particle sphericity and the bed voidage at incipient fluidisation. Ar is the Archimedes number defined as (Kunii & Levenspiel, 1991):

$$Ar = \frac{d_p^3 \rho_{gas} (\rho_p - \rho_{gas}) g}{\eta_{gas}^2} \quad (1.2)$$

where ρ_p is the particle density and g being gravity.

For particles above 100 μm the Ergun expression can be approximated by (Teunou & Poncelet, 2002 and Cryer, 1999):

$$U_{mf} = \frac{\eta_{gas}}{\rho_{gas} d_p} \left\{ (1135.7 + 0.04084 Ar)^{1/2} - 33.7 \right\} \quad , \quad d_p > 100 \mu m \quad (1.3)$$

The settling velocity U_t is the air velocity over which transportation by dragging or pneumatic conveying occurs. Above this high velocity the fluidisation will stop and the particles will be blown out of the bed. It is often desired to operate at a bed velocity between U_{mf} and U_t to avoid carryover of particles (Kunii & Levenspiel, 1991). Rules of thumb state that a proper fluidisation velocity should be found in the range of 0.2 to 0.5 times of U_t and that U_t is at least ten times larger than U_{mf} (Niro, 1992). Kunii & Levenspiel (1991) suggest the following equation for U_t :

$$U_t = \left[\frac{4 d_p (\rho_p - \rho_{gas}) g}{3 \rho_{gas} C_D} \right]^{1/2} \quad (1.4)$$

in which C_D is an experimentally determined drag coefficient for spherical particles given as (Kunii & Levenspiel, 1991):

$$C_D = \frac{24}{Re_p} + 3.3643 \cdot Re_p^{-0.3471} + \frac{0.4607 \cdot Re_p}{Re_p + 2682.5} \quad (1.5)$$

where Re_p is the particle Reynolds number defined as (Kunii & Levenspiel, 1991):

$$Re_p = \frac{d_p U_p \rho_{gas}}{\eta_{gas}} \quad (1.6)$$

where U_p is the relative velocity of the moving particles to the fluidisation gas.

For non spherical particles U_t may be found as (Kunii & Levenspiel, 1991):

$$U_t = U_t^* \left[\frac{\eta_{gas} (\rho_p - \rho_{gas}) g}{\rho_{gas}^2} \right]^{1/3} \quad (1.7)$$

where U_t^* is the dimensionless terminal velocity approximated by (Kunii & Levenspiel, 1991):

$$U_t^* = \left[\frac{18}{(d_p^*)^2} + \frac{2.335 - 1.744 \cdot \phi}{(d_p^*)^{0.5}} \right]^{-1}, \quad 0.5 < \phi < 1 \quad (1.8)$$

in which ϕ is the shape factor, which accounts for non-spherical particle shape¹ also known as the particle sphericity ϕ and d_p^* is the dimensionless particle diameter determined by (Kunii & Levenspiel, 1991):

$$d_p^* = Ar^{1/3} \quad (1.9)$$

It can be seen from equation 3.1 and 3.2 that besides the gas properties, it is the size and density of the particles that determine the fluidisation velocity needed to obtain a homogenous fluidised bed. The larger and denser the particles are, the higher the fluidisation velocity must be to keep the particles fluidised (Guignon et al., 2002). During the agglomeration process U_{mf} will increase as the granule diameter increases. As a result, the excess gas velocity² U_e will decrease and so will the overall bed mixing (Schaafsma et al., 1999).

1.3 The Geldart classification of particles

Recognizing the importance of particle size and density on fluidisation properties, Geldart has found four overall fluidisation modes and determined a general particle classification chart. For any particle of known density ρ_p and mean particle size \bar{d}_p , the Geldart chart indicates the type of fluidisation to be expected (Kunii & Levenspiel, 1991). The Geldart chart can be seen in figure 3:

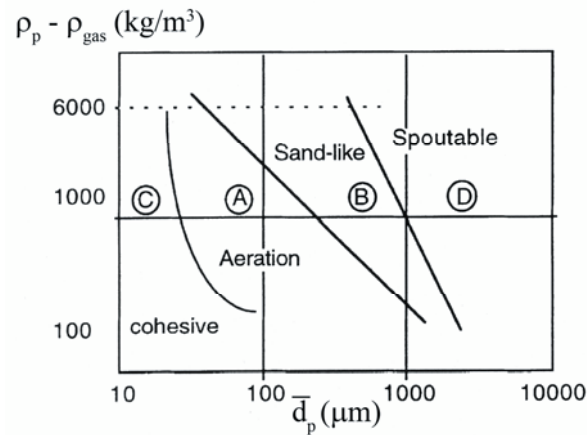


Figure 3: The Geldart classification of particles
Four types of Geldart powders being A,B,C and D (Teunou & Poncelet, 2002).

bookboon.com

Corporate eLibrary

See our Business Solutions for employee learning

[Click here](#)



[Click on the ad to read more](#)

From the smallest to the largest particles, the four groups in figure 3 are: C, A, B and D. The group C particles are cohesive or very fine powders, which are often very difficult to fluidise. Starch and flour are e.g. group C particles. Materials having a small mean particle size and/or densities less than 1.4 g/cm^3 are grouped into group A. Particles from this group fluidise well and as group A particles have the aeration properties required for coating purposes, particles suited for coating often come from this group. The group B particles are sandlike particles with mean particle diameters roughly between $40 \text{ }\mu\text{m}$ and $500 \text{ }\mu\text{m}$ and density between 1.4 and 4 g/cm^3 . The fluidisation mode of this type of particles is highly affected by the formation of gas bubbles in the bed and group B particles often fluidise well. Particles from group D are large and/or dense particles and often difficult to fluidise. As the air flow rate required to fluidise group D particles is necessarily high, group D particles are not normally processed in conventional fluid beds (Kunii & Levenspiel, 1991 and Teunou & Poncelet, 2002).

Although the division of powder particles into the four groups may seem unambiguous and rigid, it is important to note that at operating conditions above ambient temperatures and pressure, a particle may appear in a different group from that it occupies at ambient conditions. This is due to the effect of gas properties in form of ρ_{gas} in the classification chart in figure 3. As far as fluid bed processing is concerned, changes in ρ_{gas} in respect to ambient conditions often occur and thereby must be taken into consideration when using the Geldart chart (Rhodes, 1998). Nevertheless, the Geldart chart is widely used as an indication of the fluidisation possibilities for a given particle sample and often particles are simply referred to as “Geldart A particles” etc. The chart has proven useful at fluidisation conditions up to ten times U_{mf} (Kunii & Levenspiel, 1991), and although the chart has been further developed to contain areas subdividing the four particle groups, the present chart in figure 3 may serve as a helpful and quick tool concerning the choice of fluidisation operating conditions for a given particle sample with known density ρ_p and mean particle size \bar{d}_p .

1.4 Advantages and disadvantages of fluid bed operations

Fluid bed processing has many advantages over conventional wet massing and drying equipment. All the granulation processes including agglomeration, drying and coating, which require separate equipment in traditional granulation methods, can be performed in one unit saving time, transfer losses and labour costs (Summers & Aulton, 2004). Other advantages are temperature homogeneity and a fast mass and heat transfer (Teunou & Poncelet, 2002). Uniformity between e.g. the final enzyme granule batches is a necessity both regarding agglomeration and coating. Unfortunately these requirements cannot always be fulfilled and most agglomeration and coating equipment is associated with sieves and grinders to control the particles size with some possible recycling. Fluid beds have however usually low recycling ratios ($< 5\%$) compared to other types of equipment, which is an obvious advantage (Guignon et al., 2002).

A drawback is that fluid beds are expensive and that optimisation of process and product parameters needs extensive experimental work, not only initially but also during scale-up from development to production (Summers & Aulton, 2004). There are numerous apparatus, process and formulation parameters that affect the quality of the final granule produced in a fluid bed. Some of the basic parameters are listed in table 1. The extent of this list³ coupled with the fact that interactions between the parameters are intense and not yet fully understood, makes fluid bed processing still a field between science and empirical technology (Litster, 2003).

Apparatus parameters	Process parameters	Formulation parameters
Fluid bed spray type (top/bottom/Wurster or side spray)	Fluidising velocity/ temperature/ humidity	Powder particle size distributions
Batch or continuous fluid bed type	Nozzle pressure/spray rate	Powder particle material
Fluid bed vessel dimensions	Nozzle type	Binder/coating material
Air distribution plate dimensions	Spray angle	Binder/coating concentration
Nozzle height and position	Liquid droplet size	Binder/coating additives
Scale-up/scale-down	Bed load	Binder/coating solvent

Table 1: Basic apparatus, process and formulation parameters influencing fluid bed processing.

Parameters are commonly divided into three categories being equipment parameters, process parameters and formulation parameters (Based on Summers & Aulton, 2004 and Guignon et al., 2003).



Brain power

By 2020, wind could provide one-tenth of our planet's electricity needs. Already today, SKF's innovative know-how is crucial to running a large proportion of the world's wind turbines.

Up to 25 % of the generating costs relate to maintenance. These can be reduced dramatically thanks to our systems for on-line condition monitoring and automatic lubrication. We help make it more economical to create cleaner, cheaper energy out of thin air.

By sharing our experience, expertise, and creativity, industries can boost performance beyond expectations. Therefore we need the best employees who can meet this challenge!

The Power of Knowledge Engineering

Plug into The Power of Knowledge Engineering.
Visit us at www.skf.com/knowledge

SKF



Click on the ad to read more

2 The process and principles of Wet agglomeration

In the process of understanding and controlling the numerous stages and possible mechanisms taking place in a fluid bed, knowledge of the agglomeration process is essential. Whether or not agglomeration is the desired goal one should know at least the qualitative effects of the many parameters involved in the granulation process. In the following sections the stages of the agglomeration process will be presented and focus is brought onto the mechanisms and formulation and process parameters governing the granule properties and the effect upon their change.

2.1 Introduction to the stages of the granulation processes

The process of granulation has traditionally been described in terms of a number of different mechanisms, some of which is shown in figure 4 a). Such a picture of many competing mechanisms is confusing however, because the borderline between these mechanisms arbitrarily depends on the cut off size between granule and non-granular material, which again depends on the measurer's interests. Instead it has become more common to view the granulation as a combination of only three sets of separate processes: Wetting and Nucleation, Consolidation and Coalescence⁴, and Attrition and Breakage (Iveson et al., 2001a). The principle of this modern approach can be seen in figure 4 b). Even though many types of enzyme granules are not made by agglomeration, much of the theory behind the nucleation, growth and breakage mechanisms has direct parallels to the coating process of larger granules. Hence each of the three sets of processes will be presented in the following sections.

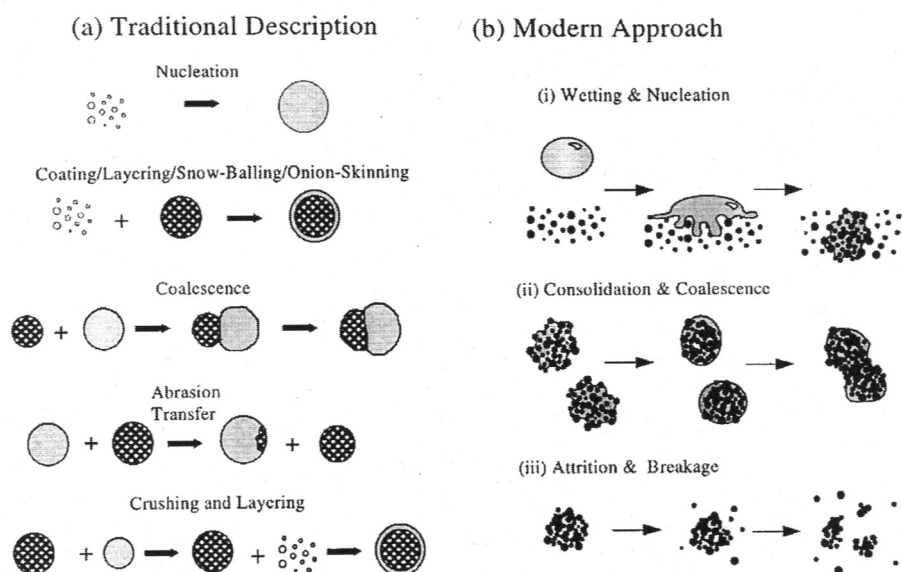


Figure 4: Schematic of granulation processes.

a) Traditional description. b) Modern approach (Iveson et al., 2001a).

2.2 Wetting and nucleation

The initial step in all wet agglomeration processes is the process of bringing liquid binder into contact with dry powder and attempt to distribute this liquid evenly throughout the powder. For simplicity the top-spray fluid-bed situation is considered although many of the following principles easily can be applied to more advanced bottom-spray or Wurster fluid beds (Rubino, 1999 and Iveson et al., 2001a).

Initially liquid droplets are formed at the spray nozzle from which they fall and impact the bed. After the initial impact the droplet wets and penetrates the bed surface by capillary action. Due to the mixing forces in the bed, the binder liquid and powder particles are mixed together to form a nucleus granule referred to as the nucleus. If the droplet is slow to penetrate the bed surface or if the flux of droplets on the surface is high, droplets will overlap and coalesce⁵. This will lead to a broad nuclei size distribution causing a broad final granule size distribution, which is often unwanted. Ideal nucleation conditions occur when one droplet produces one nucleus. This situation is referred to as “Drop controlled nucleation” (Litster et al., 2001). The principle of these five possible steps in nucleation can be seen in figure 5.

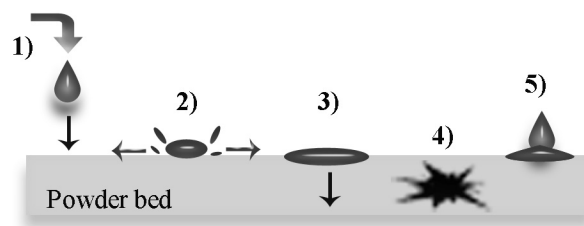


Figure 5: The five possible steps in nucleation.

1) Droplet formation at the spray nozzle. 2) Droplet impact on the powder bed surface, wetting and possible breakage of the droplet. 3) Droplet penetration into the powder bed pores). 4) Mixing of the liquid and powder by agitation forming a nucleus. 5) Possible droplet coalescence at the powder bed surface (Based on Hapgood et al., 2002).

The area of the bed where the liquid binder and powder surface first come into contact is called the spray zone⁶. Two processes are important in the spray zone. Firstly, there is the nuclei formation, which is a function of wetting thermodynamics and kinetics. Secondly, there is the mixing of the powder and binder referred to as “binder dispersion”. This latter phenomenon is a function of mainly process variables whereas nuclei formation primarily is a function of the formulation properties (Iveson et al., 2001a). These two processes are the subjects of the following sections.

2.2.1 Nucleation thermodynamics

Whether or not the binder wetting on the powder surface is energetically favourable is determined by thermodynamics. Especially two aspects have been found to have major importance. Firstly, the contact angle between the solid particle and the liquid binder and secondly, the spreading coefficient of the liquid phase over the solid phase (Iveson et al., 2001a). Both terms will be introduced in the following sections. Sufficient surface wetting as well as spreading is necessary, since a non-wetting/spreading binder liquid will either not adhere to the powder particles or only be present on or cover a very small area, thereby restricting nuclei formation (Tardos et al., 1997).

When a drop of liquid is placed in contact with a solid, three interfaces are present: The solid/liquid γ_{sl} , the solid/vapour γ_{sv} and the liquid/vapour interface γ_{lv} . Each of these interfaces has their own interfacial energy⁷. The situation can be seen in figure 6. For a droplet that partially wets a solid, as it is the case with the liquid binder impacting of the powder bed, the total interfacial energy is minimal when the horizontal components of the interfacial tensions are in equilibrium. This situation can be described by the Young equation (Kontogeorgis, 2004), where θ is the contact angle⁸ in degrees:

$$\gamma_{sv} = \gamma_{sl} + \gamma_{lv} \cdot \cos \Theta \Leftrightarrow \gamma_{sv} - \gamma_{sl} = \gamma_{lv} \cdot \cos \Theta \quad (2.1)$$

With us you can
shape the future.
Every single day.

For more information go to:
www.eon-career.com

Your energy shapes the future.

e-on



The work of adhesion⁹ for a solid/liquid interface is given by the Dupré equation (Kontogeorgis, 2004):

$$W_A = \gamma_{lv} + \gamma_{sv} - \gamma_{sl} \quad (2.2)$$

Combining the Young and the Dupré equation gives:

$$W_A = \gamma_{lv} (1 + \cos \Theta) \quad (2.3)$$

Thus by the combination, a relation between the work of adhesion and the contact angle is achieved. It is thereby obvious that if the contact angle is large (a large contact angle indicates poor wetting) the work of adhesion is small. With a low value of W_A the nuclei are expected to be small and fragile resulting in weak and friable final granules. Indeed several authors report a direct connection between the solid-liquid contact angle and the characteristics of the final granulate product. It was e.g. proved experimentally that as the contact angle of the powder-liquid mixture increases the mean granule size and strength decreases (Teipel & Mikonsaari, 2004 and Iveson et al., 2001a).

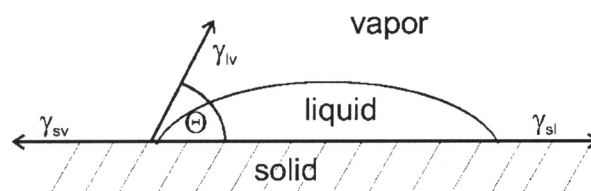


Figure 6: Droplet-solid-vapour interface.

The three interfaces present when a drop of liquid is in contact with a solid (Teipel & Mikonsaari, 2004).

The spreading coefficient λ is a measure of the tendency of a liquid and a solid combination to spread over each other. Spreading coefficients indicate whether spreading is thermodynamically favourable or not. It is related to the works of adhesion and cohesion¹⁰ being the difference between them. There are three possibilities in spreading between a powder and a liquid. Firstly, the liquid may spread over the powder particles and create a surface film (λ_{ls}) or secondly, the powder particles may spread or adhere to the liquid but no film formation occurs (λ_{sl}). The third possibility is that both the liquid and powder have high works of cohesion. The solid-liquid interfacial area will then be minimised or nonexistent (Iveson et al., 2001a). It is only the two first possibilities, which is interesting concerning nucleation. The λ_{ls} and λ_{sl} is given by the difference between the work of adhesion and the work of cohesion for a liquid and a solid respectively (York & Rowe, 1994):

$$\begin{aligned} \lambda_{ls} &= W_A - W_{CL} \\ \lambda_{sl} &= W_A - W_{CS} \end{aligned} \quad (2.4)$$

Spreading will occur spontaneously when the spreading coefficient is positive. When λ_{ls} is positive the binder will spread and form a film over the powder surface, and liquid bridges will form between most contacting powder particles creating a strong dense nucleus. When λ_{sl} is positive bonds will form only where the liquid and powder initially touch, because the liquid will not spread or form a film. Granules formed in this case have fewer bonds and consequently will be weaker and more porous (Iveson et al., 2001a). Several investigations confirm that differences in granule properties can be correlated with the spreading coefficient (Rowe, 1989 and Zajic & Buckton, 1990).

2.2.2 Nucleus formation kinetics

In practice the liquid-solid-vapour interface may not have sufficient time to reach its equilibrium state due to the interference from the agitation forces and drying occurring simultaneously in the fluid bed. Besides thermodynamics and wetting, the nuclei formation is hence also a function of kinetics. First of all the relative size of the droplets to primary powder particles will influence the nucleation mechanism. Nucleation with relatively small droplets compared to the powder bed particles will occur by distribution of the droplets on the surface of the particles, which then afterwards may start to coalesce. It will often lead to nuclei with air trapped inside (Iveson et al., 2001a). The principle can be seen in figure 7 a). This idea of distributing a liquid onto each particle is used intensively in the coating process, where the idea in that case is to avoid the subsequent coalescence from taking place, but to ensure at the same time that each granule is coated efficiently. The coating process is described in detail in later sections.

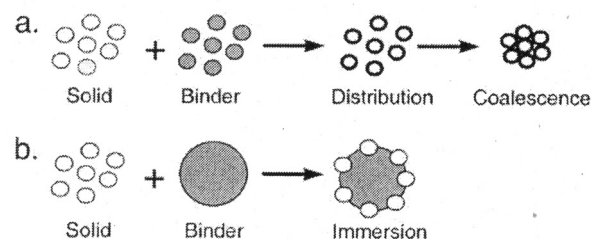


Figure 7: The dependence of the nucleation formation mechanism on the relative size of the droplets to powder particle sizes.

a) Distribution mechanism. b) Immersion mechanism (Iveson et al., 2001a).

If the droplet is large compared to the powder particles, nucleation will occur by immersion of the smaller particle into the larger droplet. The principle can be seen in figure 7 b). This produces nuclei with saturated pores. Once a large droplet of liquid binder impacts the powder bed, it penetrates into the pores of the powder bed surface to form a highly saturated initial agglomerate as indicated in figure 8. The immersion case is hence the most wanted situation in wet agglomeration (Iveson et al., 2001a).

Liquid penetration into the pores between the powder particles is driven by surface tension, contact angle and pore radius. The liquid will advance into the powder bed by flowing down successively smaller pores (Hapgood et al., 2002). Prior to depletion of the liquid, the liquid droplet has spread onto the bed surface. Denesuk et al. (1994) have showed that the spreading time τ_s is far smaller than the time of droplet penetration¹¹ τ_d indicating that as the liquid droplet contacts the bed surface, it will immediately spread to a semi-static¹² configuration followed by a slower depletion process. Each of the time constants is viscosity dependent but the ratio τ_s/τ_d has been proven not to depend on viscosity (Denesuk et al., 1994). The time it will take for a liquid droplet of binder to spread, penetrate and saturate the pores of the powder bed, and thereby prepare the initial nucleus for growth, is thereby in practice solely dependent on the droplet penetration time (Schaafsma et al., 1998).

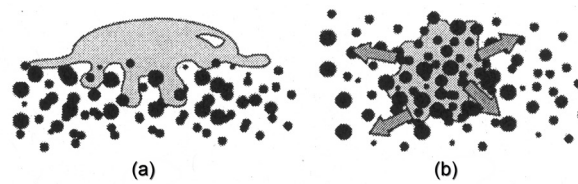


Figure 8: Single droplet nucleation.

a) Initial nucleus formation due to imbibition of the droplet into the powder bed.

b) Liquid migration within the powder bed causing dense nucleus growth (Iveson et al., 2001a).

© 2013 Accenture. All rights reserved.

be > your degree

Bring your talent and passion to a global organization at the forefront of business, technology and innovation. Discover how great you can be.

Visit accenture.com/bookboon

Be greater than.
consulting | technology | outsourcing

accenture
High performance. Delivered.

No models have yet been developed for the absorption of droplets into agitated porous powder beds but a theory exists for the penetration of a single droplet into a porous surface. A first approach for the description of a theoretical droplet penetration time τ_d was suggested by Denesuk et al. (1993 & 1994)¹³:

$$\tau_d = \frac{2V_d^2}{\pi^2 \varepsilon_{pmsp}^2 r_d^4 R_{pore}} \frac{\eta_{liq}}{\gamma_{lv} \cdot \cos \Theta} \quad (2.5)$$

where V_d is the total droplet volume, r_d the radius of the droplet, ε_{pmsp} is the porous media surface porosity, γ_{lv} is the liquid surface tension, η_{liq} is the liquid viscosity, θ is the solid-liquid contact angle and R_{pore} is the effective pore radius based on the assumption of cylindrical parallel capillary pores in the porous structure given by Kozeny approach:

$$R_{pore} = \frac{2 \cdot \varepsilon_{pmsp}}{(1 - \varepsilon_{pmsp}) \cdot s_0 \rho_p} \quad (2.6)$$

where s_0 is the particle specific surface area expressed in m^2/kg and ρ_p is the particle density (Denesuk et al., 1993).

Hapgood et al. (2002) have showed that the Kozeny approach is only valid in a well-packed powder bed with homogeneous bed structures and narrow pore size distributions. Powders in fluid beds are however agitated in motion and extremely loosely packed. Loosely packed powder beds tend to have a heterogeneous bed structure containing irregular pore structure and macrovoids between the powder particles, which will affect the flow of depletion. Taking this into account, the Denesuk approach was extended with new expressions for the R_{pore} and ε_{pmsp} and the expression of the theoretical droplet penetration time τ_d then became¹⁴ (Hapgood et al., 2002):

$$\tau_d = 1.36 \frac{V_d^{2/3}}{\varepsilon_{eff}^2 R_{eff}} \frac{\eta_{liq}}{\gamma_{lv} \cdot \cos \Theta} \quad (2.7)$$

where V_d is the total droplet volume, γ_{lv} is the liquid surface tension, η_{liq} is the liquid binder viscosity, θ is the solid-liquid contact angle and R_{eff} is an efficient bed pore radius given as:

$$R_{eff} = \frac{\phi \cdot d_{32}}{3} \frac{\varepsilon_{eff}}{(1 - \varepsilon_{eff})} \quad (2.8)$$

This equation is based on the assumption that the powder particles are approximately spherical. Application to real non-spherical particles is made through multiplication with the sphericity ϕ accounting for non-spherical particle shape and d_{32} which is the specific mean powder particles diameter defined as the diameter of a sphere with the same surface to volume ratio as the irregular particle (Hapgood et al., 2002). Hence the combination of d_{32} and ϕ can be seen as an analogy to the inverse of the product of s_0 and ρ_{pore} in equation 4.6. The effective porosity ε_{eff} can be found as (Hapgood et al., 2002):

$$\begin{aligned} \varepsilon_{eff} &= \varepsilon_{tap} (1 - \varepsilon_{lpp} + \varepsilon_{tap}) \\ \varepsilon_{tap} &= \varepsilon_{lpp} - \varepsilon_{macrovoid} \end{aligned} \quad (2.9)$$

where ε_{lpp} is the loose packed porosity of the bed and $\varepsilon_{macrovoid}$ is the fraction of macrovoids in the bed.

Based on the Hapgood model the penetration time is directly proportional to the viscosity and inversely proportional to the surface tension. In accordance with these predictions it was proven through numerous experiments that this was indeed the case. The droplet penetration time dependence on the droplet volume in the power of $\frac{2}{3}$ was proved to be quite accurate (Hapgood et al., 2002 and Litster, 2003).

In characterizing and determining the wetting behaviour of a liquid onto the powder bed the droplet penetration time is a widely used parameter in that it contains both a thermodynamic and kinetic dependence. The wetting thermodynamics dependence is represented by $(\gamma_{lv} \cdot \cos \theta)$ and the wetting kinetics by the viscosity η_{liq} and the effective pore radius R_{eff} .

2.2.3 Binder dispersion

The degree of binder dispersion indicates the quality of the mixing between the powder and the binder fluid, and it is strongly affected by the binder delivery method. Hence the binder dispersion is a matter of process properties and especially four operating variables are important and will be presented below: droplet size distribution, binder spray rate, the size and position of the spray zone and last, the size of the powder flux (Iveson et al., 2001a).

A narrow and well-defined spray droplet size distribution results in a controlled final granule size distribution, as the size and distribution of the binder droplets determines the nuclei size distribution (Tardos et al., 1997). Especially in fluid bed granulators¹⁵ a strong correlation between the droplet size and nuclei size distribution have been found according to the relation between the nucleus diameter¹⁶ d_n and the liquid binder droplet diameter d_d :

$$d_n \propto (d_d)^k \quad (2.10)$$

in which k is a correlation coefficient ranging between 0.80 and 0.89 depending on the type of powder particles and binder solution (Waldie, 1991). In addition Schaafsma et al. (1998 & 2000a) have found that there is an approximately linearly relationship between the final mass of a granule and the mass of binder liquid sprayed:

$$m_g = J \cdot m_b \quad (2.11)$$

where m_g is the mass of the granule and m_b the mass of the liquid binder sprayed. J is a proportionally constant called the “nucleation ratio”, which depends on material properties such as powder particle size distribution and the wettability of the liquid-powder interface. The better the binder liquid binds particles, which is reflected in a high nucleation ratio J , the less amount of liquid has to be used to granulate the same amount of material. This saves process time as well as money (Schaafsma et al., 2000a).

One of the most widely studied variables affecting the binder distribution is the volumetric binder spray rate \dot{V} . In fluid bed experiments the rate of nucleation increases as the binder spray rate increases. There is a general agreement among different authors that an increase in spray rate causes an increase in the final mean granule size, although the direct effect of the binder solution spray rate is difficult to determine separately (Schaafsma et al., 1999, Litster, 2003 and Liu et al., 2000). This is due to the fact that a change in spray rate usually is accompanied by a change in droplet size distribution. The droplet size may increase or decrease as the flow rate is increased depending on the type of nozzle used (Iveson et al., 2001a). Schaafsma et al. (1999) have showed in agreement with Heinrich & Mörl (1999) that spraying the binder in short pulses instead of continuous spraying leads to narrower final granule size distributions. The rate of nucleation or granule growth rate doesn't seem to be affected by this.

The location and shape¹⁷ of the spray zone is governed by the nozzle position and spray angle. Large spray angles and high nozzle positions in respect to the bed both increases the area of the bed exposed to the binder spray and increases the premature drying of binder liquid droplet before impact. This reduces the likelihood of binder droplets coalescing and reduces the sizes of the nuclei produced. There is no general agreement of how large the effect of changing the nozzle height is on the final average granule size, but some authors claim that by raising the nozzle position the average granule size is only slightly decreased (Iveson et al., 2001a and Litster et al., 2001).



"I studied English for 16 years but...
...I finally learned to speak it in just six lessons"

Jane, Chinese architect

ENGLISH OUT THERE

Click to hear me talking before and after my unique course download

Efficient powder mixing is essential to binder dispersion in all types of granulators. High powder flux through the spray zone allows more uniform distribution of the powder and the binder fluid by carrying local patches of high binder contents away and providing a constant supply of fresh powder into the spray zone. An increased powder flux through the spray zone reduces the final granule size, as there is less time and less binder volume available for nuclei formation per unit powder. Schaafsma et al. (1999 & 2000a) found that the surface mixing resulting from the powder flux was the primary determining factor to avoid overwetting of the powder resulting in a bed collapse.

Litster et al. (2001) have combined the volumetric binder spray rate with the powder flux into an equipment independent parameter called the “dimensionless spray flux”¹⁸ ψ_a :

$$\Psi_a = \frac{3 \cdot \dot{V}}{2 \cdot \dot{A} \cdot d_d} \quad (2.12)$$

where \dot{A} is the powder flux through the spray zone, \dot{V} the volumetric spray rate of spherical droplets produced by the nozzle and d_d is the liquid droplet diameter.

The dimensionless spray flux is a measure of binder coverage on the powder surface. A high value of ψ_a indicates that the binder solution is being added too quickly compared to the powder flux rate (Iveson et al., 2001a). Droplets will overlap each other on the powder surface causing droplet coalescence and a broad nuclei size distribution. A low value of ψ_a indicates on the other hand that the ratio of powder flux to binder spray rate is sufficiently high so that each liquid droplet lands separately and the nuclei are swept out of the spray zone before being rewet by another droplet. Size analysis and experiments shows that ψ_a is a parameter for the control of size and shape of the nuclei size distribution, besides being a parameter to be kept constant during equipment scaling (Litster, 2003 and Mort & Tardos, 1999). This will become more obvious with the introduction of the nucleation regime map.

2.2.4 Nucleation regime map

As described in previous sections, nucleation is a combination of single droplet behaviour (e.g. the liquid droplet penetration, contact angle, surface tension and other material properties) and multiple droplet interactions (e.g. the liquid spray flux, spray zone characteristics and other process variables). Depending on the powder and binder formulations and operating conditions, different nucleation mechanisms may dominate. Based on values of the liquid droplet penetration time τ_d , the dimensionless spray flux ψ_a and the particle circulation time¹⁹ τ_c , Litster et al. (2001) have proposed a nucleation regime map. The map is based on the postulation that three possible nucleation regimes exist: drop controlled, mechanical dispersion controlled and an intermediate regime. The nucleation regime map can be seen in figure 9.

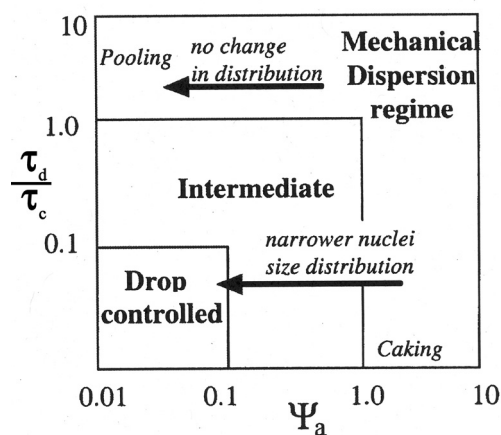


Figure 9: Nucleation regime map.

Three types of nucleation regimes have been proposed:

Droplet controlled, Intermediate and Mechanical Dispersion Regime (Litster, 2003).

In the drop controlled regime the controlling parameter is the liquid droplet size. The binder droplet penetrates into the powder bed pores almost immediately and the nuclei size distribution is reflected by the binder droplet size distribution. This is the desired region to be in. In this region one droplet tends to form one nucleus provided that two key conditions are met. The first condition is that the powder flux through the spray zone must be fast enough so that droplets, which hit the powder surface, do not overlap. This means that a low value of ψ_a is essential. Secondly the droplet must wet and penetrate into the bed completely before bed mixing brings it into contact with another partially absorbed droplet on the bed surface. This situation can be achieved having a small droplet penetration time. The borders of the drop-controlled zone have been proven by different authors (Litster, 2003 and Iveson et al., 2001a).

In the mechanical dispersion regime, nucleation and binder dispersion occurs by mechanical mixing and agitation. The binder solution delivery method and thereby the effect of droplet size distribution, nozzle height etc. on the nuclei properties is negligible. In the extreme cases either liquid droplet coalescence will happen, if the droplet penetration time is very large (and ψ_a is low), or caking of the powder bed will be the result, if the value of ψ_a is too high (and τ_d is low). In the mechanical dispersion regime often very broad nuclei size distributions are created, which is why it is undesired to operate in this regime. This type of regime is not typical to occur in fluid beds, although droplet pooling and caking can happen (Iveson et al., 2001a).

In the intermediate regime both droplet penetration dynamics and forces of dispersion are significant. Clumps of unevenly distributed binder will form if the binder flow rate exceeds the binder dispersion rate. This regime has proven to be the most difficult to control thereby being an unwanted regime to operate in (Iveson et al., 2001a).

The fact that the droplet penetration time is largely a function of formulation properties and that the dimensionless spray flux is largely a function of operating variables, makes the combination of these two parameters in a regime map a valuable and useful tool in the design of optimal nucleation and granule conditions. Based on the nucleation regime map it is possible to give reasonable predictions of the effect of changing formulation properties or operating conditions. This has proven useful in the design and scale-up or scale-down of granulation equipment (Litster, 2003).

2.3 Granule growth behavior

If wetting and nucleation is well controlled then the extent of nuclei consolidation and coalescence into granules will affect the final properties. As granules and nuclei collide with other granules/nuclei and equipment surfaces they gradually compacts. This reduces their size and porosity and squeezes liquid binder to the surface from the interior. This phenomenon is called consolidation (Iveson et al., 2001a). The low agitative forces in fluid beds are however only able to compact the granules to a confined level and the extent and importance of consolidation is limited. As an indication, the final granule porosities achieved in fluid bed granulation are often about twice the porosities²⁰ achieved in high shear mixers or mixer drums (Schaafsma et al., 2000a). A high porosity has an importance regarding mechanical strength²¹ but plays a minor role during coalescence. Hence the main focus regarding fluid bed granulation should be on coalescence rather than on consolidation phenomena (Schaafsma et al., 1998).



The advertisement features a grey background with a faint world map. In the top left is the Duke University logo: a blue square with 'DUKE' in white, and 'THE FUQUA SCHOOL OF BUSINESS' in white text below it. The text 'BUSINESS HAPPENS' is written in large, black, sans-serif capital letters. Below it is the URL 'www.fuqua.duke.edu/globalmba' in a smaller font, with 'globalmba' in blue. At the bottom left is an orange rectangular button with the text 'Learn More >' in white. On the right side is a circular collage of six diverse individuals' faces, arranged in a ring around a central grey circle containing the word 'HERE.' in bold black capital letters.



2.3.1 Granule coalescence

Granule growth behaviour depends in general on the availability of liquid at or near the granule surface and the deformability of the colliding granules. In fluid beds where the impact forces are relatively small, little permanent deformation occurs during granule collisions. Granules coalesce by viscous dissipation in the surface liquid before the granule core surfaces contact (Liu et al., 2000). As the two particles approach each other, first contact is made by the outer liquid binder layer. The liquid will subsequently be squeezed out from the space between the particles to the point where the two solid surfaces will touch. A solid rebound will occur based on the elasticity of the surface characterized by a coefficient of restitution²² e . The particles will start to move apart and liquid binder will be sucked into the interparticle gap up to the point where a liquid bridge will form. This bridge will either break due to further movement in the bed or solidify leading to permanent coalescence (Tardos et al., 1997). In the described principle, granule coalescence will occur only if there is a liquid layer present at the surface of the colliding particles. This growth principle continues until insufficient binder liquid is available at the surface to bind new particles (Schaafsma et al., 1998). The relative amount of binder liquid present at that stage is called the wetting saturation S_w and it depends on the contact angle of binder liquid and the pore structure of the granule (Tardos et al., 1997). The wetting saturation reflects the wettability of the particle and it is often approximated by the binder droplet volume divided by the pore volume of a particle, under the assumption that no drying occurs (Schaafsma et al., 2000a). Schaafsma et al. (2000a) have showed that S_w is inversely proportional to the nucleation ratio J and the mean granule porosity $\bar{\epsilon}_g$.

Ennis et al. (1991) have modelled the situation of coalescence in a fluid bed by considering the impact of two solid non-deformable spheres each of which is surrounded by a thin viscous binder layer. The situation can be seen in figure 10.

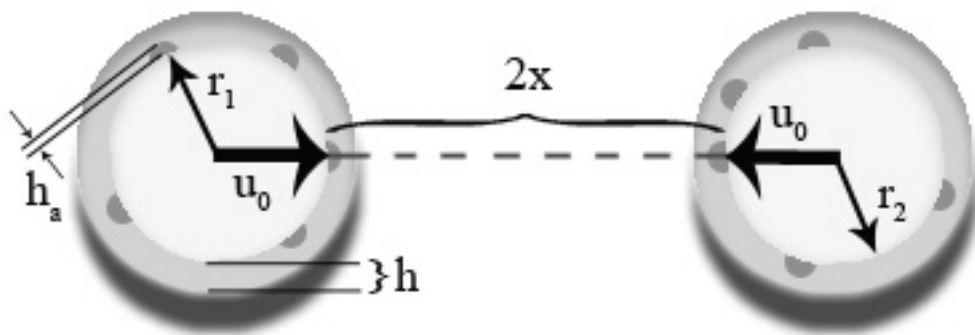


Figure 10: Schematic of two colliding granules.

Each granules is covered by a viscous binder layer of thickness h and the surface asperities have a height of h_a
(Based on Ennis et al., 1991).

The model assumes successful coalescence to occur if the kinetic energy of impact is entirely dissipated by viscous dissipation in the binder liquid layer and only elastic losses in the solid phase. The model predicts that collisions will result in coalescence when the viscous Stokes number (St_v) is less than a critical viscous Stokes number (St_v^*). The two numbers are given as (Ennis et al., 1991)²³:

$$St_v = \frac{8 \cdot \rho_g \cdot r_{\text{harm}} \cdot u_0}{9 \cdot \eta_{\text{liq}}} \quad (2.13)$$

and

$$St_v^* = \left(1 + \frac{1}{e}\right) \cdot \ln\left(\frac{h}{h_a}\right) \quad (2.14)$$

where η_{liq} is the liquid binder viscosity, e is the coefficient of restitution²⁴, ρ_g is the granule density, h is the thickness of the liquid surface, h_a is the characteristic height of the surface asperities and r_{harm} is the harmonic mean granule radius of the two spheres given as (Iveson et al., 2001a):

$$r_{\text{harm}} = \frac{2 \cdot r_1 r_2}{r_1 + r_2} \quad (2.15)$$

u_0 is the initial collision velocity which is not easily obtainable due to the various phenomena influencing the granule motion in fluid beds. A rough estimate based on the bubble rise velocity U_{br} has been presented by Ennis et al. (1991):

$$u_0 \approx \frac{12 U_{\text{br}} r_{\text{harm}}}{d_b \delta^2} \quad (2.16)$$

where d_b is the gas bubble diameter and δ the dimensionless bubble space defined as the axial fluid bed bubble spacing divided by the fluid bed gas bubble radius. Whereas the gas bubble diameter and spacing can be estimated by the dimensions of the air distributor plate or found by experiments, the bubble rise velocity is somewhat more difficult to determine. Davidson & Harrison (1963) have however proposed the following empirical relation for a fluid bed based on the bubble diameter d_b , gravity g , the minimum fluidisation velocity U_{mf} and the superficial velocity U_s measured on empty vessel basis:

$$U_{\text{br}} = U_s - U_{\text{mf}} + 0.711 \cdot (g \cdot d_b)^{1/2} \quad (2.17)$$

The Stokes viscous number St_v can be seen as the ratio of kinetic energy to the viscous dissipation. During fluid bed batch granulation St_v increases as the granules grow in size. This leads to three possible situations. The first so-called “non-inertial regime” occurs when $St_v \ll St_v^*$. All collisions result in successful coalescence regardless of the size of the colliding granules, granule kinetic energy or binder viscosity. As the granules grow larger the “inertial regime” occurs when $St_v \approx St_v^*$. The likelihood of coalescence now depends of the size of the colliding granules, and granule kinetic energy and binder viscosity begin to play a role (Iveson et al., 2001a and Abbott, 2002). It can be seen from equation 2.15 and 2.13 that the collision between two small or one small and one large granule is more likely to succeed in permanent coalescence than the collision between two large granules due to the size of r_{harm} and thereby the size of St_v versus St_v^* . This is a convenient way to understand why small particles agglomerate into larger ones (Tardos et al., 1997). Eventually the system enters the “coating regime” when $St_v \gg St_v^*$. Here all collisions between granules are unsuccessful and any further increase in the St_v will maintain the size of the granules (Iveson et al., 2001a and Tardos et al., 1997). The existence of the three regimes has been proved experimentally in different types of granulators (Ennis et al., 1991).

Granule growth is promoted by a low value of St_v and a high value of St_v^* . For instance, increasing the binder content will increase the binder layer thickness h which will increase St_v^* and hence increase the likelihood of successful coalescence. The effect of the binder viscosity is not easily predictable in that e.g increasing the value η_{liq} (lowering St_v) alters the coefficient of restitution e decreasing St_v^* as well (Iveson et al., 2001a). Although the model is limited by its many assumptions²⁵ it gives a rough number for the indication of the limit between no-agglomeration and successful agglomeration.

Tardos et al. (1997) have related the St_v to the degree of consolidation α_{cons} defined as the distance Δx at which two coalesced particles get closer by consolidation divided by the initial distance equal to the binder layer thickness $2h$. Hence for a given binder layer thickness h on each particle, the higher the Δx the higher the degree of consolidation. The relation is given by:

$$\alpha_{\text{cons}} = \frac{\Delta x}{2h} = 1 - \exp(-St_v) \quad (2.18)$$

From equation 2.18 and the expression for the St_v in equation 2.13, it is obvious that if the collision velocity u_0 is relative small (as it is the case in the low agitative fluid beds) the St_v will be small leading to $\alpha_{\text{cons}} \approx 0$. Hence through the introduction of the St_v number it is possible to give a mathematical justification for not giving much attention to the consolidation phenomenon in fluid beds.

2.3.2 Effects of different process and formulation parameters on granule growth behaviour

Although the St_v and the St_v^* are important parameters in the prediction of coalescence they are only valid for predicting the maximum size of granules which can coalesce. The parameters state nothing about the rate of granule growth. Different authors have showed however, that fast growth rates are attributed to the non-inertial regime while a slower growth is attributed to values of St_v close to or above St_v^* (Ennis et al. 1991 and Cryer, 1999). Schaafsma et al. (1998) have proved that in fluid beds the coalescence of granules is a much slower process than the initial formation of nuclei. Concerning rates of the whole granulation process, the rate of the growth stage is thereby often considered rate limiting.

Experiments by Ennis et al. (1991) have indicated that the rate of granule growth is not affected by increase in binder viscosity when operating in the non-inertial regime. The granule porosity is however increased by increasing the viscosity. Keningley et al. (1997) found in addition that a large viscosity inhibits initial growth but aids granule growth on a longer time scale, and that increased binder viscosity leads to increased granule strength even though porosity is high and pore saturation low. Further Keningley et al. (1997) found that application of low viscosity binders results in lower granule porosities as well as a faster overall growth rate. Experiments conducted by Schaafsma et al. (1998) showed that the physical shape of granules depends on the viscosity of the liquid binder. As the viscosity decreases, an increase in the deformation of the final granule shape occurs. Decreasing the viscosity leads to agglomerates, which are more susceptible to forces in the fluid bed. The final granule were found to be oval instead of spherical when a low viscous binder was used.

Join American online LIGS University!

Interactive Online programs
BBA, MBA, MSc, DBA and PhD

Special Christmas offer:

- ▶ enroll **by December 18th, 2014**
- ▶ **start studying and paying only in 2015**
- ▶ **save up to \$ 1,200** on the tuition!
- ▶ Interactive Online education
- ▶ visit ligsuniversity.com to find out more!

Note: LIGS University is not accredited by any nationally recognized accrediting agency listed by the US Secretary of Education. More info [here](#).



Rambali et al. (2001) have showed that the chance of coalescence is correlated with the moisture contents in the fluid bed. Relative high moisture contents give large granules whereas low moisture contents result in small size granules. This is due to the fact that high moisture contents will keep the binder liquid on the granule surfaces wet for a longer time thus increasing the chance of successful coalescence. This is in agreement with results found by other authors (Schaafsma et al., 1999, Iveson et al., 2001a and Faure et al., 2001) although results found by Cryer (1999) indicates that the correlation between granule size and moisture contents is far from linear and more likely consists of three domains. Schaafsma et al. (1999) have showed that increasing the relative bed humidity (rH) leads to increased deviations and scattering in the final granule size distribution. In addition they showed that rH has a high influence on the mixing behaviour in fluid beds and that above a certain critical value ranging from 45 to 60 rH% the minimum fluidisation velocity U_{mf} increases, resulting in a decreased mixing. Increasing the rH beyond the critical value will eventually lead to collapse of the bed because the bed material becomes so cohesive that fluidisation becomes impossible.

Schaafsma et al. (1999) found a distinct effect of the inlet temperature of the fluidising air on the granule growth. At lower inlet temperature of 40 °C the granules grew faster than at 60 °C due to lower drying rate at lower temperature, although the overall productivity decreased at the low temperature due to a longer drying period. In accordance with this, Härkönen et al. (1993) showed that the final granule size increases with decreasing temperature in the fluid bed, having a constant processing time. It was showed in addition, that the decrease in mean particle size at higher temperatures could be compensated by increasing the spray rate of the binder solution without overwetting the bed.

The fluidisation velocity has a complex effect on granulation growth behaviour because it alters both the frequency and energy of collisions between granules. Hence it can directly affect both the kinetics and the extent and mechanism of growth. Iveson et al. (2001a) report that increasing the excess gas velocity U_c in a top spray fluid bed leads to a decrease in the final granule size. This in agreement with what other authors report (Schaafsma et al., 1999 & 2000b) but the effect cannot be separated from the breakage and attrition phenomena which most likely also increases with increasing gas velocity, thus helping to decrease the final granule size (Watano et al., 1995).

2.4 Breakage and attrition

In the last step of the granulation process the granules grow too large to resist the agitative motions in the bed. Coalescence will be counteracted by either an attrition of debris of the granule surface or fracture of the granule either partly or totally. This is due to insufficient binder distribution or simply due to drying of the granules (Iveson et al., 2001a). A total fracture of wet or dry granules is seldom a problem in fluid bed granulation however. The low shear properties in the bed rarely give sufficient kinetic energy to fracture the granules completely (Waldie, 1991 and Schaafsma, 2000b).

Another more interesting destructive mechanism is the attrition and fracture chipping of dry granules. These phenomena lead to the generation of dusty fines. As the aim of granulation processes is to hinder dust, the attrition process is a situation to be avoided (Iveson et al., 2001a). There is limited fundamental work on fracture and attrition of wet and dry granules in fluid beds, but most of the basic theory regarding mechanical strength and breakage mechanisms is similar to breakage of the coating layer and will be discussed in combination with this in coming sections.

2.5 Simulation of the agglomeration process – a brief review on population balance theory

As an alternative to the agglomeration models generated by experimental work, the use of population balance (PB) models has received considerable attention during the last ten to fifteen years (Faure et al., 2001). A PB follows the change in granule size distribution from the birth of nuclei over granule coalescence until the granules leave the control volume, and a PB on particles can include kinetic expressions for each of the mechanisms responsible for changing the particle size (Cryer, 1999). The PB focuses only on the particle size distribution of the granules and fundamentally the entire size distribution is divided in small intervals. As the model follows the evolution of the granule growth, the model can compute how many granules that exist in each size interval at a given time. At the core of the problem with PB lies the estimation of the probability of coalescence when a granule or nucleus from interval i collide with a granule or nucleus from interval j . This probability of coalescence has been represented by a parameter β referred to as the coalescence kernel (Faure et al., 2001). The choice of kernel can dramatically affect the rate of coalescence and it is typically a function of time and the volume of the colliding particles. Much work has been done to optimise the kernel and more than ten different suggestions for an expression of β exist today (Cryer, 1999 and Liu & Litster, 2002 & 2004). There is no a priori justification of which kernels are appropriate for the given granulation system and a physical interpretation of the coalescence kernel is still missing (Faure et al., 2001 and Cryer, 1999).

Hounslow et al. (1988) proposed one of the first population balance equations used for granulation based on geometrical scaled size intervals in which the volume of the particles in the next size class is twice the volume of the particles in the current interval. The Hounslow population balance is given by (Hounslow et al, 1988):

$$\frac{dN_i}{dt} = \sum_{j=1}^{i-2} 2^{j-i+1} \beta_{i-1,j} N_j N_{i-1} + \frac{1}{2} \beta_{i-1,i-1} N_{i-1}^2 - \sum_{j=1}^{i-1} 2^{j-i} \beta_{i,j} N_j N_i - \sum_{j=1}^{\infty} \beta_{i,j} N_j N_i \quad (2.19)$$

where N_j represents the number of particles of size class j , dN_i/dt is the change of the number of particles of size class i as a function of time and $\beta_{i,j}$ is the coalescence kernel for two different discretised volume intervals. Newer more advanced models expand the discretisation. E.g. have Litster et al. (1995) made an improved discretisation by²⁶:

$$\frac{V_{i+1}}{V_i} = 2^{1/q} \quad , \quad q \in \mathbb{N} \quad (2.20)$$

This expands the original Hounslow model to (Litster et al., 1995):

$$\begin{aligned}
 \frac{dN_i}{dt} = & \sum_{j=1}^{i-S(q)-1} \beta_{i-1,j} N_j N_{i-1} \left\{ \frac{2^{(j-i+1)/q}}{2^{1/q} - 1} \right\} + \sum_{k=2}^q \sum_{j=i-S(q-k+1)-k}^{i-S(q-k+1)-k} \beta_{i-k,j} N_{i-k} N_j \cdot \\
 & \left\{ \frac{2^{(j-i+1)/q} - 1 + 2^{-(k-1)/q}}{2^{1/q} - 1} \right\} + \frac{1}{2} \beta_{i-q,i-q} N_{i-q}^2 \\
 & + \sum_{k=2}^q \sum_{j=i-S(q-k+2)-k+2}^{i-S(q-k+1)-k+1} \beta_{i-k+1,j} N_{i-k+1} N_j \left\{ \frac{-2^{(j-i)/q} + 2^{1/q} - 2^{-(k-1)/q}}{2^{1/q} - 1} \right\} \\
 & - \sum_{j=1}^{i-S(q)} \beta_{i,j} N_i N_j \left\{ \frac{2^{(j-1)/q}}{2^{1/q} - 1} \right\} - \sum_{j=i-S(q)+1}^{\infty} \beta_{i,j} N_i N_j
 \end{aligned} \tag{2.21}$$

where $S(q)$ is a summation function defined as (Litster et al., 1995):

$$S(q) = \sum_{p=1}^q p \tag{2.22}$$

At the moment the PB models are used more as a learning tool to understand processes and mechanisms rather than being a final unambiguous optimisation tool. The models are often extremely complex and require several assumptions to be made for simplification and solving. These assumptions are often made on the probability of coalescence with time and they are usually compared with experimental data, thereby confirming the validity of the models or highlighting which assumptions are valid or not. The use of PB looks promising for granulation process control but the use of PB as a tool for scale-up purposes or for the description of the breakage mechanisms has not been proven useful yet (Faure et al., 2001).

2.6 Summing up on wet agglomeration – Qualitative guidelines for parameters influencing agglomeration

Now that the basic principles of wet agglomeration have been presented it would be convenient to sum up all the important formulation and process tendencies extracted from the previous sections in one place. Some of the most important formulation and process parameters and their effect and influence on agglomeration are stated in table 2. It should be noted that the majority of the parameters are interlinked meaning that a change in one parameter may cause a change in one or several others. Many of the interactions and correlations between the different parameters are either not tested or still not fully understood. The tendencies stated in the table should thereby function only as a rough qualitative guideline for the design and optimisation of the granulation process.

	Adjustable parameter	Qualitative prediction of the effect caused by change
Formulation parameters	Binder viscosity (η_{liq})	The influence of viscosity is complex. A high η_{liq} seems to inhibit initial agglomeration but aid the long-term agglomeration tendency, increase strength but also increase porosity and decrease the growth rate. A low η_{liq} will lead to a low droplet penetration time and low porosity, high pore and wetting saturation and increased overall agglomeration rate but also to increased deformation (Keningley et al., 1997 and Schaafsma et al., 1998). Besides having influence on St_v , growth rate and extent of consolidation etc., the influence of viscosity is complicated by the fact that binder viscosity changes during drying (Abbott, 2002).
	Binder and powder surface tension (γ)	To ensure adequate wetting, the surface tension of the liquid binder must be lower than the surface tension of the powder (Kontogeorgis, 2004). Granule strength however decreases as binder liquid surface tension is lowered (Abbott, 2002).
	Binder droplet penetration time (τ_d)	A low τ_d is essential to ensure drop controlled nucleation and thereby a narrow final granule size distribution (Litster et al., 2001 and Iveson et al., 2001a).
	Size of the initial powder particles	Agglomerate strength is inversely proportional to powder particle size. The initial powder particles should be at least ten times smaller than the size of the desired granules in order to ensure appropriate final granule density and strength (Abbott, 2002).
	Powder – liquid contact angle (θ)	The contact angle θ between binder and powder particles should be as small as possible to ensure adequate wetting (Kontogeorgis, 2004 and Teipel & Mikonsaari, 2004). Granule strength decreases as the contact angle increases (Iveson et al., 2001a).
	Spreading coefficient (λ)	Having λ_s as large as possible while at the same time λ_{sl} is negligible will ensure that the binder liquid is spread properly and that a liquid film is formed on each powder particle surface. This will maximise the chance of coalescence (Iveson et al., 2001a).

Process parameters	Volumetric binder spray rate (\dot{V})	Increasing the spray rate will increase the chance of agglomeration but a change in spray rate is usually accompanied by an ambiguous change in droplet size distribution (Schaafsma et al., 1999 and Liu et al., 2000).
	Binder droplet size distribution	A uniform droplet size distribution is a prerequisite for a narrow final granule size distribution. To ensure that the nucleation occurs by immersion instead of distribution, the liquid droplets should be considerably larger than the initial powder particles (Waldie, 1991 and Iveson et al., 2001a).
	Binder droplet volume (V_d)	A small binder droplet volume V_d will help to lower the droplet penetration time τ_d but a too low V_d will lead to coating of the powder particles and result in fragile nuclei (Iveson et al., 2001a).
	Spray nozzle height	The effect of changing the nozzle position in vertical direction is ambiguous but there are indications that raising the nozzle height will decrease the chance of agglomeration resulting in smaller final granules (Iveson et al., 2001a and Litster et al., 2001).
	Powder flux (\dot{A})	A high powder flux through the spray zone will help to hinder binder droplet overlap and ensure a narrow nucleus/granule size distribution. The chance of agglomeration decreases with increasing powder flux (Iveson et al., 2001a and Litster, 2003).
	Fluidisation velocity (U)	The effect of the fluidisation velocity is complex because it influences both powder flux, drying rate and breakage phenomena. Tendencies indicate however that increasing the fluidisation velocity decreases the final granule size (Schaafsma et al., 1999 and Schaafsma, 2000b).
	Inlet temperature (T_{inlet})	A decreasing inlet temperature often leads to faster agglomeration and larger granules although a too low inlet temperature will lead to overwetting and bed collapse (Schaafsma et al., 1999 and Abbott, 2002).
	Fluid bed temperature (T_{bed})	Decreasing the bed temperature leads to increased agglomeration and thereby an increase in granule size. At high temperature the chance of agglomeration is low (Härkönen et al., 1993, Guignon et al., 2002 and Iveson et al., 2001a).
	Relative bed humidity (rH)	A high bed rH value increases the chance of agglomeration although increasing rH may also cause scattering in the final granule size distribution. Above a critical value the rH affects the fluidisation velocity (Watano et al., 1995 and Schaafsma et al., 1999).
	Dimensionless spray flux (ψ_a)	A low value of ψ_a is necessary to ensure that the powder flux \dot{A} is high enough to avoid binder droplet overlap on the powder bed surface. Having a value of ψ_a below 0.1 combined with a low droplet penetration time τ_d will ensure drop controlled nucleation (Litster, 2003).
	St_v versus St_v^*	The size of St_v versus St_v^* will determine the chance of coalescence. To ensure successful coalescence one should operate in the non-inertial regime having $St_v \ll St_v^*$ (Simons & Fairbrother, 2000 and Iveson et al., 2001a).

Table 2: Agglomeration summary.

Summary of some of the important formulation and process parameters and their influence on agglomeration.

3 Granule coating principles and properties in fluid beds

The initial step of the coating and agglomeration process is always the same: The successful collision between a liquid droplet and a particle. In analogy with wet agglomeration a liquid coating is sprayed onto the agitated particle bed during coating. Where it was the coalescence phenomenon, which was desired in the agglomeration process, much effort is put into the coating process to avoid coalescence (Link & Schlünder, 1997). In the coating process it is desired to let the surface of solid granules be covered completely by a solid layer (as indicated in figure 8 a.) and this is achieved by exposing the granule to many succeeding spraying-drying cycles. This shell- or onion-like structure will capsule the original granule more or less homogeneously depending on the choice of process and formulation parameters and the number of spraying-drying cycles (Guignon et al., 2003). Coating of solid granules may be considered as an active packaging located on the surface of the granules. For particles of 0.1 to 10 mm in diameter the coating layer is often only about 10 to 15 μm thick. Nevertheless the coating layer has several important purposes (Guignon et al., 2002).



ie business school

#1 EUROPEAN BUSINESS SCHOOL
FINANCIAL TIMES 2013

#gobeyond

MASTER IN MANAGEMENT

Because achieving your dreams is your greatest challenge. IE Business School's Master in Management taught in English, Spanish or bilingually, trains young high performance professionals at the beginning of their career through an innovative and stimulating program that will help them reach their full potential.

- Choose your area of specialization.
- Customize your master through the different options offered.
- Global Immersion Weeks in locations such as Rio de Janeiro, Shanghai or San Francisco.

Because you change, we change with you.

www.ie.edu/master-management | mim.admissions@ie.edu | [f](#) [t](#) [in](#) [YouTube](#) [v](#)

There are many advantages of granule coating. The coating layer can protect unstable ingredients in the granule from degradation factors such as heat, moisture, air and light. It can provide controlled or delayed release and reduce hygroscopicity. The coating layer also helps in changing the physical characteristics of the original material such as dust reduction, appearance and density modifications (Teunou & Poncelet, 2002). In addition the compressibility and mechanical strength of the granules can be improved through coating. Coating can also result in a more uniform particle size distribution and smoother granule surfaces, which improves handling, flowability and further processing (Guignon et al., 2003 and Kerkhof, 2000).

3.1 Parameters describing the coating process and result

There is a significant analogy between the coating phenomena and the phenomena existing in the wet agglomeration process, including wetting, adhesion, spreading, drying, chance of coalescence, attrition and more. A description of the coating system should ideally take all these aspects into account, which is difficult not just because of the number of simultaneous phenomena, but also due to the fact that many process and formulation parameters are interlinked and in addition change during the process. One way to describe the coating process is to find the thickness of the coated layer. Assuming spherical coated granules, Dewettinck (1997) and Dewettinck et al. (1999a) have found a relation to calculate the coating thickness ζ_c based on measurable parameters²⁷:

$$\zeta_c = \left[\left(\left(\frac{\rho_{\text{core}}}{\rho_{\text{cm}}} \right) \cdot \left(\frac{m_{\text{core}} + m_{\text{dep}}}{m_{\text{core}}} - 1 \right) + 1 \right)^{1/3} - 1 \right] \cdot \left(\frac{d_{\text{core}}}{2} \right) \quad (3.1)$$

where d_{core} is the diameter of the core granule (the uncoated granule), ρ_{core} the density of the core granule, ρ_{cm} the density of the coating material, m_{core} the mass of the core material and m_{dep} is the deposited mass of coating defined as (Teunou & Poncelet, 2002):

$$m_{\text{dep}} = m_{\text{core}} \frac{w}{1 - w} \quad (3.2)$$

where w is the coating contents of the coated granule in kg/kg. Experiments by Sudsakorn & Turton (2000) in a batch fluidised bed have showed that the amount of coating deposited on a granule m_{dep} is often proportional to d_{core} to the power of 3.1–3.6.

Often the coating performance is defined in simpler manner as the “coating efficiency” E_c defined as the mass of coating deposited divided by the mass of coating sprayed (Teunou & Poncelet, 2002):

$$E_c = \frac{m_{\text{dep}}}{m_{\text{cs}} \cdot Dm} \quad (3.3)$$

where m_{cs} is the mass of coating solution and Dm is the coating solution dry matter content in kg/kg.

As indicated in equation 3.3, E_c is a type of material efficiency expressing relations between masses. Other types of efficiencies²⁸ can be derived as well, but it is often the coating efficiency, which is interesting regarding the final granule properties. The coating efficiency E_c itself depends on many factors in and around the bed. Among the important factors are: Bed temperature, bed humidity, coating droplet size, coating spray rate, fluidisation velocity and the composition of the coating material (Maronga & Wnukowski, 1997a), each of which will be described in the next section.

3.2 Product, system and operating parameters affecting the coating process and efficiency

The temperature and humidity inside the fluid bed are the driving force behind the drying of the coating solution on the granule surface. When the temperature is too high there is little or no coating growth because of rapid surface drying and premature spray-drying of the coating solution before impact (Guignon et al., 2002). At too high humidity and/or low temperature on the other hand, the bed is likely to collapse due to wet quenching (Maronga & Wnukowski, 1998). It is often a basic assumption that all granules have the same temperature and moisture contents and that for all granules the coating and drying history is the same. This might be a reasonable overall assumption if the granule circulation time τ_c is low (Kerkhof, 2000). Results by Maronga & Wnukowski (1998) indicate however, that the temperature and humidity during the coating process in a top spray fluid bed varies significantly with radial and vertical position. During the coating process pockets of low temperature and high humidity are formed deep inside the bed, causing fluctuations in temperature of more than 10% on a °C scale. Based on these systematic fluctuations, the top spray fluid bed was formally divided into four zones, which can be seen in figure 11.

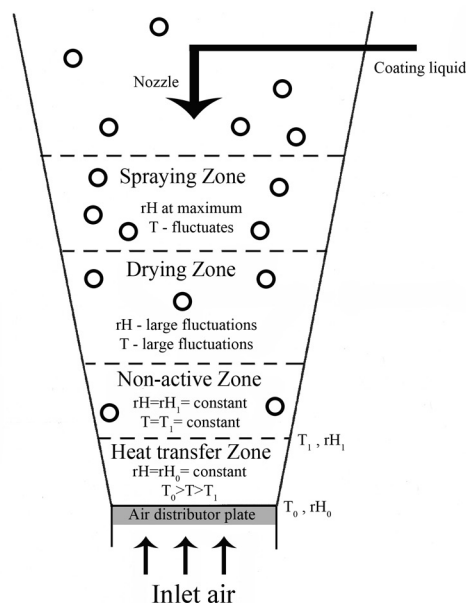


Figure 11: Zones in a top spray fluid bed during coating.

Basically four zones exist in a top-spray fluid bed during wet granulation being the spraying zone, Primary drying zone, the Non-active zone and the Heat transfer zone (Based on Maronga & Wnukowski, 1998).

As seen in figure 11, the highest humidity and the lowest temperature are situated closest to the bed surface in the spraying zone. The size and rate of transfer to this zone are important factors because granules are coated if and only if they visit this zone. Maronga & Wnukowski (1997b) report that the actual size of the spraying zone is only a few percent of the bed volume. Increasing the size of the spraying zone decreases the variance of the coating distribution (Maronga & Wnukowski, 1997b). The highest T and rH fluctuations are reached in the drying zone although zones of low temperature and high humidity not always are correlated or identical. In the heat transfer zone the conditions are that of the inlet air. Between the inlet heat transfer zone and the drying zone a non-active zone exists, where neither temperature nor humidity changes significantly (Maronga & Wnukowski, 1998). The minimisation of this zone may at first seem advantageous to the coating process in order to decrease the particle circulation time. Nevertheless the non-active zone acts as a safeguard against the chance of wet quenching the bed. Hence the fluid bed coating process has to be operated with a significant size of the non-active zone (Maronga & Wnukowski, 1997b).

Dewettinck et al. (1999a) proved that the size of the liquid coating droplet has an effect on the coating efficiency as well. A large droplet size results in less premature droplet evaporation before impact and therefore a higher coating efficiency E_c . This can also be understood through equation 3.2 and 3.3. As the coating content of the granule w increases in equation 3.2 with increasing droplet size, the coating efficiency E_c in equation 3.3 will increase as well. Larger droplets may however also increase the chance of agglomeration. Kleinbach & Riede (1995) suggest that small droplets with a narrow size distribution favour homogeneous final coating and Guignon et al. (2002) report that the droplet-granule size ratio must be at most 1 to 10.

The liquid spray rate increases with the air pressure through the nozzle. Experiments have showed that air pressure P_{nozzle} during coating should be between 0.5 and 3.5 bar depending on coating liquid viscosity, size of the particles being coated, distance from the nozzle to the bed etc. The higher the pressure the smaller the jet angle is, leading to small droplets and higher penetration depth into the bed. Above 3.5 bar the droplets become less than 10 μm and a too high extent of premature drying occurs (Dewettinck et al., 1999a and Guignon et al., 2002). Increasing the coating spray rate means a shorter wetting time but also a necessary longer drying time in order to avoid agglomeration (Guignon et al., 2002). Low viscosity is a necessity in order to facilitate proper pumping through the nozzle. The coating solution is often added at ambient temperature, but preheating may be used to decrease the viscosity further (Guignon et al., 2002).

The fluidisation air is used to ensure a homogenous partition of all granules and also to dry the coating solution sprayed onto the granules. The granule flow pattern will directly affect the amount of coating liquid a granule will receive (Abbott, 2002). Hence the fluidisation velocity is an important parameter in coating as well. Giugnon et al., (2002) report that in a top spray fluid bed, the fluidisation velocity should be significantly higher than the minimal fluidisation velocity U_{mf} in order for the coating growth rate to depend primarily on the coating spray rate and at the same time have negligible agglomeration. During the coating process by repeated wetting-drying cycles, the quantity of coating deposit is rather small leading to a variation in granule size and density of usually only a few percent. This does not affect the fluidisation in the same manner, as it is the case during agglomeration. Hence adapting and adjusting the fluidisation velocity during coating may not be as important as during agglomeration (Guignon et al., 2002).

The composition and properties of the coating material is vital not just for the mass based coating efficient but also for the quality of the final coating. The optimisation of the coating liquid is more of a fundamental chemical rather than a process challenge and several attempts have been made to find the right coating compositions with sufficient properties. A selection of additives such as surfactants, plasticisers, texturisers, emulsifiers, anti-adherent agents and stabilisers can indeed improve the coating properties and avoid unwanted agglomeration. Such additions will however often cause other problems such as decreased adhesion on the granules and/or reduced mechanical or leaching properties (Abbott, 2002).

SMS from your computer

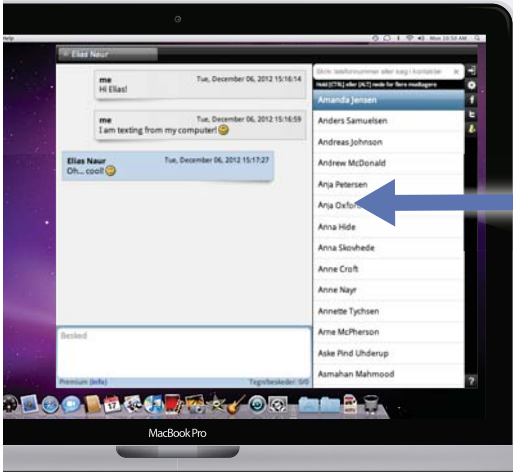
...Sync'd with your Android phone & number


FREE
30 days trial!

Go to

BrowserTexting.com

and start texting from
your computer!




BrowserTexting

In industrial scale it is often difficult to add new compounds. Compromises must be found between the composition of the coating solution, economics, process conditions and legislation. Hence it is often a limited amount of new additives, which in practice may be chosen from. Often the choice is to optimise on the already given coating solution. One idea is to simply change the solute concentration (Teunou & Poncelet, 2002). Guignon et al. (2002) report that the chance of adhesion of the coating layer to the core material increases with solute concentration and surface tension for a number of coating materials. Both are parameters that increase during coating droplet drying. The stronger the adhesion is, the more likely is the tendency of unwanted agglomeration however. In the pursuit of suppressing agglomeration tendency in coatings Nakano et al. (1999) have added small concentrations of widely used salts to an existing type of polymer coating HPMC (hydroxypropyl methyl cellulose). It was found that granule agglomeration was strongly suppressed by adding even small concentrations (0.01 M) of salt to the polymer coating liquid, and the tendency increased with increasing concentrations. The coating efficiency increased with increasing concentration as well (Nakano & Yuasa, 2001). The suppressing effect was suggested to result from a reduction in viscosity of the coating solution caused by a salting-out of the polymer coating. Especially potassium citrate and sodium citrate proved superior to other well-known and used salts as: Na_2SO_4 , NaCl , K_2SO_4 and CaSO_4 . Na_2SO_4 was the third best salt in full accordance with the ranking based on salting-out power of anions given in the Hofmeister series²⁹ (Nakano et al. 1999). The final coating including sodium/potassium citrate showed however decreasing mechanical strength with increasing salt concentration (Nakano & Yuasa, 2001).

3.3 Influence of product and formulation variables on coated granule morphology

Link & Schlünder (1997) have used SEM (Scanning Electron Microscopy) to study the coating process using different coating materials and drying-wetting conditions. First the same types of particles were coated under identical conditions with different coating solutions. Using a low viscous lactose or PVP solution led to the formation of uniform non-porous surfaces without holes. This indicated that after impact the coating droplets spread evenly over the granule surface and the dried coating remained attached to the granule as small patches. A layer was gradually developed as the wetting-drying cycle was repeated. The PVP coating layer however had fine cracks caused by shrinkage of the coated layer perhaps due to too fast drying-wetting cycles. If drying happens very fast, the coated layer dries first at the surface to form a shell-structure containing unvaporised coating solution inside. As the solvent inside the solid shell starts to evaporate, the volume inside the shell will decrease causing shrinkage and cracking in the surface shell-structure.

Using solutions of NaCl and Ca(OH)_2 with higher viscosity than PVP led to rough and raspberry-like structures. This indicated that after impact, capillary forces in the granule quickly dewatered the droplets. As a result the dewatered droplets stick on the surface almost unchanged in their original shape. The raspberry effect however decreased as the salt concentration decreased due to the decrease in viscosity and increase in drying time. This led to an increase in the merging of droplets before drying and a smoother surface. Guignon et al. (2002) report that the chance of a smooth and homogenous coating layer is improved if the granule surface before coating is smooth and with few pores, although adhesion of the coating liquid is improved by surface roughness. Examples of SEM pictures of smooth, raspberry-like and crackled coatings can be seen in figure 12.

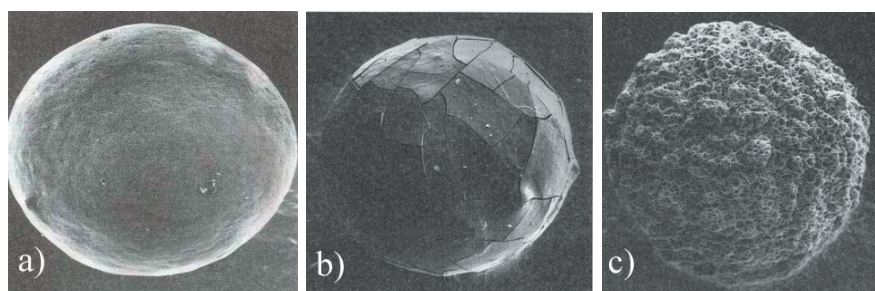


Figure 12: SEM pictures of coated single aluminium spheres having a diameter of about 1.3 mm.
a) Smooth coating by aqueous solution of lactose. b) Smooth coating with cracks by aqueous solution of PVP.
c) Raspberry structure by aqueous solution of NaCl (Link & Schlünder, 1997).

Next the liquid properties were kept constant and only the drying and wetting conditions were varied. The coating under high drying temperatures and long drying times led to highly porous surfaces with sharp-edged crystal structures, whereas coating under low temperatures and short drying cycles produced less porous surfaces with almost amorphous crystal structures. Reducing the droplet impact velocity to one half while keeping the drying-wetting cycle conditions constant led to an increase in raspberry structures. Further experiments with bed temperatures up to 120 °C and addition of surfactants to the coating solution created smooth and uniform coating layers with amorphous structures (Link & Schlünder, 1997). Whether or not the coating layer forms crystals is of great importance. Besides changing important properties as hygroscopicity and solubility, the mechanical properties of the coating layer is highly influenced by the extent of crystal formation. The formation of crystals will often lead to a stratified, porous and flaky coating layer with a high possibility of being degraded by attrition (Canselier, 1993). In later sections more on the mechanical properties and types of coating destruction mechanisms will be described in detail.

3.4 Agglomeration or Coating?? – Qualitative trends and attempts of finding a boundary parameter

As discussed in previous sections, agglomeration in fluid beds is caused by collisions between wetted surfaces establishing a liquid bridge that gradually solidifies. One way to hinder the chance of agglomeration is to ensure that the moisture contents of the granules is low (Guignon et al., 2003). The moisture contents of the fluidised granules depend on the wetting and drying conditions. Besides coating spray rate, fluidisation velocity and bed temperature, the circulation rate of the granules determines the moisture contents of the granules at the moment of collision. Rowe (1972) reports a simple equation³⁰ for the calculation of the average circulation time τ_c during fluidisation with moderate gas velocities:

$$\tau_c = \frac{h_{mf}}{0.6 \cdot (U_s - U_{mf}) \cdot [1 - (U_s - U_{mf})/U_{br}]}$$
 (3.4)

where h_{mf} is the bed height at minimum fluidisation velocity U_{mf} , U_s is the superficial gas velocity (measured on an empty vessel basis) through the bed and U_{br} the bubble rise velocity of gas bubbles in the bed. Usually τ_c should be only a few seconds to keep the moisture contents low and hence reduce the chance of agglomeration (Link & Schlünder, 1997). Abbott (2002) reports that the uniformity regarding size of coated granules is highly affected by the value of τ_c in a batch fluid bed. If the circulation time is too high, the number of time each granule will pass through the spray zone varies from granule to granule. This will lead to significant variations in coating levels and increase the chance of agglomeration even when the initial granule size distribution prior to coating was narrow. The tendency of agglomeration seems to increase drastically after a number of drying-wetting cycles indicating that agglomeration is negligible without a certain amount of coating layer (Teunou & Poncelet, 2002).

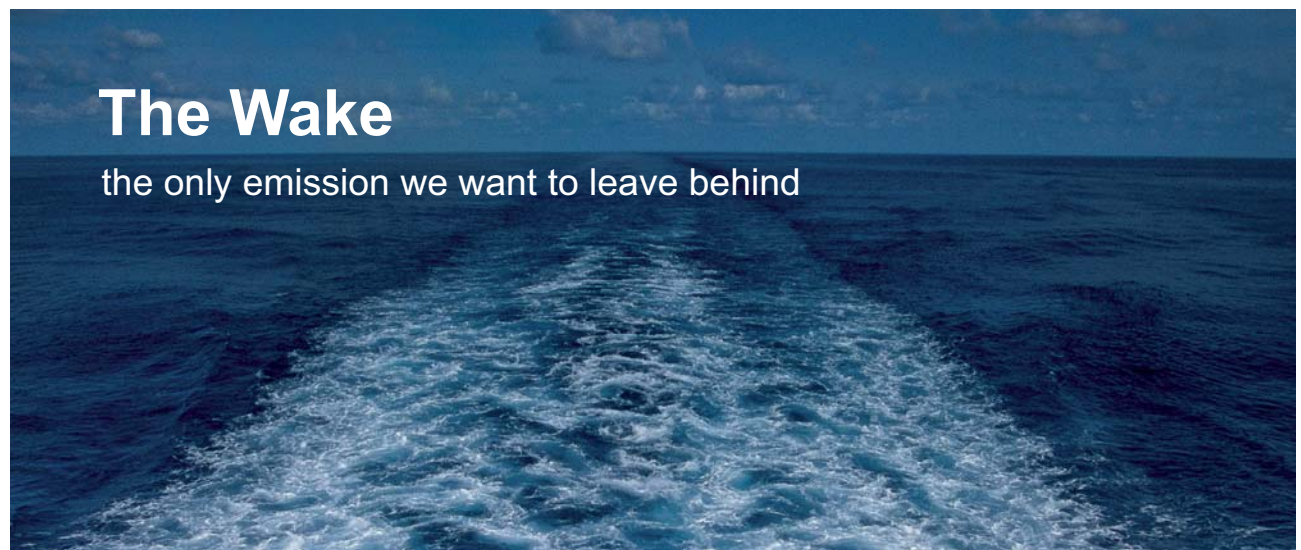
Dewettinck et al. (1999a) & Maa et al. (1996) report that unwanted agglomeration during coating primarily is influenced by the type of coating and its hygroscopicity, water binding capacity and viscosity. Link & Schlünder (1997) report in addition in agreement with Guignon et al. (2002) that the probability of agglomeration is correlated with viscosity. With increasing viscosity the adhesion-probability and hence the chance of coalescence is increased. This is somewhat in agreement with results found by Keningley et al. (1997) presented earlier.

Experiments by Maa et al. (1996) showed that the larger the coating chamber is, the less likely is the chance of agglomeration. In addition their results indicate that top spraying always causes higher degrees of agglomeration than with the Wurster coater. Further Maa et al. (1996) report that the higher the granule/droplet ratio, the lower is the extent of agglomeration. Agglomeration tendency was found to increase as the granule diameter decreased.

From experiments with a top spray fluid bed, Dewettinck et al. (1999a) found that the agglomeration was an all or nothing phenomenon meaning that for some conditions no agglomeration happened but at another condition severe agglomeration occurred accompanied by coverage of reactor walls and nozzle with agglomerated granules. The boundary was found to correlate with the evaporation efficiency E_{evap} given as:

$$E_{\text{evap}} = \frac{aH_{\text{outlet}} - aH_{\text{inlet}}}{aH_{\text{sat,bed}} - aH_{\text{inlet}}} \quad (3.5)$$

where aH_{inlet} is the inlet air absolute humidity, aH_{outlet} the outlet air absolute humidity and $aH_{\text{sat,bed}}$ the saturated air absolute humidity at the given bed temperature. One of the advantages of defining the coating-agglomeration boundary by E_{evap} is that the inlet humidity and bed temperature in some fluid beds quite easily can be changed step by step thereby accurately determining the agglomeration boundary value for E_{evap} . Typically values for E_{evap} where agglomeration occurs lies in the range of 0.3 to 0.6 depending on process and coating formulation conditions. E_{evap} is however only an empirical parameter, and it is still not possible to find the critical value for E_{evap} based on initial formulation or process parameters (Dewettinck et al., 1999a).



The Wake


the only emission we want to leave behind

[Low-speed Engines](#) [Medium-speed Engines](#) [Turbochargers](#) [Propellers](#) [Propulsion Packages](#) [PrimeServ](#)

The design of eco-friendly marine power and propulsion solutions is crucial for MAN Diesel & Turbo. Power competencies are offered with the world's largest engine programme – having outputs spanning from 450 to 87,220 kW per engine. Get up front! Find out more at www.mandieselturbo.com

Engineering the Future – since 1758.

MAN Diesel & Turbo




Click on the ad to read more

Other authors have defined the boundary between coating and agglomeration by means of a critical or maximum liquid spray flow rate \dot{m}_{\max} (Guignon et al., 2003). It indicates the maximum amount of coating liquid that can be sprayed on the bed pr. min without agglomeration. Guignon et al. (2003) have found that \dot{m}_{\max} is dependent on the granules as well as the chemical properties of the coating droplets such as surface tension, viscosity and drying characteristics. This dependency on numerous parameters makes the maximum liquid flow rate unsuitable for other things than comparing different coating solutions during experiments.

Based on statistical considerations, Litster (2003) has related the fraction of particles that agglomerate to the dimensionless spray flux by:

$$f_{\text{agglom}} = 1 - \exp(-4 \cdot \Psi_a) \quad (3.6)$$

Although first validations in high shear mixers seems promising, the formula has still not been validated in fluid bed experiments.

As mentioned earlier, the Stokes viscous number versus the critical stokes number can be used to distinguish between agglomeration and coating. The coating regime occurs when $St_v \gg St_v^*$. In this regime all collisions between granules are unsuccessful meaning that agglomeration is negligible (Simons & Fairbrother, 2000). The difficulties in determining the coefficient of restitution e and the collision velocity u_0 makes the viscous Stokes theory difficult to apply without experiments (Abbott, 2002).

All in all there is still no single parameter for the unambiguous determination of the boundary between agglomerating and coating based on simple process or formulation parameters. The need for empirical experimental work is thereby still extensive.

3.5 Qualitative description of key parameters governing the coating process – a first attempt to encircle an operating window

As indicated in previous sections, it is still not possible to state the quantitative optimal conditions for each of the parameters involved in the coating process. Based on the tendencies found in reported coating experiments in literature, it is however possible to give rough qualitative guidelines to avoid agglomeration and at the same time ensure proper coating. In a first attempt to encircle an operating window, some of the most important parameters are presented in table 3:

	Adjustable parameter	Qualitative prediction of the effect caused by change
Formulation parameters	Coating liquid viscosity (η_{liq})	As it is the case for wet agglomeration theory, the effect of viscosity is complex because the viscosity plays many roles in different phenomena during coating. Experiments indicate that increasing the viscosity increases the chance of agglomeration. In addition, increased viscosity can lead to rough and raspberry structures. Low viscosity coatings may on the other hand mean that the coating droplet size becomes too small thereby causing a high degree of premature drying prior to droplet impact on the core surface. A low coating droplet viscosity may further cause a high extent of droplet drainage into the core material if the core has a significant porosity. Hence either a too high or too low viscosity may cause poor coating quality (Link & Schlünder, 1997 and Guignon et al., 2002).
	Granule surface prior to coating	In order to improved the chance of a strong, homogenous and smooth coating layer the granule surface before coating should be rather smooth and with few pores. Adhesion of the coating liquid is however improved by granule surface roughness (Guignon et al., 2002).
	Coating additives	Additions of surfactants, emulsifiers, anti-adherent agents etc. may reduce the chance of agglomeration but also reduce the mechanical and leaching properties of the final coated granule (Abbott, 2002, Nakano & Yuasa, 2001 and Nakano et al., 1999).
	Granule size vs. coating liquid droplet size	The chance of agglomeration is reduced as the granule diameter is increased and the droplet-granule ratio should be at most 1 to 10 in order to reduce the chance of agglomeration and at the same time ensure homogenous coating (Maa et al., 1996, Guignon et al., 2002 and Kleinbach & Riede, 1995).
Process parameters	Type of fluid bed	The Wurster fluid bed seems to produce more homogenous coating layer than top spray especially with granule diameter less than 125 μm . In addition, the chance of agglomeration is lowered the larger the coating chamber is (Maa et al., 1996).
	Bed temperature and drying time	Experiments have shown that if the bed/drying temperatures are too high, porous, raspberry-like and crystalline coating layers may result. The chance of agglomeration is however significantly smaller at high temperatures (Guignon et al., 2002). Amorphous coatings with lower porosities and improved mechanical properties can be achieved by combination of high bed temperatures, short drying cycles and the addition of surfactants to the coating solution (Link & Schlünder, 1997).
	Fluidisation velocity (U)	Experimental indications suggest that U should be significantly higher than U_{mf} . This will ensure that the circulation time τ_c is low enough to reduce the chance of agglomeration and at the same time enhance the chance of uniform coating (Guignon et al., 2002).
	Coating spray rate (\dot{V}) and nozzle pressure (P_{nozzle})	The pressure through the nozzles governs the spray rate and experiments indicate that the nozzle pressure should be between 0.5 and 3.5 bar. This will ensure proper coating droplet size and proper droplet impact velocity. If the droplet impact velocity is too low, raspberry structure may result (Dewettinck et al., 1999a, Guignon et al., 2002 and Link & Schlünder, 1997).
	Particle circulation time (τ_c)	Link & Schlünder (1997) suggest that τ_c should not exceed a few seconds in order to keep the moisture contents low and reduce the chance of agglomeration. If τ_c however becomes too small, shrinkage and cracking in the coating may happen due to inhomogeneous drying of the coated layer (Link & Schlünder, 1997).
	Size of the spray zone	Maronga & Wnukowski (1997b) have showed that as the size of the spray zone increases, the variance of the coating distribution decreases.

Table 3: Summary of important process and formulation parameters involved in the coating process.

Attempt to highlight key parameters governing the coating process and product and their qualitative tendencies.

4 Mechanical properties of granules and coating layer – strength and breakage mechanisms

As indicated in previous sections, a final coated granule consists of typically several different species combined in a heterogeneous way. In a physical sense a granule is often considered a composite material (Iveson et al., 2001a). Given the heterogeneity of coated granules, it is not obvious that their mechanical properties can be described by the properties used for the description of metals, ceramics and other conventional solids. Granule deformation and destruction mechanisms are however fundamentally similar to other solids (Bika et al., 2001). As in other composite materials, the stress in a granule is transformed non-uniformly, meaning that it is concentrated in preferred paths, where some areas experience high stress loads and others little or no load. Another common characteristic is the distribution of defects (e.g. pores or grains) and internal and surface cracks that may dominate the macroscopic response to stress (Bika et al., 2001). These similarities imply that the description of failure in conventional solids can be applied to granules as well and that granule strength is directly related to failure mechanisms (Scarlett et al. 2002). Likewise can the mechanical properties of a granule crudely be described by the same set of properties used for characterising solids: The Young's modulus³¹, yield strength, tensile strength, ductility/brittleness, fracture toughness and hardness (Bika et al., 2001). Each of these properties will briefly be introduced in the following section in respect to granules.

4.1 Properties characterising the granule strength

The degree to which a structure deforms or strains, depends on the magnitude of the imposed stress. For some materials that are stressed in tension at low levels, stress and strain are proportional through (Callister, 2001):

$$\sigma = E \cdot \Gamma \quad (4.1)$$

where Γ is the strain, σ is the stress and E is the Young's modulus. This modulus may be thought of as stiffness or the resistance of a material to deform elastically. The stiffer the material, the greater the modulus. The Young's modulus in granules is often determined by compression or indentation tests³² (Jørgensen, 2002).

Deformation in which stress and strain are proportional is called elastic deformation, which is a non-permanent deformation meaning that as the applied load is released, the granule returns to its original shape (Callister, 2001). Increasing the stress-strain rate further will lead to permanent plastic deformation and eventually to breakage. The point where plastic deformation starts to occur is called the yield stress or yield strength σ_y . Some of the simplest tests for determining σ_y are indentation or confined compression tests (Iveson et al., 2001a).

The maximum point in the strain-stress curve is called the tensile strength σ_t . This point corresponds to the maximum stress that can be sustained by a structure in tension. If this stress is applied and maintained, fracture will result (Callister, 2001). The stress to failure σ_f of a spherical agglomerate with uniform structure of radius R_{sph} under compression load F_c in one dimension can be found as:

$$\sigma_f = b \cdot \frac{F_c}{\pi R_{sph}^2} \quad (4.2)$$

where b is a constant depending on the size of contact area between the granule and the impact plate with values ranging from 0.4 – 0.7 (Bika et al., 2001).

TURN TO THE EXPERTS FOR SUBSCRIPTION CONSULTANCY

Subscribe is one of the leading companies in Europe when it comes to innovation and business development within subscription businesses.

We innovate new subscription business models or improve existing ones. We do business reviews of existing subscription businesses and we develop acquisition and retention strategies.

Learn more at [linkedin.com/company/subscribe](https://www.linkedin.com/company/subscribe) or contact Managing Director Morten Suhr Hansen at mha@subscribe.dk

SUBSCRIB✓**BE** - to the future



Experimental tensile strength is not always a readily measured property in granules because stress concentration may cause brittle fracture at much lesser values than the true tensile strength. The experimental determined tensile strength of granules has long been known to be a variable depending on the specimen size but not linearly. Hence a statistic data treatment is necessary. The Weibull two-parameter distribution can be used to express the probability $P_s(\sigma)$ of a granule sample to survive a given stress σ (Bika et al., 2001):

$$P_s(\sigma) = \exp \left[- \left(\frac{\sigma}{\sigma_0} \right)^{n_{\text{Weibull}}} \right] \quad (4.3)$$

where n_{Weibull} is the Weibull modulus related to the range of flaw sizes present in the granule. The n_{Weibull} can be considered as a measure of the brittleness of the sample. The smaller the value of n_{Weibull} , the more brittle the sample. The second parameter σ_0 is the Weibull constant being a characteristic strength value of the material. More precisely it is the stress at which $1/\exp(1) = 37\%$ of the specimens remain unbroken (Bika et al., 2001).

Brittleness and ductility are important terms in describing the mechanical properties of a granule. Ductility is a measure of the degree of plastic deformation that has been sustained at fracture. A material that experiences very little or no plastic deformation upon fracture is termed brittle. Ductile materials on the other hand may experience large extent of plastic deformation without fracture (Callister, 2001). Granules are often considered semi-brittle in that limited plastic deformation can occur besides brittle fracture (Iveson et al., 2001a).

The fracture toughness K_c of a granule defines the elastic stress field in the granule ahead of a propagating crack. In other words it is a measure of granule resistance to crack propagation. Fracture toughness is typically measured on a macroscopic scale in a special indentation test in which a specimen containing a sharp crack of known length is subjected to an applied load F , which is increased during the course of the test until the specimen fails. For such specimen, the magnitude of the stress near the crack tip is described by the stress intensity factor K , which in turn depends on the stress to failure σ_f , the crack length c , the radius of the granule r_g and a dimensionless specimen dependent factor M according to (Efunda, 2005):

$$K = M \cdot \sigma_f \sqrt{\pi \cdot (c + r_g)} \quad (4.4)$$

The fracture toughness K_c is defined as the magnitude of the stress intensity factor K at the point of crack extension (Leeds, 2005). Iveson et al. (2001a) suggest the following simplified expression for the determination of K_c in granules:

$$K_c = \chi \sqrt{\frac{E}{H}} \frac{F}{c^{3/2}} \quad (4.5)$$

where χ is the proportionality constant depending on the indenter dimensions and H is the hardness. The hardness is a measure of a granule resistance to plastic deform. It is defined as the applied load divided by the projected area of the indent after unloading (Jørgensen, 2002). A hard material is often brittle and typically less resistant to propagation of cracks. As seen from equation 4.5 a hard granule should have a low fracture toughness, which indeed has been reported by Bika et al. (2001). The inverse proportionality between K_{c} and the radial crack length c is obvious. The longer the crack length the weaker the material gets, resulting in lower fracture toughness.

Having defined some of the most important properties and parameters for characterising the mechanical properties of granules, the next section is devoted to the description of breakage mechanisms.

4.2 Types of breakage mechanisms

The existence of cracks and the extent of crack propagation is of high importance in semi-brittle materials as granules. Several types of destruction can be traced back to the existence of cracks in the granule surface or cracks in the core. A distinction between lateral and radial cracks has been made by Ghadiri & Zhang (2002). Radial cracks propagate radially from the surface to the inner of the granule whereas lateral cracks propagate closely parallel to the granule surface.

The principle of a granule failing by radial crack propagation can be seen in figure 13. The tensile stress concentrates near the crack tip and is much higher than the applied stress leading to local yielding near the crack tip. This zone is called the “process zone³³” (Iveson et al., 2001a). The crack will thereby gradually propagate from the edge of the process zone to the interior of the granule causing degradation of the granule mechanical strength. The principle of lateral crack propagation is analogous but the strength degradation only concerns the outer layer of the granule. Often radial and lateral cracks propagate simultaneously (Iveson et al., 2001a).

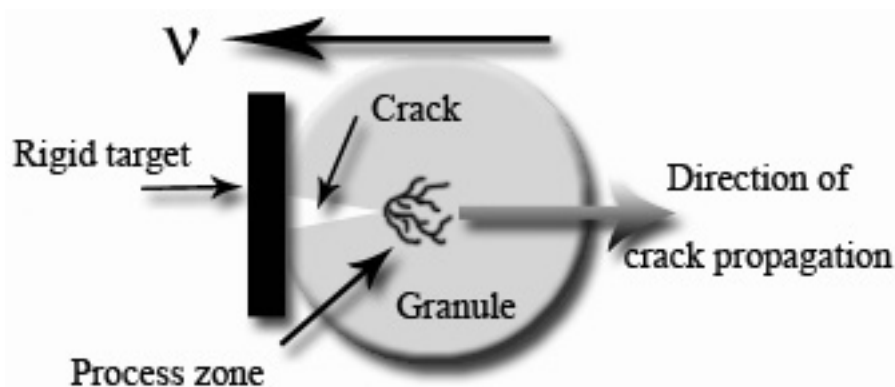
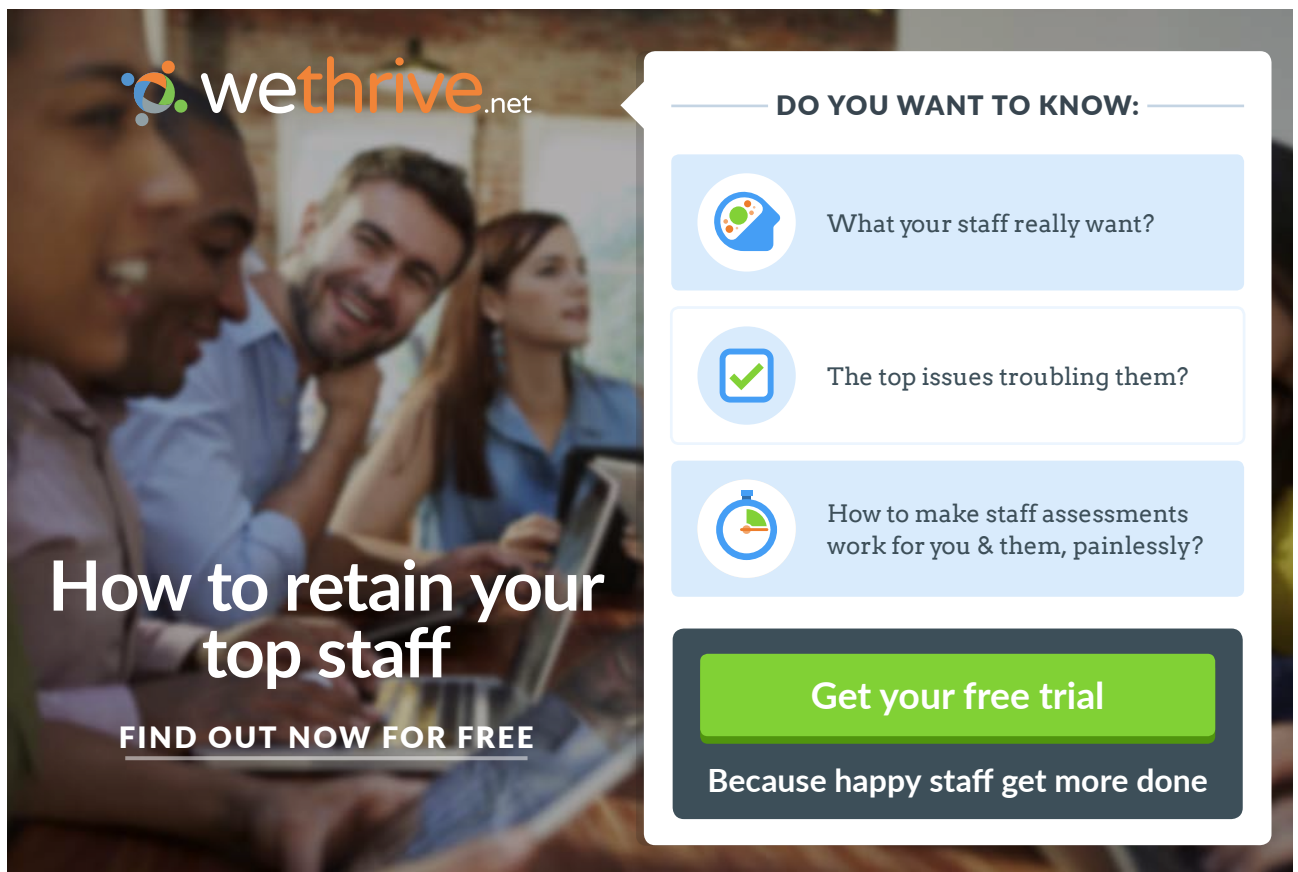


Figure 13: Fracture of a granule (semi-brittle) by radial crack propagation.

As the granule impact a rigid target or simply just another granule the crack will propagate in the opposite direction of the direction of the impact velocity (based on Iveson et al., 2001a and Jørgensen, 2002).

The process zone plays a large role in the mechanisms of granule breakage. The size of the process zone in respect to the granule size along with the main type of crack propagation will determine the type of destruction. E.g. will granules with a small process zone in comparison to the size of the granule break by a brittle fracture mechanism. This mechanism is called fragmentation or fracture³⁴ (Iveson et al., 2001a). Fracture of a granule is major internal breakage due to the application of very large or repeated external forces head-on. Due to fracture there is drastic reduction in the granule size and the resulting daughter particles are large compared to the original mother granule (Pitchumani et al., 2003). Fracture is the most severe kind of breakage because the original granule structure is completely destructed and the granule core is exposed to the surroundings (Jørgensen et al., 2004).

For fracture to occur, the granule must be able to concentrate enough elastic energy to propagate single radial cracks throughout the granule structure. This is harder to do as the size of the process zone increases. Hence fracture will only occur if the process zone is significantly smaller than the granule size (Iveson et al., 2001a). Thornton et al. (2004) and Mishra & Thornton (2001) have showed that fracture is often associated with dense granules whereas other more porous and more loosely packed granules destruct by other type of mechanisms.



wethrive.net

How to retain your top staff

FIND OUT NOW FOR FREE

DO YOU WANT TO KNOW:

- What your staff really want?
- The top issues troubling them?
- How to make staff assessments work for you & them, painlessly?

Get your free trial

Because happy staff get more done



Click on the ad to read more

Another type of fracture is chipping. If the granule is applied to large external forces tangentially instead of head-on³⁵, deep lateral cracks will propagate and the surface area of the granules is damaged and some material is chipped off. Next to fracture chipping is a very severe type of damage. Due to chipping, the granule surface will become rougher and exposure of the inner coating layers and even the granule core may occur, although the inner granule core structure is usually kept intact (Jørgensen et al., 2004 and Pitchumani et al., 2003). A formal classification of the different types of breakage mechanisms can be seen in table 4. The last two types are presented below.

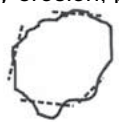



Force	Normal force	Tangential force
Small force (only local damage)	<i>Wear</i>	
	Attrition (by erosion, peeling or fatigue) 	Abrasion 
Large force (widespread damage)	<i>Fracture</i>	
	Fragmentation 	Chipping 

Table 4: Formal classification and summary of possible granule breakage mechanisms.

Basically four types of granule failure mechanisms have been proposed being attrition, abrasion, fragmentation and chipping (Based on Beekman, 2000 and Pitchumani et al., 2003).

For many granules the process zone is of the order of the granule size and fracture of granules and especially coated granules is rare (Ennis & Sunshine, 1993). Instead other types of destructive mechanisms occur. Wear is the overall term for gradual surface damage that merely peels off or polishes the granule leaving the original shape more or less unchanged (Pitchumani et al., 2003). Abrasion is wear caused by low magnitude tangential forces. The small tangential forces lead to polishing and rounding of the granules. This will generate fine particles and the mother granules become more and more spherical and smoother with time by gradually losing primarily the coating layer (Jørgensen et al., 2004 and Pitchumani et al., 2003).

Wear caused by low magnitude of head-on forces leading to the propagation of lateral cracks is called attrition. The forces acting on the granule result in the removal of sharp edges producing a more spherical granule shape. Beekman (2000) have subdivided the attrition phenomena into two subgroups: attrition by fatigue and attrition by erosion. Often impact forces causes attrition and it is often observed that it takes many impact events before any damage of the granules can be observed. During the impact events, cracks propagate and finally lead to damage with an ever-increasing rate of loss of mass with time (Beekman, 2000). This type of attrition damage is called fatigue and depending on the depth of the crack propagation this may eventually lead to chipping or even fracture.

Erosion is the attrition mechanism occurring when a granule gradually loses mass mainly from the outside of the granule. Uneven parts of the granule surface are eroded and the rate at which the granule loses mass is constant or decreasing with time (Beekman, 2000). When erosion only affects a specific surface layer it is called peeling. Initially the rate of erosion will be constant but decrease after the weak layer is removed. Peeling is often observed for granules that have a layered structure such as coated granules (Beekman, 2000, Jørgensen, 2002 and Jørgensen et al., 2004).

4.3 Towards a quantitative prediction of breakage mechanisms

In order to try to quantify the different breakage mechanisms it is desirable to describe the mechanisms by fracture mechanical parameters such as the fracture toughness K_c and by mechanical properties that define deformability (Young's modulus E , yield strength σ_y and hardness H). It has long been realised that the type of breakage mechanism is also controlled by external factors such as temperature, pressure, impact velocity, type of load application (e.g. shear, tensile or compression impacts) and most importantly loading rate and granule history (Bika et al., 2001). The limited number of experiments so far allows only approximate relations to be suggested. These relations are however an important step towards a thorough quantitative prediction of the extent and type of breakage mechanism.

Iveson et al. (2001a) suggest in agreement with Bika et al. (2001) the following relation based on experimental studies between the fractional volume removed by abrasive wear V_{abrasion} per granule impact and the following parameters:

$$V_{\text{abrasion}} \propto \frac{d_g v^n \rho_g}{K_c^{3/2} H^{1/2}} \quad (4.6)$$

where ρ_g is the granule density, d_g is the granule diameter, v is the impact velocity and n is a number ranging from 2.5 and 4. An unambiguous velocity dependence has however not been determined yet due to severe problems in testing abrasive wear mechanisms without the influence of other types of destructive mechanisms. Instead another more widely proved relation for indenter analysis of abrasion has been suggested by Bika et al. (2001) based on fracture mechanics theory as well as experimental data fitting:

$$V_{\text{abrasion}} \propto \frac{d_g^{1/2}}{A_i^{1/4} K_c^{3/4} H^{1/2}} F^{5/4} \quad (4.7)$$


where A_i is the apparent area of indenter contact and F is the total applied indenter load.

It is worth noting that in both equation 4.6 and 4.7, V_{abrasion} is inversely dependent on both the fracture toughness K_c and the hardness H . Several authors have proved these tendencies (Bika et al., 2001 and Ennis & Sunshine, 1993) although Mullier et al. (1991) suggest that V_{abrasion} should depend on $1/K_c$ instead of $1/K_c^{3/4}$ in equation 6.7.

Attrition is the most studied of the four overall breakage phenomena possible because it is the most observed mechanism in fluid bed equipment. Another reason may be that experiments exposing granules to head-on forces by impact tests are easier to conduct than tangential force tests. Unfortunately some attrition experiments show signs of surface deterioration by several of the mechanisms simultaneously. This is especially the case when large numbers of granules are tested together in bulk tests. It is thereby not always possible to determine the mechanisms individually and often the observed breakage mechanism is simply referred to as attrition without further specification (Beekman, 2000). As indicated, “attrition” should only refer to wear by head-on forces, but the widespread use of the term has resulted in the use of “attrition” to describe all kinds of material losses from attrition by fatigue to fracture. Hence the attrition relations presented below may also be applied for the description of fracture mechanisms (Bika et al., 2001).

There still exists no unified description or method to assess, quantify or predict attrition although several attempts have been made. Ghadiri & Zhang (2002) suggests the following proportionality between the fractional volume removed per impact by attrition $V_{\text{attrition}}$ and the following parameters³⁶:

$$V_{\text{attrition}} \propto \frac{\rho_g v^2 d_g H}{K_c^2} \quad (4.8)$$



Struggling to get interviews?

Professional CV consulting & writing assistance from leading job experts in the UK.

[Visit site](#)



Take a short-cut to your next job!
Improve your interview success rate by 70%.



TheCVagency
Visit theagency.co.uk for more info.



Click on the ad to read more

It is interesting to notice from equation 6.8 that the fractional loss is proportional to the impact kinetic energy $\rho_g v^2$ and that it varies linearly with particle size d_g . That $\rho_g v^2 d_g$ should be depend linearly with $V_{\text{attrition}}$ complies fully with results found by Beekman et al. (2002) who showed a direct proportionality.

Comparing equation 6.6 with 6.8 indicates that impact attrition is more sensitive to fracture toughness K_c than abrasive wear. The velocity dependence in both equations are in accordance with experimental evidence. The higher the velocity the more material is lost, meaning that the more severe the type of breakage mechanism is. There is a general agreement in literature that breakage of granules increases with increasing impact velocity (Subero et al., 1999, Mishra & Thornton, 2001, Scarlett et al., 2002 and Jørgensen et al., 2004). At increased impact velocity, the primary breakage mechanism is changed from attrition/abrasion to chipping and finally fracture. In addition it can be seen by comparison that the effect of hardness H on attrition is the opposite of that for abrasion. It can be seen from equation 6.8 that a high value of H promotes chipping/fragmentation. Hardness acts to concentrate stress for fracture during impact and it seems plausible that the fractional volume of a granule removed by attrition depends linearly on the hardness H (Iveson et al., 2001a). The dependence on hardness is however not ambiguous. Liu et al. (2003) have tested several polymer coatings and found that the degree of attrition increases (although not much) with decreased coating hardness, whereas Ghadiri & Zhang (2002) suggest a direct linear relationship between H and $V_{\text{attrition}}$.

As late as 1969 by Gwyn et al. proposed an empirical model for the prediction of the weight fraction Y of a granule sample, that has undergone attrition as a function of time t in a fluid bed. The parameter Y thereby goes from zero at no attrition to the size of one at point where all the granules in the sample have undergone attrition. The empirical relation was found to be (Gwyn, 1969):

$$Y_{\text{attrition}} = Q \cdot t^{n_{\text{Gwyn}}} \quad (4.9)$$

where n_{Gwyn} is an empirical constant and Q is a constant dependent on the initial granule size. Where Q represents the severity of attrition and the initial attritability of the granule, n_{Gwyn} concerns the change in attritability with time. Hence the two parameters are descriptive of both the material properties and the attrition process (Neil & Brigdwater, 1999). Results by Neil & Brigdwater (1999) indicate that n_{Gwyn} could be split up into two parameters such that $n_{\text{Gwyn}} = \xi \cdot \phi_{\text{attrition}}$ where ξ is a term describing the rate of granule degradation and $\phi_{\text{attrition}}$ is a material property of attrition. This expansion should help adapting the formula to different types of equipment and take into account the different attrition rates in erosion and fatigue. The Gwyn formula has been studied intensively and it has been found to characterise the extent of attrition successfully in many types of equipment besides fluid beds.

As it is the case with the Gwyn formula, the previously presented relations describing the volumetric wear rates are primarily found on the basis of homogenous granules with an isotropic structure. The case is somewhat more complicated when dealing with coated granules. Hence the presented relations may only help to give a qualitative prediction of the effect of the different parameters. There are still extensive needs for empirical experience concerning the mechanical properties of coated granules.

4.4 Qualitative trends of parameters affecting breakage

Although only very few attempts have been made to quantify the types of breakage mechanisms, a number of qualitative trends (besides the already mentioned) have been reported in literature. These tendencies have not yet been incorporated into models or equations but knowledge of them is nevertheless important. A brief review of some of the most interesting trends is presented below.

Guignon et al. (2002) report that in fluid bed experiments the extent of attrition is lowered the more uniform the shape of the granule surface is. In addition, experiments by Jørgensen et al. (2004) indicate in agreement with Pitchumani et al. (2003) that the type and extent of breakage depends on surface friction as well as initial granule shape. Further Jørgensen et al (2004) showed that the stronger the core the better the breakage resistance of the final coated granule. Coating layers of inorganic salts and water-soluble polymers enhance the breakage resistance of the granules tremendously (Jørgensen et al., 2004). This is in agreement with results found by Liu et al. (2003) and Beekman et al. (2003). Their experiments indicate that the coating attrition rate is highly affected by both the core granule composition as well as the binder properties of the coating layer.

Experiments by Scarlett et al. (2002) indicate that the type of breakage mechanism is nearly independent of granule size. This is somewhat in contradiction to Guignon et al. (2002) who report that in fluid bed experiments, the extent of attrition is lowered the smaller the granules are. Guignon et al. (2002) report further that attrition during the drying-wetting cycles is decreased by combining a short intense drying time with the addition of a surfactant to the coating solution to improve adhesion.

Impact tests of granules made by Salman et al. (2004 & 2002) showed that change of impact angle away from normal 90° had little influence on the type and extent of breakage mechanism. However for impact angles less than 10° no fragmentation was observed regardless of the impact velocity. Other interesting aspects regarding fragmentation were found by Salman et al. (2002). Experiments showed that the impact target thickness and material has a significant effect on particle fragmentation. In order to reduce the chance of fragmentation, the impact target should be thin and/or soft. This becomes relevant not just for the fluid bed design, but also when designing storage tanks and conveying systems.

4.5 Modern approach – a brief review on computer simulation of granule breakage

Besides the attempts to find experimental-based relations, some researchers have taken a different approach to predict granule breakage behaviour using primarily DEM (Discrete Element Models³⁷) (e.g. Subero et al., 1999, Thornton et al. 2004 and Mishra & Thornton, 2001). In DEM, particles are treated as discrete entities, which interact with each other at the interface when they are in contact. The used particle interaction principles are based on well-established contact mechanics theories (Mishra & Thornton, 2001). This simulation technique can be used to simulate two-dimensional breakage behaviour in granules with randomly generated spherical packing. The breakage pattern upon impact with a rigid target is then studied (Salman et al., 2004). Improvements by Subero et al. (1999) have made it possible to simulate three-dimensional granules upon impact. Problems in quantifying the breakage phenomena makes the use of population balance modelling difficult although first attempts have been reported by Salman et al. (2003). Potapov & Campbell (1994) have used another approach to simulate the breakage behaviour of homogeneous elastic solids impacting against a rigid wall. Instead of discrete elements, the elastic solid is divided into contiguous polygonal elements, which are considered broken when the tensile force is found to exceed a certain limit. This type of approach made it possible to simulate and study fracture patterns for a number of solids.

gaiteye®
Challenge the way we run

**EXPERIENCE THE POWER OF
FULL ENGAGEMENT...**

.....

**RUN FASTER.
RUN LONGER..
RUN EASIER...**

**READ MORE & PRE-ORDER TODAY
WWW.GAITEYE.COM**

Simulations have primarily been used to support qualitative trends found by experiments. Only in the last few years, simulations have been used for the investigation of the effect of the macroscopic granule mechanical properties such as modulus of elasticity, hardness and fracture toughness. In general, the results from computer simulations rely heavily on the accuracy of the equipment producing the empirical data, which the simulation results are held up against. Recent use of fine scale equipment such as nano-indentation and AFM (Atomic Force Microscopy) along with faster computers, have allowed advanced simulation of impact breakage on three-dimensional granules with random packing (Subero et al., 1999). Still no simulation is able to take into account all the random breakage phenomena that can take place during fluid bed processing and many of the tendencies found by simulation are only valid as qualitative support for the specific equipment (Thornton et al., 2004). Industrial granules consisting of several materials with different mechanical properties are still too complex to simulate (Beekman, 2000). There is however no doubt that the combination of computer simulation with careful fine scale measurement remains an open area for future research in the coming years.

4.6 Strength test methods – a brief review

In early literature most of the attention was focussed on the energy used to cause breakage and some of the tests used were small scale grinding machines operated at prescribed conditions. These test were unfortunately very dependent on the equipment and poor repeatability was often a problem. In later improvements the operating, equipment and material variables were to be separated and focus was brought onto mechanical strength as a function of load, velocity and stress (Linoya et al., 1990 and Beekman, 2000). Modern tests are often optimised to determine tendencies with high repeatability and little equipment dependence (Beekman et al., 2002 and Beekman, 2000). A general challenge for particle tests is that granules often are of a complex structure containing different materials in the core and coating layer (Pitchumani et al., 2003). Modern tests are conveniently divided into either bulk or single particle tests. There are numerous test methods in both categories and the following sections will not go into detail with each method. Instead a brief overall introduction will be given in order to present the possibilities, advantages and limitations of the different granule test types.

4.6.1 Bulk test methods

A bulk test is useful for determining the average strength of a sample of particles. Multiple particle tests offer the advantages of testing a great number of particles simultaneously and they show the closest resemblance to particle handling in process equipment (Jørgensen et al., 2004). The types of equipment used for bulk tests are often closely related to the process equipment used to produce the granules. Examples of different bulk test methods can be seen in figure 14:

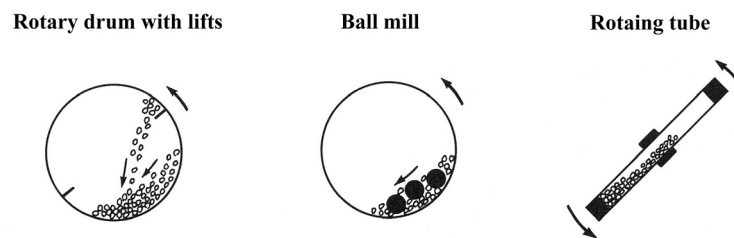


Figure 14: Examples of bulk particle test methods.
Rotary drum apparatus, ball mill and rotating tube (Linoya et al., 1990).

Much attention must be attained to secure that each granule experiences approximately the same treatment in the test. Otherwise the results are statistically useless. There are several problems associated with bulk tests. E.g. are many of the tests highly dependent on the initial particle size distribution. One of the newest approaches by Beekman (2000) indicates however that it is in fact possible to design a bulk test method, which is independent of granule properties. Other interactions between the tested granules can result in complex mechanical effects leading to unsystematic breakage phenomena. The building up of static charge e.g. has been known to influence to reproducibility of results from bulk tests (Beekman, 2000).

Bulk particle tests often give statistically reproducible results but are more empirical in nature (Beekman, 2000). A bulk test is sometimes sufficient for quality control purposes and to provide data that is useful for direct applications in the industry, but a specific strength value usually cannot be interpreted and used to develop a better process or product. Neither do bulk tests usually reveal the basic failure mechanisms (Salman et al., 2004). This is due to the fact that bulk test often show large breakage variances and results difficult to generalise. In the case of product optimisation, the use of single particle tests is needed as well (Beekman et al., 2002).

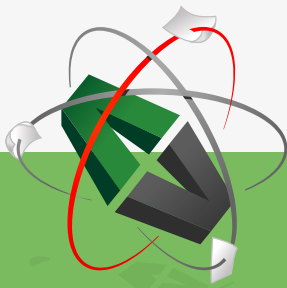
4.6.2 Single particle test methods

Any single particle test method aims to first subject the particle to a controlled but variable stress and then to determine the damage caused. Modern single particle methods are categorised on the basis of the stress mechanisms e.g. normal, tangential, compression or impact. The single particle tests measure each particle individually and only by testing a number of particles, statistically predictions of a whole sample can be made (Beekman et al., 2002 & 2003).

In general, most single particle breakage tests exert the stress on the particle either by compression or by impact. In a single-particle crushing test a single granule is compressed between two hard platens and the stress-strain behaviour is recorded until fracture. The compression test measures the applied stress directly. In an impact test a granule is accelerated to a certain velocity and smashed into a rigid target. An impact test does not usually record the force that causes failure but rather indicates the chance that breakage will occur at the given velocity (Beekman et al., 2002). Although not as accurate as the compression test there are two major advantages of the impact test. Firstly, the granule is not necessarily destructed completely by the impact. This is an advantage when surface damage is to be analysed. Secondly, there is only one point of contact meaning that crack propagation only will origin from one position on the granule surface. In repeated impact tests the same granule is exposed to a well-defined number of impacts. It is thereby possible to investigate fatigue and erosion phenomena closely (Beekman et al., 2003).

Impact and compression tests are complementary. The major difference between impact and compression tests is that the rate of strain is inevitably high during impact but can be controlled during compression. The impact test determines attrition better and the compression test determines fracture better. The impact test is often more convenient to use than compression tests (Beekman et al., 2003).

This e-book
is made with
SetaPDF



PDF components for **PHP** developers

www.setasign.com



Click on the ad to read more

The primary disadvantage with single-particle test is that granules in practice never exist as isolated entities but rather in bulks. Results from bulk tests show clearly that interparticle interactions are likely to have a large effect on granule breakage types and rates. It is only through single particle studies however, that a mechanistic understanding of granule breakage can be achieved (Salman et al., 2003 and Beekman, 2000).

4.7 Summing up on granule strength

The diversity of the reported trends and approaches presented in the previous sections imply that the mechanical strength of particles and especially coated granules is a fairly unexplored area and that quantitative descriptions and predictions lie far ahead. Nevertheless, the identity between several of the reported trends should help to demonstrate that qualitative predictions of granule breakage are possible to a limited extent. Some of the most important properties and parameters concerning granule strength and breakage are summed up in table 5:

Parameter	Qualitative description
Hardness (H)	Although not unambiguously determined, it seems that the higher the value of H, the more severe the type of breakage mechanism. A hard granule is often brittle and less resistant to crack propagation (Ghadiri & Zhang, 2002 and Iveson et al., 2001a).
Fracture toughness (K_{IC})	A high value of K_{IC} will hinder crack propagation and reduce the amount of the fractional volume removed per impact (Ghadiri & Zhang, 2002).
Mean granule porosity ($\bar{\epsilon}_g$) and density (ρ_g)	The suggested formulas indicate that the smaller the density the less material is removed per impact. A correlation with porosity however cannot be made directly because highly porous granules often destruct by an all or nothing fracture mechanism. Granules with high porosity are generally weak and fragile. (Bika et al., 2001 and Iveson et al., 2001a).
Size of the process zone	The larger the process zone is compared to the granule diameter, the less severe is the type of breakage mechanism (Bika et al., 2001 and Guignon et al., 2002).
Granule diameter (d_g)	Although not fully agreement among the authors, there are indications that the extent of attrition is lowered as the granule diameter decrease (Guignon et al., 2002 and Beekman et al., 2002).
Granule surface	The more uniform the granule surface is, the less severe is the amount and type of breakage (Guignon et al., 2002).
Impact velocity (v)	There is general agreement that the higher the impact velocity the more severe is the type of breakage mechanism (e.g Subero et al., 1999 and Mishra & Thornton, 2001).
Impact angle and impact material	The smaller the impact angle and the softer and thinner the target material is, the less severe will the type of damage be (Salman et al., 2002 & 2004)
Influence of coating layer	The coating layer can enhance the breakage resistance of the whole granule depending on the coating material and amount and type of coating solution additives (Liu et al., 2003, Beekman et al., 2003 and Jørgensen et al., 2004).

Table 5: Summary of some of the important properties and parameters concerning granule strength.

5 Summary

Besides providing an overall introduction to fluid bed processing and parameters, the text gives a comprehensive presentation of agglomeration and fluid bed coating theory and principles regarding strength and breakage mechanisms of granules. Focus is brought onto theoretical considerations and models as well as practice and experience presented in the scientific literature. Selected results from some of the newest articles are cited in order to give an up-to-date presentation of the fluid bed granulation field.

The variety of parameters influencing the granules makes fluid bed granulation seem somewhat chaotic. The situation is complicated not just by the variety of influencing parameters but also because many of the parameters are interlinked and influence each other. The text does however indicate that it is possible to give rough qualitative indications of the effect of some of the main parameters governing coating/agglomeration and granule coating strength. A summary of these trends and tendencies are presented in the text in three main tables concerning respectively: Parameters important for agglomeration, key parameters governing the coating process and product and last, important properties and parameters concerning granule strength. These tables may function as rough initial guidelines for an operating window, where successful coating of granules leads to unagglomerated granules with high mechanical strength. The validation of these guidelines seems nevertheless to be highly dependent on verification by systematic experimental results.

Interestingly, it was seen from the study of modern scientific articles that fluid bed agglomeration and coating still is a widely unexplored field and to some extent still more of an empirical-based technology rather than science. Many experiments and attempts have been conducted in order to explain some of the phenomena taking place in a fluid bed during coating/agglomeration, but no single model contains all the parameters needed for a full description. In addition, it was seen that yet no model or single parameter makes it possible to predict whether or not excessive agglomeration will occur during the coating process. Nor is it possible to precisely predict the mechanical strength of coated granules based on initial process and formulation parameters. Both issues are highly relevant subjects in the process of improving the mechanical strength of granules while at the same time reduce the tendency of agglomeration during processing. Such models may further help to verify and explain some of the various fluid bed product and process tendencies emphasised in the present text.

Table of symbols

Nomenclature	Unit (SI-system)
a_d	Area covered by each droplet
\dot{a}_d	Total projected area of droplets per time
aH_{inlet}	Absolute humidity of inlet air
aH_{outlet}	Absolute humidity of outlet air
$aH_{sat,bed}$	Absolute humidity of saturated air at bed temperature
A_s	Spray area
A_p	Powder flux
A_i	Apparent area of indenter contact
A_b	Cross sectional area occupied by bubbles
A_{bed}	Cross sectional area of the bed
$A_{chamber}$	Chamber surface area
$A_{cylinder}$	Surface area of cylinder part of the fluidising chamber
$A_{frustum}$	Surface area of frustum part of the fluidising chamber
Ar	Archimedes number
b	Proportionality constant
c	Crack length
c_{air}	Heat capacity of air
c_{water}	Heat capacity of water
$C_{diss.mat.}$	Concentration of dissolved material
C_D	Drag coefficient
D_m	Dry matter contents of coating solution
d_b	Gas bubble diameter
$d_{chamber}$	Chamber diameter
d_{core}	Granule core diameter
d_n	Nucleus diameter
d_d	Liquid droplet diameter
d_g	Granule diameter
d_p	Particle diameter
\bar{d}_p	Mean particle diameter
d_p^*	Dimensionless particle diameter
d_{32}	Specific mean powder particle diameter
e	Particle coefficient of restitution
e_i	The i 'th residual
E	Young modulus
E_{evap}	Evaporation efficiency
E_{Free}	Free energy
E_c	Coating efficiency
f_{agglom}	Fraction of particles agglomerated
F	Applied force/load
F_c	Compression load
g	Gravity
h	Binder layer thickness covering colliding granules
h_a	Characteristic length scales of surface asperities
h_{bed}	Bed height
h_{inner}	Heat transfer number inside the chamber
h_{mf}	Bed height at minimum fluidisation velocity
h_{outer}	Heat transfer number outside the chamber
h_p	Liquid droplet penetration depth
H	Hardness
H_{mf}	Bed height at U_{mf}
H_{vap}	Heat of vaporisation
i	Experiment number
	m^2
	m^2/s
	$kg\ H_2O/kg\ dry\ air$
	$kg\ H_2O/kg\ dry\ air$
	$kg\ H_2O/kg\ dry\ air$
	m^2
	m^2/s
	m^2
	m^2
	m^2
	m^2
	m^2
	m^2
	Dimensionless
	Dimensionless
	m
	$kJ/(kg\ ^\circ C)$
	$kJ/(kg\ ^\circ C)$
	$w/w\%$
	Dimensionless
	kg/kg
	m
	m
	m
	m
	m
	m
	m
	m
	Dimensionless
	m
	Dimensionless
	Dimensionless
	N/m^2
	$\%$
	J
	$\%$
	$\%$
	$\%$
	N
	N
	m/s^2
	m
	m
	m
	$J/(m^2\ s\ ^\circ C)$
	m
	$J/(m^2\ s\ ^\circ C)$
	m
	N/m^2
	m
	kJ/kg
	Dimensionless

J	Nucleation ratio	Dimensionless
k	Correlation coefficient	Dimensionless
k_{steel}	Thermal conductivity of the stainless steel chamber	$\text{J}/(\text{m s } ^\circ\text{C})$
K	Stress intensity factor	$\text{N}/\text{m}^{3/2}$
K_c	Fracture toughness	$\text{N}/\text{m}^{3/2}$
l	Path length of light (Cuvette width)	m
L_D	Distance above the distributor plate	m
m_b	Mass of liquid bindersprayed	kg
m_{core}	Mass of core material	kg
m_{cs}	Mass of coating solution	kg
m_{dep}	Deposited mass of coating	kg
$m_{\text{dust created}}$	Amount of dust created by impact	kg
m_{harm}	Harmonic mean granule mass	kg
\dot{m}_{max}	Maximum liquid flow rate before agglomeration	m^3/s
m_g	Mass of granule	kg
m_{sample}	Amount of sample	kg
M	Specimen dependent factor	Dimensionless
n	Correlation number	Dimensionless
\dot{n}_b	Number of bubbles pr. second crossing a horizontal plane	$1/\text{s}$
n_d	Number of droplets	Dimensionless
\dot{n}_d	Nozzle droplet production rate	$1/\text{s}$
n_{exp}	Number of experiments	Dimensionless
n_{Gwyn}	The Gwyn relation exponent factor	Dimensionless
$n_{\text{Gwyn adj}}$	The adjusted Gwyn relation exponent factor	Dimensionless
n_{Weibull}	Weibull modulus	Dimensionless
N_i	Number of particles from class i	Dimensionless
N_j	Number of particles from class j	Dimensionless
N_D	Distributor plate orifice density	Number of holes/ m^2
Nu	Nusselts number	Dimensionless

**YOU THINK.
YOU CAN WORK
AT RMB**

**RAND
MERCHANT
BANK**
A division of FirstRand Bank Limited
Traditional values. Innovative ideas.

Rand Merchant Bank uses good business to create a better world, which is one of the reasons that the country's top talent chooses to work at RMB. For more information visit us at www.rmb.co.za

Thinking that can change your world

Rand Merchant Bank is an Authorised Financial Services Provider



Click on the ad to read more

p	Summation number	Dimensionless
p_{model}	Number of model parameters	Dimensionless
P	Pressure	Pa
P_{actual}	Actual vapour pressure	Pa
P_{nozzle}	Nozzle/atomising pressure	bar
Pr	Prandtls number	Dimensionless
P_{sat}	Saturated vapour pressure	Pa
$P_s(\sigma)$	Probability of a granule sample to survive the stress σ	%
q_{air}	Fluidisation air flow rate	kg/min or m ³ /min
q_{at}	Atomising air volumetric flow rate	m ³ /s
q_{cl}	Coating liquid volumetric flow rate through the nozzle	m ³ /s
$q_{\text{coating solut.}}$	Coating solution volumetric flow rate	kg/min or m ³ /min
$q_{\text{nozzle air}}$	Nozzle air volumetric flow rate	kg/min or m ³ /min
q_{water}	Water flow rate	kg/min
Q	Proportionality factor	Dimensionless
Q_{adj}	Adjusted Gwyn relation proportionality factor	Dimensionless
Q_b	Volumetric bubble flow	m ³ /sec
r	Radius	m
r_1, r_2	Radius of granule 1 and 2 respectively	m
r_{app}	Apparent surface contact radius	m
r_{core}	Granule core radius	m
r_d	Radius of droplet	m
r_f	Radius of drop footprint on the powder bed surface	m
r_g	Granule radius	m
r_{harm}	Harmonic mean granule radius	m
rH	Relative humidity	%
Re	Reynolds number	Dimensionless
Re_p	Particle Reynolds number	Dimensionless
R_{eff}	Effective bed pore radius	m
R_{pore}	Radius of parallel capillary pores in porous media	m
R_{sph}	Radius of a sphere	m
R^2	R-squared	Dimensionless
R^2_{adj}	Adjusted R-squared	Dimensionless
R^2_{pred}	Predicted R-squared	Dimensionless
S_0	Particle specific surface area	m ² /kg
St_v	Viscous Stokes number	Dimensionless
St_v^*	Critical viscous Stokes number	Dimensionless
S_w	Wetting saturation	Dimensionless
t	Time	s
T	Temperature	K
T_{bed}	Bed temperature	K
T_{cart}	Heating cartridge outlet temperature	K
T_{inlet}	Temperature of inlet fluidisation gas	K
T_{inner}	Temperature inside fluidising chamber	K
$T_{\text{nozzle, inlet}}$	Inlet temperature of nozzle air	K
T_{outlet}	Temperature of outlet fluidisation gas	K
T_{room}	Room temperature	K
$T_{\text{water, inlet}}$	Inlet temperature of water being purged	K
T_{wall}	Chamber wall temperature	K
u	Scalar granule collision velocity	m/s
u_a	Granule rebound velocity	m/s
u_0	Initial granule collision velocity	m/s
u_{liq}	Liquid velocity	m/s
U	Fluidisation velocity	m/s
U_{br}	Bubble rise velocity for a fluid bed	m/s
U_{down}	Average particle velocity downwards	m/s
U_e	Excess gas velocity	m/s

U_{hc}	Heat conduction number	$\text{kJ}/(\text{m}^2 \text{ min } ^\circ\text{C})$
U_{mf}	Minimum fluidisation velocity	m/s
U_p	Relative velocity of the moving particles to the fluid. gas	m/s
U_s	Superficial gas velocity	m/s
U_{t*}	Terminal velocity of falling particle	m/s
U_t	Dimensionless terminal velocity of falling particle	Dimensionless
U_{up}	Average particle velocity upwards	m/s
V	Volume	m^3
\dot{V}	Volumetric spray rate	m^3/s
V_{abrasion}	Fractional volume removed by abrasive wear per impact	m^3
$V_{\text{attrition}}$	Fractional volume removed by attrition per impact	m^3
V_b	Bubble volume	m^3
V_d	Droplet volume	m^3
V_p	Liquid volume in a single pore	m^3
V_s	Droplet volume at porous media surface	m^3
w	Coating contents of the coated granule	kg/kg
W_A	Work of adhesion for an interface	N/m
W_{CL}	Work of cohesion for a liquid	N/m
W_{CS}	Work of cohesion for a solid	N/m
x	Distance	m
x_{cwt}	Chamber wall thickness	m
X	Coded parameter	Dimensionless
$Y_{\text{attrition}}$	Weight fraction of a granule sample that has undergone attrition	Dimensionless
Y_i	The i 'th response	Dimensionless
\hat{Y}_i	The i 'th response predicted by the model	Dimensionless
\bar{Y}	Mean response	Dimensionless
Y_{PIG}	Impact strength parameter	Dimensionless

Greek

α_{cons}	Degree of consolidation	%
β	Coalescence kernel	Varies
β_{E1}, β_{E2}	Ergun parameters	Dimensionless
χ	Prefactor depending on indenter geometry	Dimensionless
δ	Dimensionless bubble spacing	Dimensionless
ε_A	Absorptivity	$\text{w/w} \%^{-1} \text{ m}^{-1}$
ε_{eff}	Effective porosity (void fraction)	%
$\bar{\varepsilon}_g$	Mean granule porosity (void fraction)	%
ε_{gs}	Granule surface porosity (void fraction)	%
$\varepsilon_{\text{macrovoid}}$	Macrovoid fraction (void fraction)	%
ε_b	Fraction of bed occupied by bubbles (void fraction)	%
ε_{ipp}	Loose packed bed porosity (void fraction)	%
$\varepsilon_{\text{pmsp}}$	Porous media surface porosity (void fraction)	%
ε_{tap}	Tapped porosity (void fraction)	%
ϕ	Particle shape factor (sphericity)	Dimensionless
$\phi_{\text{attrition}}$	Material property of attrition	Dimensionless
σ	Stress	N/m^2
σ_0	Weibull constant	N/m^2
σ_f	Stress to failure	N/m^2
σ_t	Tensile strength	N/m^2
σ_y	Yield stress/strength	N/m^2
Γ	Strain	Dimensionless
ζ_c	Coating thickness	m
γ_{cl}	Coating liquid surface tension	N/m
γ_{lv}	Interfacial tension between liquid and vapour	N/m
γ_{sv}	Interfacial tension between solid and vapour	N/m
γ_{sl}	Interfacial tension between solid and liquid	N/m

κ	Constant	Dimensionless
η_{cl}	Coating liquid viscosity	mPa s
η_{liq}	Liquid (binder/coating) viscosity	kg/m s
η_{gas}	Fluidisation gas viscosity	kg/m s
λ_{ls}	Spreading coefficient (liquid over solid)	N/m
λ_{sl}	Spreading coefficient (solid over liquid)	N/m
ξ	Term describing the rate of granule degradation	Dimensionless
θ	Contact angle	°
ρ_{core}	Granule core density	kg/m ³
ρ_{cl}	Coating liquid density	kg/m ³
ρ_{cm}	Density of coating material	kg/m ³
ρ_g	Granule density	kg/m ³
ρ_{gas}	Gas density	kg/m ³
ρ_p	Particle density	kg/m ³
ρ_{pore}	Density of powder particle pores	Number of pores/m ²
ψ_a	Dimensionless spray flux	Dimensionless
μ_{JT}	Joule-Thomson coefficient	K/bar
τ_b	Bubble residence time	s
τ_c	Average particle circulation time	s
τ_d	Droplet penetration time	s
τ_{drying}	Droplet drying time	s
$\tau_{res,dry}$	Residence time in the drying zone	s
τ_s	Spreading time	s
v	Impact velocity	m/s
v_{air}	Air velocity passing the outer chamber wall	m/s
v_{rel}	Relative velocity between nozzle and fluidisation air	m/s



Discover the truth at www.deloitte.ca/careers

Deloitte.

© Deloitte & Touche LLP and affiliated entities.



Click on the ad to read more

Literature

Abbott, A.: *Boundary Between Coating and Granulation*, Master Thesis, Department of Chemical Engineering, The University of Queensland, **2002**.

Amsterdam. Universiteit van Amsterdam. Visit on the homepage: www.uva.nl, April **2005**.

Aqualon. *Blanose Cellulose Gum – Physical and Chemical Properties*, Hercules Aqualon, **1998**.

Austin, G.T.: *Shreve's Chemical Process Industries*, 5th Edition, McGraw-Hill Inc., New York, **1984**.

Bach, P. Various conferences with Poul Bach, Principal Scientist at Solids Products Development, Novozymes A/S, February – June **2005**.

BASF Pharma. *Coating of tablets and capsules*, BASF Pharma Ingredients Generic Drug Formulation, **2001**.

BASF. BASF Corporation United States. Visit on the homepage: www.basf.com, April **2005**.

Beekman, W.J.: *Measurement of the Mechanical Strength of Granules*, Ph.D. Thesis, Technische Universiteit Delft, **2000**.

Beekman, W.J., Meesters, G.M.H., Scarlett, B. and Becker, T.: *Measurement of Granule Attrition and Fatigue in a Vibrating Box*, Particle System Characterisation, No. 19, pp. 5–11, **2002**.

Beekman, W.J., Meester, G.M.H., Becker, T., Gaertner, A., Gebert, M. and Scarlett, B.: *Failure mechanism determination for industrial granules using a repeated compression test*, Powder Technology, No. 130, pp. 367–376, **2003**.

Bika, D.G, Gentzler, M and Michaels, J.N.: *Mechanical properties of agglomerates*, Powder Technology, No. 117, pp. 98–112, **2001**.

Callister, W.D. Jr.: *Fundamentals of Materials Science and Engineering – An Interactive e-Text*, John Wiley & Sons Inc., 5th edition, New York, **2001**.

Canselier, J.P.: *The effect of surfactants on crystallization phenomena*, Journal of Dispersion Science Technology, No. 14, pp. 625–644, **1993**.

ChemIndustry. Visit on the homepage: www.chemindustry.com, April **2005**.

Christensen, G., Both, E. and Sørensen, P.Ø.: *Mekanik*, Institut for Fysik, DTU, **2000**.

Clement, K.H., Fangel, P., Jensen, A.D. and Thomsen, K.: *Kemiske Enhedsoperationer*, 5th Edition, Polyteknisk Forlag, **2005**.

Cryer S.A.: *Modelling Agglomeration Processes in Fluid-Bed Granulation*, AIChE Journal, Vol. 45, No. 10, pp. 2069–2078, **1999**.

Davidson, J.F. and Harrison, D.: *Fluidized Particles*, Cambridge University Press, New York, **1963**.

Denesuk, M., Smith, G.L., Zelinski, B.J.J., Kreidl, N.J., and Uhlmann, D.R.: Capillary Penetration of Liquid Droplets into Porous Materials, *Journal of Colloid Interface Science*, No. 158, pp. 114–120, **1993**.

Denesuk, M., Zelinski, B.J.J., Kreidl, N.J., and Uhlmann, D.R.: *Dynamics of Incomplete Wetting on Porous Materials*, *Journal of Colloid Interface Science*, No. 168, pp. 141–151, **1994**.

Depypere, F.: Email correspondence with Frédéric Depypere, Ph.D. student at the University of Ghent, March **2005**.

Dewettinck, K.: *Fluidized Bed Coating in Food Technology: Process and Product Quality*, Ph.D. Thesis, Universiteit of Gent, **1997**.

Dewettinck, K. and Huyghebaert, A.: *Top-Spray Fluidized Bed Coating: Effect of Process Variables on Coating Efficiency*, *Lebensmittel-Wissenschaft und Technologie*, Vol. 31, pp. 568–575, **1998**.

Dewettinck, K., Messens, W., Derro, L. and Huyghebaert, A.: *Agglomeration Tendency during Top-Spray Fluidized Bed Coating with Gelatin and Starch Hydrolysate*, *Lebensmittel-Wissenschaft und Technologie*, No. 32, pp. 102–106, **1999a**.

Dewettinck, K. and Huyghebaert, A.: *Fluidized bed coating in food technology*, *Trends in Food & Technology*, No. 10, pp. 163–168, **1999b**.

Efunda. Engineering Fundamentals. Visit on the homepage: www.efunda.com, March **2005**.

Eklund, F.: Email correspondence with Frank Eklund, AVEBE Sweden, March **2005**.

Engineering Toolbox. Visit on the homepage: www.engineeringtoolbox.com, March-June **2005**.

Ennis, B.J., Tardos, G. and Pfeffer, R.: *A microlevel-based characterization of granulation phenomena*, Powder Technology, No. 65, pp. 257–272, **1991**.

Ennis, B.J. and Sunshine, G.: *On Wear as a mechanism of granule attrition*, Tribology International, Butterworth-Heinemann Ltd., pp. 319–327, **1993**.

Faure, A., York, P. and Rowe, R.C.: *Process control and scale-up of pharmaceutical wet granulation processes: a review*, European Journal of Pharmaceutics and Biopharmaceutics, No. 52, pp. 269–277, **2001**.

Felder, R.M. and Rousseau, R.W.: *Elementary Principles of Chemical Processes*, 3rd Edition, John Wiley & Sons Inc., New York, **2000**.

Flick, D., Rock T.C. and Kolter, K.: *Granulation of Theophylline with Kollicoat SR30D or Kollicoat EMM 30D for Sustained-Release Action*, BASF Aktiengesellschaft, Product Development Pharma/Food, Ludwigshafen, Germany, **2005**.

GEA. *Aeromatic-Fielder Strea-1 brochure*, Niro Pharma Systems, GEA Powder Technology Division, **2005**.

Ghadiri, M. and Zhang, Z.: *Impact attrition of particulate solids. Part 1: A theoretical model of chipping*, Chemical Engineering Science, No. 57, pp. 3659–3669, **2002**.

I WANT TO CHANGE DIRECTION,
AND THE WORLD.

GOT-THE-ENERGY-TO-LEAD.COM

We believe that energy suppliers should be renewable, too. We are therefore looking for enthusiastic new colleagues with plenty of ideas who want to join RWE in changing the world. Visit us online to find out what we are offering and how we are working together to ensure the energy of the future.

RWE
The energy to lead



Goodwin, J.: *Colloids and Interfaces with Surfactants and Polymers – An Introduction*, John Wiley & Sons Ltd., Chichester, **2004**.

Guignon, B., Duquenoy, A. and Dumoulin, E.D.: *Fluid Bed Encapsulation of Particles: Principles and Practice*, *Drying Technology*, No. 20, pp. 419–447, **2002**.

Guignon, B., Regalado, E. Duquenoy, A. and Dumoulin, E.D.: *Helping to choose operating parameters for a coating fluid bed process*, *Powder Technology*, No. 130, pp. 193–198, **2003**.

Gwyn, J.E.: *On the Particle Size Distribution Function and the Attrition of Cracking Catalysts*, *AIChE Journal*, Vol. 15, No.1, **1969**.

Hansen, L.A.: *Enhedsoperationer i den kemiske industri*, 4th Edition, Polyteknisk Forlag, **1999**.

Hapgood, K.P., Litster, J.D., Biggs, S.R. and Howes, T.: *Drop penetration into Porous Powder Beds*, *Journal of Colloid Interface Science*, No. 253, pp. 353–366, **2002**.

Heinrich, S. and Mörl, L.: *Description of the Temperature, Humidity and Concentration Distribution in Gas-Liquid-Solid Fluidized Beds*, *Chemical Engineering Technology*, No. 22, pp. 118–122, **1999**.

Hede, P.D. *Fluid bed granulation and coating*, Master Thesis, Department of Chemical Engineering, Technical University of Denmark, pp. 1–227, **2005**.

Hede, P.D. *Towards Mathesis Universalis: Modern aspects of modelling batch fluid bed agglomeration and coating systems – review*, Department of Chemical Engineering, Technical University of Denmark, pp. 1–100, **2006**.

Hinds, W.C.: *Aerosol Technology. Properties, Behaviour and Measurement of Airborne Particles*, John Wiley & Sons Inc., 2nd Edition, New York, **1999**.

Hounslow, M.J., Ryall, R.L. and Marshall, V.R.: *A Discretized Population Balance for Nucleation, Growth and Aggregation*, *AIChE Journal*, No. 34, pp. 1821, **1988**.

Härkönen, H., Koskinen, M., Linko, P. Siika-aho, M. and Poutanen, K.: *Granulation of Enzyme Powders in a Fluidized Bed Spray Granulator*, *Lebensmittel-Wissenschaft und Technologie*, Vol. 26, pp. 235–241, **1993**.

IGME. The Geological and Mining Institute of Spain, Madrid, Spain. Visit on the homepage: www.igme.es, April **2005**.

Iveson, S.M., Litster, D.L., Hapgood, K. and Ennis, B.J.: *Nucleation, growth and breakage phenomena in agitated wet granulation processes: a review*, Powder Technology, No. 117, pp. 3–39, **2001a**.

Iveson, S.M., Wauters, P.A.L., Forrest, S., Litster, J.D., Meesters G.M.H. and Scarlett, B.: *Growth regime map for liquid-bound granules: further development and experimental validation*, Powder Technology No. 117, pp. 83–87, **2001b**.

Iveson, S.M. and Franks, G.V.: *Particle Technology Demonstrations for the Classroom and Laboratory*, University of Newcastle-Callaghan, New South Wales, Australia, **2003**.

Jackson, L.S and Lee, K.: *Microencapsulation and the Food Industry*, Lebensmittel-Wissenschaft und Technologie, Vol. 24, pp. 289–297, **1991**.

Jørgensen, K.: *Design of a Shear and Impact Resistant Enzyme Granule*, Master Thesis, Department of Chemical Engineering, Technical University of Denmark, **2002**.

Jørgensen, K., Bach, P. and Jensen, A.D.: *Impact and attrition shear breakage of enzyme granules and placebo particles-application to particle design and formulation*, Powder Technology, No. 149, pp. 157–167, **2004**.

Keningley, S.T., Knight, P.C. and Marson, A.D.: *An investigation into the effects of binder viscosity on agglomeration behaviour*, Powder Technology, No. 91, pp. 95–103, **1997**.

Kerkhof, P.J.A.M.: *Some modelling aspects of (batch) fluid-bed drying of lifescience products*, Chemical Engineering and Processing, No. 39, pp. 69–80, **2000**.

Kleinbach, E. and Riede, T: *Coating of Solids*, Chemical Engineering and Processing, No. 34, pp. 329–337, **1995**.

Kontogeorgis, G.M.: *Notes in Course 28315: Colloid and Surface Chemistry*, **2004**.

Kunii, D. and Levenspiel, O.: *Fluidization Engineering*, 2nd Edition, Butterworth-Heinemann, Stoneham, **1991**.

Leeds. Institute of Particle Technology, University of Leeds. Visit on the homepage: www.particles.leeds.ac.uk, January **2005**.

Link, K.C. and Schlünder, E.U.: *Fluidized bed spray granulation. Investigation of the coating process on a single sphere*, Chemical Engineering and Processing, No. 36, pp. 443–457, **1997**.

Linoya, K., Gotoh, K. and Higashitani, K.: *Powder Technology Handbook*, 1st Edition, Marcel Dekker Inc., New York, **1990**.

Litster, J.D., Smit, J. and Hounslow, M.J.: *Adjustable Discretized Population Balance for Growth and Aggregation*, AIChE Journal, Vol. 41, No. 3, pp. 591-603, **1995**.

Litster, J.D., Hapgood, K.P., Michaels, J.N., Sims, A., Roberts, M., Kameneni, S.K. and Hsu, T.: *Liquid distribution in wet granulation: dimensionless spray flux*, Powder Technology, No. 114, pp. 32-39, **2001**.

Litster, J.D.: *Scaleup of wet granulation processes: Science not art*, Powder Technology, No. 130, pp. 35-40, **2003**.

Liu, L.X., Litster, J.D., Iveson, S.M. and Ennis, B.J.: *Coalescence of Deformable Granules in Wet Granulation Processes*, AIChE Journal, Vol. 46, No. 3, pp. 529-539, **2000**.

Liu, L.X. and Litster, J.D.: *Population balance modelling of granulation with a physically based coalescence kernel*, Chemical Engineering Science, No. 57, pp. 2183-2191, **2002**.

Liu, L.X., Golchert, D., Page, N.W., Page, D. and Litster, J.D.: *Strength and attrition resistance of agglomerates and particulate coatings*, Powder Technology, No. 130, pp. 415-420, **2003**.

bookboon.com

Corporate eLibrary

See our Business Solutions for employee learning

Click here

Management Time Management

Problem solving Self-Confidence Effectiveness

Project Management Goal setting Motivation Coaching

73

Click on the ad to read more

Download free eBooks at bookboon.com

Liu, L.X. and Litster, J.D.: *Modelling Coalescence in Granulation*, University of Queensland, Not yet published, **2004**.

Maa, Y., Nguyen, P. and Hsu, C.C.: *Spray-coating of rhDNase on lactose: effect of system design operational parameters and protein formulation*, International Journal of Pharmaceutics, No. 144, pp. 47–59, **1996**.

Marmur, A., Schrader, M.E. and Loeb, G.: *Modern Approach to Wettability*, Plenum Press, New York, **1992**.

Maronga, S.J. and Wnukowski, P.: *Establishing temperature and humidity profiles in fluidized bed particulate coating*, Powder Technology, No. 94, pp. 181–185, **1997a**.

Maronga, S.J. and Wnukowski, P.: *Modelling of the three-domain fluidized-bed particulate coating process*, Chemical Engineering Science, No. 17, pp. 2915–2925, **1997b**.

Maronga, S.J. and Wnukowski, P.: *The use of humidity and temperature profiles in optimising the size of fluidized bed in a coating process*, Chemical Engineering and Processing, No. 37, pp. 423–432, **1998**.

Menon, A., Dhodi, N. Mandella, W. and Chakrabarti, S.: *Identifying fluid-bed parameters affecting product variability*, International Journal of Pharmaceutics, No. 140, pp. 207–218, **1996**.

Mishra, B.K. and Thornton, C.: *Impact breakage of particle agglomerates*, International Journal of Mineral Processing, No. 61, pp. 225–239, **2001**.

Montgomery, D.C.: *Design and Analysis of Experiments*, 4th Edition, John Wiley & Sons Inc., NY, **1997**.

Mort, P.R. and Tardos, G.I.: *Scale-up of agglomeration processes using transformations*, Kona, No. 17, **1999**.

Mullier, M.A., Seville, J.P.K. and Adams, M.J.: *The effect of agglomerate strength on attrition during processing*, Powder Technology, No. 65, pp. 321–333, **1991**.

Nakano, T., Yuasa, H. and Kanaya, Y.: *Suppression of Agglomeration in Fluidized Bed Coating. III. Hofmeister Series in Suppression of Particle Agglomeration*. Pharmaceutical Research, No. 10, pp. 1616–1620, **1999**.

Nakano, T. and Yuasa, H.: *Suppression of agglomeration in fluidized bed coating. IV. Effects of sodium citrate concentration on the suppression of particles agglomeration and the physical properties of HPMC film*, International Journal of Pharmaceutics, No. 215, pp. 3–12, **2001**.

Nebraska. Institute of Agricultural and Natural Resources, University of Nebraska-Lincoln. Visit on the homepage: www.ianrpubs.unl.edu, April **2005**.

Neil, A.U. and Bridgwater, J.: *Towards a parameter characterising attrition*, Powder Technology, No. 106, pp. 37–44, **1999**.

NIST. NIST Chemistry Webbook. Visit on the homepage: webbook.nist.gov, June **2005**.

Niro. *Notes on Fluidized Beds*, Niro Atomizer A/S, **1992**.

Niskinaka, M and Iljima, H.: *Enzyme-granulating method and granular composition containing enzyme*. Patent US 4740649, **1988**.

Novozymes. *Enzymes at work*, Novozymes A/S, **2004**.

Petrucelli, J.D., Nandram, B. and Chen, M.: *Applied statistics for engineers and scientists*, 1st Edition, Prentice-Hall Inc., Upper Saddle River, NJ, **1999**.

PharmSciTech. AAPS PharmSciTech Online Journal, visit on the homepage: www.aapspharmscitech.org, May **2005**.

PHYWE. *Laboratory Experiments: Joule-Thomson effect*, PHYWE Systeme GmbH, Göttingen, Germany, **2005**.

Pietsch, W.: *Size Enlargement by Agglomeration*, John Wiley & Sons Ltd., Chichester, **1991**.

Pitchumani, R., Meesters, G.M.H. and Scarlett, B.: *Breakage behaviour of enzyme granules in repeated impact test*, Powder Technology, No. 130, pp. 421–427, **2003**.

Potapov, A.V. and Campbell, A.V.: *Computer simulations of impact-induced particle breakage*, Powder Technology, No. 81, pp. 207–216, **1994**.

Rambali, B., Baert, L. and Massart, D.L.: *Using experimental design to optimise the process parameters in fluidised bed granulation on a semi-full scale*, International Journal of Pharmaceutics, No. 220, pp. 149–160, **2001**.

Rhodes, M.: *Introduction to Particle Technology*, John Wiley & Sons Ltd., Chichester, **1998**.

Rowe, P.N.: *Estimation of solids circulation rate in a bubbling fluidised bed*, Chemical Engineering Science, No. 28, pp. 979–980, **1972**.

Rowe, R.C.: *Binder-substrate interactions in granulation: a theoretical approach based on surface free energy and polarity*, International Journal of Pharmaceutics, No. 52, pp. 149–154, **1989**.

Rubino, O.P.: *Fluid-Bed Technology. Overview and Criteria for Process Selection*, Pharmaceutical Technology, No. 23, pp. 104–117, **1999**.

Rumpf, H.: *Particle Technology*, English Edition, Chapman and Hall, London, **1990**.

Räsänen, E., Antikainen, O. and Yliruusi, J.: *A New Method to Predict Flowability Using a Microscale Fluid Bed*, AAPS PharmSciTech, No. 4, **2003**.

Salman, A.D., Biggs, C.A., Fu, J., Angyal, I., Szabó, M. and Hounslow, M.J.: *An experimental investigation of particle fragmentation using single particle impact studies*, Powder Technology, No. 128, pp. 36–46, **2002**.

Salman, A.D., Reynolds, G.K. and Hounslow, M.J.: *Particle Impact Breakage in Particulate Processing*, KONA, No. 21, pp. 88–98, **2003**.

Salman, A.D., Reynolds, G.K., Fu, J.S., Cheong, Y.S., Biggs, C.A., Adams, M.J., Gorham, D.A., Lukenics, J. and Hounslow, M.J.: *Descriptive classification of the impact failure modes of spherical particles*, Powder Technology, No. 143–144, pp. 19–30, **2004**.

An advertisement for SKF. It features a woman with long dark hair smiling in the foreground. In the background, a large white wind turbine is visible against a blue sky. The text 'Brain power' is written in large white letters on the left. On the right, there is a block of text about wind energy and SKF's role. At the bottom left, there is a call to action to visit the SKF website. The SKF logo is in the bottom right corner.

Brain power

By 2020, wind could provide one-tenth of our planet's electricity needs. Already today, SKF's innovative know-how is crucial to running a large proportion of the world's wind turbines.

Up to 25 % of the generating costs relate to maintenance. These can be reduced dramatically thanks to our systems for on-line condition monitoring and automatic lubrication. We help make it more economical to create cleaner, cheaper energy out of thin air.

By sharing our experience, expertise, and creativity, industries can boost performance beyond expectations.

Therefore we need the best employees who can meet this challenge!

The Power of Knowledge Engineering

Plug into The Power of Knowledge Engineering.
Visit us at www.skf.com/knowledge

SKF

Saujanya. Manufactures & Exporters of Dyes, Dye intermediates and Chemicals, Ahmedabad, India. Visit on the homepage: www.saujanya.com, April **2005**.

Scarlett, B., Beekman, W.J., Meesters, G.M.H. and Pitchumani, R.: *Particles – Their Strengths and Weaknesses*, Key Engineering Materials, Vol. 230-232, pp. 203–212, **2002**.

Schaafsma, S.H., Vonk, P., Segers, P. and Kossen, N.W.F.: *Description of agglomerate growth*, Powder Technology, No. 97, pp 183–190, **1998**.

Schaafsma, S.H., Kossen, N.W.F., Mos, M.T., Blauw L. and Hoffman A.C.: *Effects and control of humidity and particle mixing in fluid-bed granulation*, AIChE Journal, Vol. 45, No. 6, pp. 1202–1210, **1999**.

Schaafsma, S.H., Vonk, P., and Kossen, N.W.F.: *Fluid bed agglomeration with a narrow droplet size distribution*, International Journal of Pharmaceutics, No. 193, pp. 175–187, **2000a**.

Schaafsma, S.H.: *Down-scaling of a fluidised bed agglomeration process*, Rijkuniversiteit Groningen, **2000b**.

Shao, Z.J., Morales, L., Diaz, S. and Muhammad, N.A.: *Drug Release From Kollicoat SR 30D-Coated Nonpareil Beads: Evaluation of Coating Level, Plasticizer Type and Curing Conditions*, AAPS PharmSciTech, No. 3, **2002**.

Simons, S.J.R. and Fairbrother, R.J.: *Direct observations of liquid binder-particle interactions: the role of wetting behaviour in agglomeration growth*, Powder Technology, No. 110, pp. 44–58, **2000**.

Skoog, D.A., West, D.M. and Holler, F.J.: *Fundamentals of Analytical Chemistry*, 7th Edition, Saunders College Publishing, New York, **1997**.

Smith, J.M., Van Ness, H.C. and Abbott, M.M.: *Introduction to Chemical Engineering Thermodynamics*, 6th Edition, McGraw Hill Inc., New York, **2001**.

Snabre, P. and Magnifotcham, F.: *Formation and rise of a bubble stream in a viscous liquid*, The European Physical Journal B, No. 4, pp. 369–377, **1998**.

Spiegel, M.R. and Liu, J.: *Mathematical Handbook of Formulas and Tables*, 2nd Edition, McGraw Hill Inc., New York, **1999**.

Spliid, H.: *Design and Analysis of Experiments with k Factors having p Levels*, Lecture notes in the Design and Analysis of Experiments, Informatics and Mathematical Modelling, DTU, **2002**.

Subero, J., Ning, Z., Ghadiri, M. and Thornton, C.: *Effect of interface energy on the impact strength of agglomerates*, Powder Technology, No. 105, pp. 66–73, **1999**.

Sudsakorn, K. and Turton, R.: *Nonuniformity of particle coating on a size distribution of particles in a fluidized bed coater*, Powder Technology, No. 110, pp. 37–43, **2000**.

Summers, M. and Aulton, M.: *Granulation*, through forum at www.fleshandbones.com, December **2004**.

Tardos, G.I., Irfan-Khan, M. and Mort, P.R.: *Critical parameters and limiting conditions in binder granulation of fine powders*, Powder Technology, No. 94, pp. 245–258, **1997**.

Tardos, G.I.: Email correspondence with Gabriel I. Tardos, D.Sc., Professor and Deputy, Department of Chemical Engineering, The City College of the City University of New York, June **2005**.

Teipel, U. and Mikonsaari, I.: *Determining Contact Angles of Powder by Liquid Penetration*, Particle System Characterization, No. 21, pp. 255–260, **2004**.

Teunou, E. and Poncelet, D.: *Batch and continuous fluid bed coating – review and state of the art*, Journal of Food Engineering, No. 53, pp. 325–340, **2002**.

Thornton, C., Ciomocos, M.T. and Adams, M.J.: *Numerical simulations of diametrical compression test on agglomerates*, Powder Technology, No. 140, pp. 258–267, **2004**.

Waldie, B.: *Growth mechanism and the dependence of granule size on drop size in fluidized-bed granulation*, Chemical Engineering Science, No. 46, pp. 2781–2785, **1991**.

Watano, S., Harada, T., Terashita, K. and Miyanami, K.: *Development and application of moisture control system with IR moisture sensor to aqueous polymeric coating process*, Chemical Pharmaceutical Bulletins, No. 41, pp. 580–585, **1993**.

Watano, S., Morikawa, T. and Miyanami, K.: *Kinetics of Granule Growth in Fluidized Bed Granulation with Moisture Control*, Chemical and Pharmaceutical Bulletins, No. 43, **1995**.

Wedel, S.: Email correspondence with Stig Wedel, lector at KT, DTU, March **2005**.

Williams R.O. and Liu, J.: *Influence of processing and curing conditions on beads coated with an aqueous dispersion of cellulose acetate phthalate*, European Journal of Pharmaceutics and Biopharmaceutics, No. 49, pp. 243–252, **2000**.

York, P. and Rowe, R.C.: *Monitoring granulation size enlargement processes using mixer torque rheometry*, First International Particle Technology Forum, Denver, **1994**.

Zajic, L. and Buckton, G.: *The use of surface energy values to predict optimum binder selection for granulations*, International Journal of Pharmaceutics, No. 59, pp. 155–164, **1990**.

With us you can
shape the future.
Every single day.

For more information go to:
www.eon-career.com

Your energy shapes the future.

e-on



Appendix A1: Derivation of the equation 2.5

Based on: Denesuk et al. (1993 & 1994), Iveson & Franks (2003), Rumpf (1990), Hansen (1999), Teipel & Mikonsaari, 2004 and Hapgood et al. (2002).

Consider the three phases present when a liquid droplet is in contact with a porous media as indicated in figure A1:

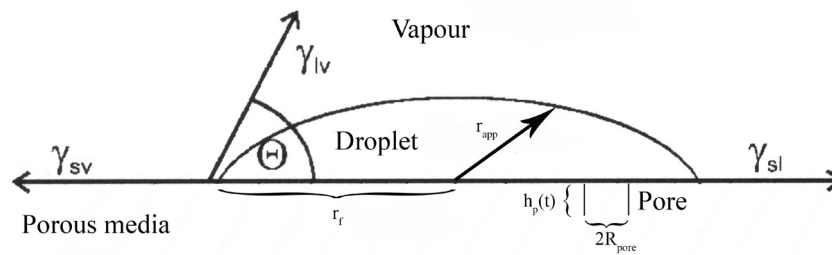


Figure A1: Droplet-Solid phase-vapour interface.

The three interfaces present when a liquid droplet is in contact with a porous solid media
(Based on Teipel & Mikonsaari, 2004 and Denesuk et al., 1993).

As long as the γ_{sl} is smaller than γ_{sv} , surface energy considerations will favour the replacement of solid-vapour interfaces by solid-liquid interfaces and liquid will be drawn into the pores at a rate determined by the pore geometry, surface energies and the viscosity of the liquid.

The interfacial interactions constitute a pore liquid penetration pressure ΔP that can be expressed in terms of the partial change in free energy for a given volume of liquid taken into a pore:

$$\frac{\partial E_{\text{Free}}}{\partial V} = \Delta P \quad (\text{A.1})$$

The change in free energy for a given differential depth of liquid penetration into a cylindrical pore dh_p with radius R_{pore} can be expressed as:

$$dE_{\text{Free}} = (\gamma_{sv} - \gamma_{sl}) 2 \cdot \pi \cdot R_{\text{pore}} \cdot dh_p \quad (\text{A.2})$$

Relating the associated differential volume to the differential penetration depth $dV = \pi R_{\text{pore}}^2 dh_p$ gives by insertion into equation A.1:

$$\Delta P = \frac{2(\gamma_{sv} - \gamma_{sl})}{R_{\text{pore}}} \quad (\text{A.3})$$

Equation A.3 is the Young-Laplace equation describing the capillary pressure driving force.

Neglecting any droplet curvature as well as gravitationally³⁸ induced pressure, one may take the above pressure relation in equation A.3 to constitute the total pressure difference driving the advance of the liquid and use the Hagen-Poiseuille law to obtain the rate of droplet advance. This will be shown below. The Hagen-Poiseuille equation describes the viscous resistance to laminar flow and is given by:

$$\Delta P = \frac{8u_{\text{liq}} h_p \eta_{\text{liq}}}{R_{\text{pore}}^2} \quad (\text{A.4})$$

where u_{liq} is the liquid velocity in m/s and h_p is the length of the pore filled. By equating equation A.4 with A.3 one achieves:

$$u_{\text{liq}} = \frac{R_{\text{pore}}(\gamma_{\text{sv}} - \gamma_{\text{sl}})}{4h_p \eta_{\text{liq}}} = \frac{dh_p}{dt} \quad (\text{A.5})$$

Equation A.5 is known as the Washburn equation and by simple integration from $t'=0$, $h_p = 0$ to $t' = t$, $h_p' = h_p$ one can easily obtain a solution expressed by:

$$h_p(t) = \sqrt{\frac{(\gamma_{\text{sv}} - \gamma_{\text{sl}})R_{\text{pore}}}{2\eta_{\text{liq}}}} \sqrt{t} \quad (\text{A.6})$$

This solution thereby expresses the depth of liquid penetration into a given pore as function of time.

Assuming radial symmetry of the liquid and of the porosity parameters, a differential volume of liquid drawn into the pores dV_p can be expressed as the product of the differential volume of liquid in a single pore (given as $\pi R_{\text{pore}}^2 dh_p$) and the differential number of pores in a thin annulus of the porous substrate between r and $r + dr$ (given as $\rho_{\text{pore}} 2\pi r dr$):

$$dV_p = \pi R_{\text{pore}}^2 dh_p \rho_{\text{pore}} 2\pi \cdot r dr \quad (\text{A.7})$$

By differentiation of equation A.6 with respect to t , dh_p can be related to dt and give by insertion into equation A.7:

$$dV_p = \pi^2 R_{\text{pore}}^2 \rho_{\text{pore}} \sqrt{\frac{(\gamma_{\text{sv}} - \gamma_{\text{sl}})R_{\text{pore}}}{2\eta_{\text{liq}}}} \frac{r}{\sqrt{t}} dr dt \quad (\text{A.8})$$

Equation A.8 can be integrated to give the total volume of liquid drawn into the porous solid. Hence the total volume of a liquid in the porous solid at a given time t may be obtained by integrating from $t' = 0$ to $t' = t$ and from $r = 0$ to $r = r_f$ where r_f is the radius of the footprint of the droplet on the porous surface:

$$V_p(t) = \pi^2 R_{\text{pore}}^2 \rho_{\text{pore}} \sqrt{\frac{(\gamma_{\text{sv}} - \gamma_{\text{sl}})R_{\text{pore}}}{2\eta_{\text{liq}}}} \int_0^t \int_0^{r_f(t')} \frac{r}{\sqrt{t'}} dr dt' \quad (\text{A.9})$$

Besides the volume of liquid in the porous solid, there is a volume of liquid present at the porous media surface V_s which may be expressed as a function of an apparent surface contact radius³⁹ $r_{app}(t)$ and the contact angle θ between the porous media and the wetting liquid. Hence the total droplet volume may at a given time be expressed as:

$$V_d = V_s(t) + V_p(t) \quad (A.10)$$

By further manipulation it is possible to obtain a general complex equation describing how the apparent radius r_{app} varies as a function of V_d , R_{pore} , θ , r_f and time. This relationship is a pseudo indication of the drop penetration time but the equation cannot easily be solved because of the difficulty of determining how the droplet footprint on the porous media surface r_f varies as a function of time.

It has however been observed that during imbibition, droplets often have a constant drawing area (CDA) meaning that the three-phase contact line remains stationary. Hence the droplet radius is constant during drainage (and r_f may be considered constant and equal to the droplet radius r_d), whereas the contact angle slowly decreases as the liquid drains from the droplet into the porous surface. The principle can be seen in figure A2.

© 2013 Accenture. All rights reserved.

be > your degree

Bring your talent and passion to a global organization at the forefront of business, technology and innovation. Discover how great you can be.

Visit accenture.com/bookboon

Be greater than.
consulting | technology | outsourcing

accenture
High performance. Delivered.

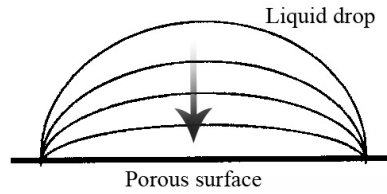


Figure A2: Constant drawing area.

The constant drawing area (CDA) case of liquid drop penetration into a porous surface.

(Based on Hapgood et al., 2002).

The CDA case can be considered as a limiting case of the general model and it can be shown by assumption of $r_f = r_d = \text{constant}$ that the apparent radius r_{app} can be expressed as:

$$r_{\text{app}}(t) = r_d \left(1 - \sqrt{\frac{t}{\tau_d}} \right)^{1/3} \quad (\text{A.11})$$

where τ_d is the droplet penetration time given as:

$$\tau_d = \left(\frac{V_d}{r_d^2 \kappa} \right)^2 \quad \text{where} \quad \kappa = \pi^2 R_{\text{pore}}^2 \rho_{\text{pore}} \sqrt{\frac{(\gamma_{\text{sv}} - \gamma_{\text{sl}}) R_{\text{pore}}}{2 \eta_{\text{liq}}}} \Rightarrow$$

$$\tau_d = \frac{2 V_d^2}{\pi^4 r_d^4 \rho_{\text{pore}}^2 R_{\text{pore}}^5} \cdot \frac{\eta_{\text{liq}}}{(\gamma_{\text{sv}} - \gamma_{\text{sl}})} \quad (\text{A.12})$$

By introducing the porous media surface porosity $\varepsilon_{\text{pmsp}} = \pi R_{\text{pore}}^2 \rho_{\text{pore}}$ and by application of the Young equation: $\gamma_{\text{sv}} - \gamma_{\text{sl}} = \gamma_{\text{lv}} \times \cos(\theta)$ one finally ends at:

$$\tau_d = \frac{2 V_d^2}{\pi^2 \varepsilon_{\text{pmsp}}^2 r_d^4 R_{\text{pore}} \gamma_{\text{lv}} \cdot \cos \Theta}, \text{ Q.e.d.} \quad (\text{A.13})$$

Appendix A2: From equation 2.5 to equation 2.7

Based on: Hapgood et al. (2002) and Denesuk et al. (1993).

Although not obvious at first, the Hapgood equation 4.7 describing the droplet penetration time τ_d is basically the Denesuk equation 4.5 in a different form. The main differences between the two equations are the expressions describing the pore radii (R_{pore} and R_{eff}) and the porosities ($\varepsilon_{\text{pmsp}}$ and ε_{eff}). It will be shown below how the Hapgood equation is derived from the Denesuk equation. Beginning with the Denesuk equation 4.5 derived in appendix A1:

$$\tau_d = \frac{2V_d^2}{\pi^2 \varepsilon_{\text{pmsp}}^2 r_d^4 R_{\text{pore}}} \frac{\eta_{\text{liq}}}{\gamma_{\text{lv}} \cdot \cos \Theta} \quad (\text{A.14})$$

Exchanging $\varepsilon_{\text{pmsp}}$ with ε_{eff} and R_{pore} and R_{eff} and assuming that the volume of a droplet V_d can be assumed to be spherical thereby being expressed as:

$$V_d = \frac{4}{3} \pi \cdot r_d^3 \Leftrightarrow r_d = \frac{(6V_d)^{1/3}}{2\pi^{1/3}} \quad (\text{A.15})$$

and by insertion into equation A.14:

$$\begin{aligned} \tau_d &= \frac{2V_d^2 16\pi^{4/3}}{\pi^2 \varepsilon_{\text{eff}}^2 (6V_d)^{4/3} R_{\text{eff}}} \frac{\eta_{\text{liq}}}{\gamma_{\text{lv}} \cdot \cos \Theta} \Leftrightarrow \\ \tau_d &= \frac{2 \cdot 16\pi^{4/3}}{\pi^2 (6)^{4/3}} \frac{V_d^{2/3}}{\varepsilon_{\text{eff}}^2 R_{\text{eff}}} \frac{\eta_{\text{liq}}}{\gamma_{\text{lv}} \cdot \cos \Theta} \end{aligned} \quad (\text{A.16})$$

Thereby ending at:

$$\tau_d = 1.36 \frac{V_d^{2/3}}{\varepsilon_{\text{eff}}^2 R_{\text{eff}}} \frac{\eta_{\text{liq}}}{\gamma_{\text{lv}} \cdot \cos \Theta}, \text{ Q.e.d.} \quad (\text{A.17})$$

Appendix A3: Derivation of the dimensionless spray flux

Based on: Litster et al. (2001).

Assume that a spray nozzle with the volumetric spray rate \dot{V} produces spherical droplets with an average droplet size diameter d_d . The number of spherical droplets \dot{n}_d produced by the nozzle per unit time is thus:

$$\dot{n}_d = \frac{\dot{V}}{\frac{1}{6} \cdot \pi \cdot d_d^3} \quad (\text{A.18})$$

If it is assumed that the area covered by each droplet is equal to the cross-sectional area of the spherical droplet⁴⁰, the area covered by each droplet is thereby:

$$a_d = \frac{\pi \cdot d_d^2}{4} \quad (\text{A.19})$$

The total projected area of droplets produced by the nozzle per time unit is then:

$$\dot{a}_{dT} = a_d \dot{n}_d = \frac{3 \cdot \dot{V}}{2 \cdot d_d} \quad (\text{A.20})$$

This area of droplets is distributed over a spray area A on the powder bed surface and this surface area is traversing the spray zone with a powder flux⁴¹ \dot{A} . The dimensionless spray flux is thereby given as:

$$\Psi_a = \frac{3 \cdot \dot{V}}{2 \cdot \dot{A} \cdot d_d}, \text{ Q.e.d.} \quad (\text{A.21})$$

Appendix A4: Derivation of the Stokes viscous number and the Stokes critical viscous number

Based on: Ennis et al. (1991), Tardos et al. (1997) and Wedel, (2005).

Consider two individual spherical granules with masses and radii m_1, r_1 and m_2, r_2 respectively, as indicated in figure A3:

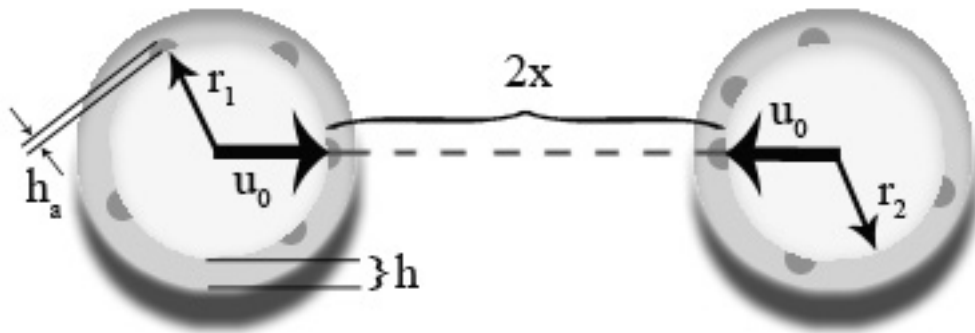


Figure A3: Colliding granules.

Schematic of two colliding granules each of which is covered by a viscous binder layer of thickness h
(Based on Ennis et al., 1991).

Assuming that the two granules are approaching one another at an initial relative velocity of $2u_0$ and that each are covered with a binder layer thickness h . As the individual binder layers come into contact a dynamic pendular bridge will form between the colliding granules now separated by a gap of distance $2h$. For sufficiently large binder viscosity, the bridge will dissipate the relative kinetic energy of the colliding granules preventing rebound. To determine the minimum velocity required for particle rebound, a force balance on an individual granule can be considered. Ignoring the effect of capillary forces and assuming creep flow between the two granules, the force balance equation of motion (Newton's second law) for the approach stage can be expressed as:

$$m_{\text{harm}} \frac{du}{dt} = \frac{3}{2} \pi \eta_{\text{liq}} r_{\text{harm}}^2 \frac{dx}{dt} \frac{1}{x} \quad (\text{A.22})$$

where x is half of the dimensional gap distance at a given time t and m_{harm} and r_{harm} are the harmonic mean mass and radius for the unequal granules given by:

$$m_{\text{harm}} = \frac{m_1 m_2}{m_1 + m_2} \quad \text{and} \quad r_{\text{harm}} = \frac{r_1 r_2}{r_1 + r_2} \quad (\text{A.23})$$

A solution to equation A.22 can easily be obtained by integrating the left side between $u' = u_0$ and u and the right side between $x' = h$ and x . The solution can be expressed as:

$$u = u_0 \left(1 - \frac{1}{St_v} \ln \left(\frac{h}{x} \right) \right) \quad (\text{A.24})$$

where St_v is the viscous Stokes number given by:

$$St_v = \frac{2m_{\text{harm}} u_0}{3\pi \cdot \eta_{\text{liq}} r_{\text{harm}}^2} \quad (\text{A.25})$$

Assuming that the granules have an equal density of ρ_g and that they are completely spherical, one may assume:

$$m_{\text{harm}} = \frac{4}{3} \pi r_{\text{harm}}^3 \rho_g \quad (\text{A.26})$$

and by insertion into equation A.25 one finally ends at:

$$St_v = \frac{2 \frac{4}{3} \pi r_{\text{harm}}^3 \rho_g u_0}{3\pi \cdot \eta_{\text{liq}} r_{\text{harm}}^2} \Leftrightarrow St_v = \frac{8 \cdot \rho_g \cdot r_{\text{harm}} \cdot u_0}{9 \cdot \eta_{\text{liq}}}, \text{ Q.e.d.} \quad (\text{A.27})$$

"I studied English for 16 years but...
...I finally learned to speak it in just six lessons"

Jane, Chinese architect

ENGLISH OUT THERE

Click to hear me talking before and after my unique course download

For rebound of the colliding granules to occur, the Stokes number must exceed a critical value of St_v^* . With the initial velocity of u_0 , let the velocity of the colliding granule upon reaching a distance of h_a be u_a , where h_a represents a characteristic length scale of surface asperities. The initial rebound velocity is then $e u_a$ where e is the particle coefficient of restitution with the presence of binder layer. Realising that the granule velocity u is a scalar velocity and thereby a sign-depend parameter⁴², the situation of the two granules colliding and afterwards rebounding can be split up into two situations analogously to equation A.22:

$$\text{Approach: } m_{\text{harm}} \frac{du}{dt} = \frac{3}{2} \pi \cdot \eta_{\text{liq}} r_{\text{harm}}^2 \frac{dx}{dt} \frac{1}{x} \quad (\text{A.28})$$

$$\begin{aligned} \text{with the boundary conditions:} \quad & \text{At} \quad t = 0: \quad x = h \text{ and } u = u_0 \\ & \text{and at:} \quad t = t_1: \quad x = h_a \text{ and } u = u_a \end{aligned}$$

$$\text{Rebound: } -m_{\text{harm}} \frac{du}{dt} = \frac{3}{2} \pi \cdot \eta_{\text{liq}} r_{\text{harm}}^2 \frac{dx}{dt} \frac{1}{x}$$

$$\begin{aligned} \text{with the boundary conditions:} \quad & \text{At} \quad t = t_1: \quad x = h_a \text{ and } u = e u_a \\ & \text{and at:} \quad t = t_2: \quad x = h \text{ and } u = 0 \end{aligned}$$

By integrating equation A.28 between its boundaries one achieves:

$$m_{\text{harm}} (u_a - u_0) = -\frac{3}{2} \pi \cdot \eta_{\text{liq}} r_{\text{harm}}^2 \ln \frac{h}{h_a} \quad (\text{A.30})$$

Analogously, one achieves by integration of equation A.29 between its boundaries:

$$m_{\text{harm}} \cdot e \cdot u_a = \frac{3}{2} \pi \eta_{\text{liq}} r_{\text{harm}}^2 \ln \frac{h}{h_a} \quad (\text{A.31})$$

and by insertion of equation A.31 into equation A.30 one achieves:

$$\begin{aligned} m_{\text{harm}} u_0 - \frac{1}{e} \frac{3}{2} \pi \cdot \eta_{\text{liq}} r_{\text{harm}}^2 \ln \frac{h}{h_a} &= \frac{3}{2} \pi \cdot \eta_{\text{liq}} r_{\text{harm}}^2 \ln \frac{h}{h_a} \Leftrightarrow \\ \frac{2m_{\text{harm}} u_0}{3\pi \cdot \eta_{\text{liq}} r_{\text{harm}}^2} &= \left(1 + \frac{1}{e}\right) \ln \frac{h}{h_a} \end{aligned} \quad (\text{A.32})$$

By exploiting the result in equation A.25 one finally ends at:

$$St_v^* = \left(1 + \frac{1}{e}\right) \cdot \ln \left(\frac{h}{h_a}\right), \text{ Q.e.d.} \quad (\text{A.33})$$

Appendix A5: Derivation of equation 3.1 describing the coating thickness

Based on: Depypere (2005) and Dewettinck et al. (1999a).

Although equation 5.1 seems somewhat confusing at first, it is basically nothing more than a calculation of what the coating thickness ζ_c theoretically would be if a known mass of coating m_{dep} were added to a known mass of core particles m_{core} , assuming hereby that all the core particles have equal diameters d_{core} and that the core particles as well as the coated particles are spherical. First the mass of a coating as well as the mass of a core particle in terms of density and volume are expressed as:

$$m_{core} = \frac{4\rho_{core}\pi(r_{core})^3}{3} \quad \text{and} \quad (A.34)$$

$$m_{dep} = \frac{4\rho_{cm}\pi((r_{core} + \zeta_c) - r_{core})^3}{3}$$

and by the dividing m_{dep} with m_{core} one obtains:

$$\frac{m_{dep}}{m_{core}} = \frac{\rho_{cm}((r_{core} + \zeta_c) - r_{core})^3}{\rho_{core}(r_{core})^3} \Leftrightarrow \quad (A.35)$$

$$\frac{m_{dep}\rho_{core}}{m_{core}\rho_{cm}} \cdot r_{core}^3 = \zeta_c^3 + 3r_{core}\zeta_c^2 + 3r_{core}^2\zeta_c$$

By dividing by r_{core}^3 and afterwards adding 1 on both sides one achieves:

$$\frac{m_{dep}\rho_{core}}{m_{core}\rho_{cm}} + 1 = \frac{\zeta_c^3}{r_{core}^3} + \frac{3\zeta_c^2}{r_{core}^2} + \frac{3\zeta_c}{r_{core}} + 1 \quad (A.36)$$

Realising that:

$$\frac{\zeta_c^3}{r_{core}^3} + \frac{3\zeta_c^2}{r_{core}^2} + \frac{3\zeta_c}{r_{core}} + 1 = \left(\frac{\zeta_c}{r_{core}} + 1 \right)^3 \quad (A.37)$$

one achieves:

$$\frac{m_{\text{dep}}\rho_{\text{core}}}{m_{\text{core}}\rho_{\text{cm}}} + 1 = \left(\frac{\zeta_c}{r_{\text{core}}} + 1 \right)^3 \Leftrightarrow$$

$$\left(\frac{m_{\text{dep}}\rho_{\text{core}}}{m_{\text{core}}\rho_{\text{cm}}} + 1 \right)^{1/3} - 1 = \frac{2\zeta_c}{d_{\text{core}}} \quad (\text{A.38})$$

and then finally ends at:

$$\zeta_c = \left(\left(\left(\frac{\rho_{\text{core}}}{\rho_{\text{cm}}} \right) \cdot \left(\frac{m_{\text{core}} + m_{\text{dep}}}{m_{\text{core}}} - 1 \right) + 1 \right)^{1/3} - 1 \right) \cdot \left(\frac{d_{\text{core}}}{2} \right), \text{ Q.e.d.} \quad (\text{A.39})$$

DUKE
THE FUQUA
SCHOOL
OF BUSINESS

BUSINESS HAPPENS

HERE.

www.fuqua.duke.edu/globalmba

Learn More >



Click on the ad to read more

Appendix A6: Derivation of equation 3.4

Based on: Kunii & Levenspiel (1991), Rowe (1972) and Link & Schlünder (1997).

It has been well proven among different authors that gas bubbles in fluidised beds causes an upward drift of particles along its vertical path and also carries particles upwards in a captive wake. Examinations by Rowe (1972) indicate that the upward drift is a roughly conical shape with a volume of approximately 0.35 times the gas bubble volume V_b , whereas the wake volume is approximately 0.25 times the bubble volume. Hence, each gas bubble displaces upwards a total volume of particles of approximately $0.6 \cdot V_b$. Figure A4 illustrates the different volumes as well as the different types of motion occurring during the rise of a bubble.

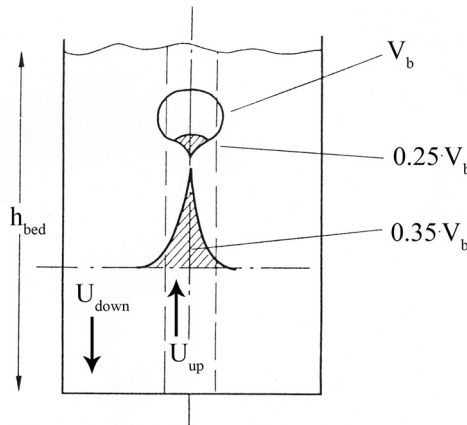


Figure A4: Model of particle movement due to the rise of a bubble in a bubbling fluidised bed. Notice how part of the particles are moved by the wake and another part by the bubble itself (Based on Rowe, 1972).

If n_b bubbles per. second cross a horizontal plane through the bed, the volumetric bubble flow Q_b will be given as:

$$Q_b = \dot{n}_b V_b \quad (A.40)$$

If the h_{bed} is the bed height and U_{br} is the bubble rise velocity then the residence time of a single bubble in the bed is given by:

$$\tau_b = \frac{h_{bed}}{U_{br}} \quad (A.41)$$

and by combination of equation A.40 and A.41 one achieves the hold-up of bubbles:

$$Q_b \tau_b = \frac{\dot{n}_b V_b h_{bed}}{U_{br}} \quad (A.42)$$

The fraction of bubble space in the bed is given by:

$$\varepsilon_b = \frac{Q_b}{U_{br} A_{bed}} \quad (A.43)$$

where A_{bed} is the cross-sectional area of the bed. Equation A.43 is also the fraction of the bed cross-sectional area occupied by bubbles A_b/A_{bed} and thereby:

$$A_b = \frac{Q_b}{U_{br}} \quad (A.44)$$

A_b is the cross-sectional area through which the upward particles flow of $0.6 \cdot Q_b$ is assumed to occur. Hence the average upwards particle velocity is then given by:

$$U_{up} = \frac{0.6 \cdot Q_b}{A_b} = 0.6 \cdot U_{br} \quad (A.45)$$

and since there is no net particle movement out of the bed, the average downward particle velocity must be given as:

$$U_{down} = \frac{0.6 \cdot Q_b}{(A_{bed} - A_b)} = 0.6 \left(\frac{A_{bed}}{Q_b} - \frac{1}{U_{br}} \right) \quad (A.46)$$

The average particle circulation time τ_c around the bed will then be:

$$\tau_c = h_{bed} \left(\frac{1}{U_{up}} + \frac{1}{U_{down}} \right) \quad (A.47)$$

By inserting equation A.45 and A.46 into equation A.47 one easily obtains:

$$\tau_c = \frac{h_{bed} A_{bed}}{0.6 \cdot Q_b} \quad (A.48)$$

Because the derived equation A.48 depends on the bed height h_{bed} , which again depends on the particle properties and fluidisation velocity, it is desirable to exchange h_{bed} with other parameters that more easily can be determined. Equation A.42 describing the bubble hold-up can in other terms be expressed as:

$$Q_b \tau_b = A_{bed} (h_{bed} - h_{mf}) \quad (A.49)$$

where h_{mf} is the bed height at minimum fluidisation velocity U_{mf} . Combining equation A.49 with equation A.41 gives:

$$h_{bed} = \frac{h_{mf}}{\left(1 - \frac{Q_b}{A_{bed} U_{br}}\right)} \quad (A.50)$$

Hence by insertion of equation A.50 into equation A.48 one obtains:

$$\tau_c = \frac{h_{mf} A_{bed}}{0.6 \cdot Q_b \left(1 - \frac{Q_b}{A_{bed} U_{br}}\right)} \quad (A.51)$$

It should be noted that $h_{mf} \cdot A_{bed}$ in equation A.51 is the volume of the bed at minimum fluidisation conditions. According to the two-phase theory, the cross-sectional area of the bed A_{bed} at minimum fluidisation conditions can be found from the following equation describing the volumetric bubble flow as function of the superficial fluidisation velocity U_s and the minimum fluidisation velocity U_{mf} :

$$Q_b = A_{bed} (U_s - U_{mf}) \quad (A.52)$$

By combination of equation A.52 and A.51 one finally ends at:

$$\tau_c = \frac{h_{mf}}{0.6 \cdot (U_s - U_{mf}) \cdot [1 - (U_s - U_{mf})/U_{br}]}, \text{ Q.e.d.} \quad (A.53)$$

Join American online LIGS University!

Interactive Online programs
BBA, MBA, MSc, DBA and PhD

Special Christmas offer:

- ▶ enroll **by December 18th, 2014**
- ▶ **start studying and paying only in 2015**
- ▶ **save up to \$ 1,200** on the tuition!
- ▶ Interactive Online education
- ▶ visit ligsuniversity.com to find out more!

Note: LIGS University is not accredited by any nationally recognized accrediting agency listed by the US Secretary of Education. More info [here](http://ligsuniversity.com).



Notes

1. The sphericity is defined as the surface of a sphere divided by the surface of an irregular particle both having the same volume (Kunii & Levenspiel, 1991).
2. The excess gas velocity U_e is the part of the gas above minimum fluidisation that is not necessary for fluidisation. Ideally it is defined as the given fluidisation velocity U minus U_{mf} . In practice an adjustment for the volume fraction of the bed occupied by gas bubbles has to be made (Schaafsma, 2000b).
3. The list is expanded and further specifications are made in coming sections.
4. This second set of the granulation process is sometimes referred to as “Consolidation and Growth” (e.g. Iveson et al., 2001b) or “Growth and Compaction” (e.g. Pietsch, 1991).
5. This phenomenon is sometimes referred to as “Drop pooling” (Iveson et al., 2001a).
6. Sometimes referred to as the “Wetting zone” or “Nucleation zone” (Schaafsma et al., 1999).
7. Even though this theory is developed for a plane solid surface there is a complete analogy to the wetting of spherical particles (Marmur et al., 1992).
8. The contact angle depends on the composition of the binder solution and the physical properties of the powder particle, especially roughness, porosity and affinity for the binder solution (Guignon et al., 2002). Contact angles of powder particles are generally determined by either Goniometry or Wilhelmy tensiometry. In both principles the particles are compressed to produce a flat surface before being wet by a drop and determination of the resulting contact angle (Marmur et al., 1992).
9. The work of adhesion W_A is the work required to separate an interface into two separate surfaces (Kontogeorgis, 2004).
10. The work of cohesion W_C is the work required to separate a unit cross-sectional area of a material from itself. For a solid $W_{CS} = 2\lambda_{sv}$ and for a liquid $W_{CL} = 2\lambda_{lv}$ (Iveson et al., 2001a).
11. The droplet penetration time is defined as the time it takes for the liquid droplet to penetrate completely into the porous substrate with no liquid remaining on the surface. Besides the “droplet penetration time” it is often referred to as the “time of depletion” (Denesuk et al., 1994) or “Wicking time” (Hapgood et al., 2002).
12. It is considered a semi-static configuration in the sense that it changes very little on a time scale comparable to the depletion time (Denesuk et al., 1994).
13. Please refer to appendix A1 to see the formal derivation of equation 2.5.
14. Please refer to appendix A2 to see the how the Hapgood formula is obtained from the Denesuk formula.
15. The droplet size has a negligible effect on nuclei size in other types of high agitation granulation equipment. In high shear mixers e.g., the granule product size appears almost independent of the binder droplet size, as the intensive shear forces crush the initial flocks and agglomerates formed during the nucleation stage (Iveson et al., 2001a).
16. The nucleus diameter obviously cannot be measured during processing. Instead particle samples are taken from the fluid bed at different early stages of the spray process. The sample thereby contains nuclei rather than final agglomerated granules. Size measurements of these samples will thereby give the nucleus diameter (Waldie, 1991 and Iveson et al., 2001a).

17. It may be circular, flat or annular depending on the nozzle type, nozzle position and spray angle (Iveson et al., 2001a).
18. Please refer to appendix A3 to see the derivation of equation 2.12.
19. The time it takes for a particle to circulate a complete wetting-drying cycle. It depends primarily on the fluidisation velocity and bed height (Link & Schlünder, 1997), as it will be presented in section 3.4.
20. The porosity of fluid bed granules varies typically between 0.4–0.5 whereas granules made in high shear or drum mixers have porosities in the range of 0.2 to 0.3 (Schaafsma et al., 2000a).
21. High porosities are often correlated with weak and friable granules (Schaafsma et al., 1998).
22. The coefficient of restitution is the ratio of the difference in velocity before and after the collision. In the case of two colliding particles it is the difference in the velocities of the two colliding particles after the collision divided by the difference in their velocity prior to collision. Perfect elastic collisions has $e = 1$ (Christensen et al., 2000). The coefficient of restitution e thereby accounts for the viscous dissipation in the binder phase being sufficient to dissipate the energy of collision (Liu et al., 2000).
23. Please refer to appendix A4 to see the derivation of equation 2.13 and equation 2.14.
24. The difficulty of determining a uniform value of e for granules means that precise values of St_v^* has to be determined experimentally or by numerical integration (Tardos et al., 1997).
25. For instance that there exists a uniform granule collision velocity or that in coalescence, capillary forces can be neglected (Ennis et al., 1991). Especially the difficulty of determining a precise collision velocity u_0 makes the viscous Stokes theory difficult to exploit fully in practice (Abbott, 2002).
26. The original Hounslow model is hereby made a special case where $q = 1$ (Cryer, 1999).
27. Please refer to appendix A5 to see the derivation of equation 3.1.
28. e.g. energy efficiency, quality efficiency, evaporation efficiency or productivity efficiency etc.
29. The order of salting-out power is generally known as the Hofmeister series. It governs many colloidal phenomena including the viscosity of hydrosols such as polymers in salt solutions. The salting-out power increases from the left to the right in the following series for anions bounded with the same cation: $\text{citrate}^{3-} > \text{SO}_4^{2-} > \text{acetate}^- > \text{Cl}^- > \text{Br}^- > \text{I}^- > \text{SCN}^-$. The smaller the cation associated with the given anion in the series, the larger the salting-out effect (Goodwin, 2004 and Nakano et al., 1999).
30. Please refer to appendix A6 to see the derivation of equation 3.4
31. Often referred to as the “modulus of elasticity” (Callister, 2001).
32. In an indentation test a conical diamond point is indented into the material with a known maximum applied force F . After that, the length of radial cracks c is measured versus F . This test can be used on real granules down to 50 μm to determine several strength parameters (Iveson et al., 2001a and Jørgensen, 2002).
33. In some articles referred to as the “Damage zone” or “Yielding zone” (Bika et al., 2001).
34. Actually the term “fracture” is the overall term for “chipping” as well as “fragmentation”, but almost all authors mix fragmentation and fracture or use the terms as synonyms.
35. Chipping is sometimes also used as a general term for small fracture damage even when the applied force is not tangential (Jørgensen et al., 2004).
36. The proportionality is derived on the basis of various observed proportionalities gained from experimental studies. Although derived on the basis of indentation tests on cubes of uniform material, the relation has proven well when compared to granule data (Iveson et al., 2001a and Beekman et al., 2002).
37. Also sometimes referred to as DEA – Distinct Element Analysis (Subero et al., 1999).

- 38. The neglect of gravity may seem wrong at first, but Denesuk et al. (1993) have made rough estimations of the effect and concluded that the neglect of gravity should be valid for essentially all porous media.
- 39. This radius is the contact radius associated with the spherical droplet cap (please refer to figure A1). It decreases as the droplet is drained into the porous media but not linearly.
- 40. An assumption analogue to the assumption of $r_f = r_d$ stated in the derivation of τ_d in appendix A1.
- 41. Often approximated by the product of the powder velocity past the spray in m/s and the width of the powder being wet in m. Both are apparatus/process dependent parameters that can be found experimentally.
- 42. For the rebound, u is decreased as x increases whereas during approach u decreases as x decreases.